1992

Alteration of the degree of crystallinity in a liquid crystalline polymer by thermal processing

Robert S. Turk
San Jose State University

Order Number 1351082

Alteration of the degree of crystallinity in a liquid crystalline polymer by thermal processing

Turk, Robert Stanley, M.S.

San Jose State University, 1992

U·M·I
300 N. Zeeb Rd.
Ann Arbor, MI 48106

ALTERATION OF THE DEGREE OF CRYSTALLINITY IN A LIQUID CRYSTALLINE POLYMER BY THERMAL PROCESSING

A Thesis

Presented to

The Faculty of the Department of Materials Engineering

San Jose State University

In Partial Fulfillment

of the Requirements for the Degree

Master of Science

By

Robert S. Turk

December, 1992

APPROVED FOR THE DEPARTMENT OF MATERIALS ENGINEERING

Linda L. Clements

Dr. Linda L. Clements

Guna Selvaduray

Dr. Guna Selvaduray

Ronald M. Horn

Dr. Ronald M. Horn

APPROVED FOR THE UNIVERSITY

Serena M. Stanford

ABSTRACT

ALTERATION OF THE DEGREE OF CRYSTALLINITY IN A LIQUID CRYSTALLINE POLYMER BY THERMAL PROCESSING

by Robert S. Turk

The effects of thermal processing on the degree of crystallinity for a liquid crystalline polymer, marketed under the Trade Name XYDAR^{R} SRT-300, were studied.

The thermal processing consisted of four annealing cycles, and the pre-annealing specimen preparation conditions. Differential scanning calorimetry (DSC) and X-ray diffraction were used to evaluate the condition of the specimens following thermal exposure. Both techniques show that there are distinct differences between the as-pressed, quenched and annealed specimens.

While the DSC studies show that there is some kind of reversible change which takes place as a consequence of the annealing conditions, the X-ray diffraction results do not clearly show that the level of crystallinity is enhanced.

The exact nature of the change detected by DSC is not clear. It is thought that this is due to a minor increase in molecular ordering which cannot be detected by X-ray diffraction.

ACKNOWLEDGEMENTS

I wish to thank Dr. Linda L. Clements for her time, technical guidance and direction. Her seemingly endless supply of patience with question after question was greatly appreciated. I would also like to thank the other members of my committee, Dr. Guna Selvaduray, and Dr. Ronald M. Horn for there patience, guidance and the contribution of their time.

Many people helped me in this endeavor but lack of space requires that I list only a few. My thanks to: Mr. Milton F. Custer at Hexcel for providing the initial problem for this thesis, along with samples of the resin; Greg Fazzio for his help with the DSC and numerous other things; Mike Pyzyna for his help in getting the X-ray diffractometer running; Marty Carswell for his moral support and running some early TGAs; and Doug Matson for his encouragement (harassment), and moral support.

I particularly thank my parents, Al and Mima; my in-laws Joe and Frances; and especially my wife Maria for their support and patience. They have all sacrificed something for this endeavor, but we made it.

Finally, I especially wish to thank my wife Maria for her time and energy in entering most of the X-ray diffraction data into the computer, and proof reading the text.

TABLE OF CONTENTS

		Page
ABSTRACT		iii
ACKNOWLEDGEMENTS		iv
TABLE OF CONTENTS		v
LIST OF FIGURES		ix
LIST OF TABLES		xiv
Chapter 1.	INTRODUCTION	1
Chapter 2.	PARTIAL MOLECULAR ORDERING DURING PHASE TRANSFORMATIONS	5
	2.1 Disordered Crystal Mesophases	6
	2.2 Ordered Fluid Mesophases	6
	2.3 Ordering Within Liquid Crystals	7
	2.4 Classification of Liquid Crystalline Materials	15
	2.5 Order Transformations Between Mesophases	16
	2.6 Mesophase vs Phase Nomenclature	20
	2.7 The Molecular Structures of Liquid Crystalline Materials	21
Chapter 3.	XYDAR^{R} SRT-300 RESIN	29
	3.1 The XYDAR^{R} Family of Resins	29

		Page
	3.1.1 Family Characteristics of XYDAR^R Resins	31
	3.1.2 Current Uses for XYDAR^R Resins	35
	3.2 The Specific Structure and Properties of XYDAR^R SRT-300	36
	3.2.1 The Chemical Structure of XYDAR^R SRT-300	36
	3.2.2 Reported Mechanical Properties for XYDAR^R SRT-300	41
	3.3 Thermal Transformations Which Occur in XYDAR^R SRT-300	50
Chapter 4.	RESEARCH METHODS FOR ALTERING THE DEGREE OF CRYSTALLINITY	53
	4.1 Preparation of Suitable Specimens	53
	4.2 Thermal Treatment	62
	4.2.1 Quench Treatment	62
	4.2.1.1 Oven Set-up	63
	4.2.1.2 Quench Treatment Procedure	66
	4.2.2 Annealing	68
	4.2.2.1 Annealing Treatment Procedures	69
	4.3 X-ray Diffraction	71

		Page
	4.4 Differential Scanning Calorimetry Analysis	77
Chapter 5.	EXPERIMENTAL RESULTS AND DISCUSSIONS	80
	5.1 Specific Differential Scanning Calorimetry Results	80
	5.1.1 As-pressed Specimens	80
	5.1.2 Quenched Specimens	105
	5.1.3 Specimens Annealed at 300°C For 1 Hour	108
	5.1.4 Specimens Annealed at 300°C For 24 Hours	109
	5.1.5 Specimens Annealed at 360°C For 1 Hour	111
	5.1.6 Specimens Annealed at 360°C For 1 Hour	113
	5.2 General DSC Results	114
	5.3 Overall X-ray Diffraction Results	126
	5.3.1 Diffraction Traces of As-pressed Specimens	140
	5.3.2 Diffraction Traces for Quenched Specimens	141
	5.3.3 Specimens Annealed at 300°C for 1 Hour	142

Page

5.3.4 Specimens Annealed at 300°C for 24 Hours 143

5.3.5 Specimens Annealed at 360°C for 1 Hour 143

5.3.6 Specimens Annealed at 360°C for 24 Hours 144

5.3.7 Injection Molded Specimens 145

5.4 Correlation of DSC and X-ray Diffraction Results 147

5.5 Indications that the Level of Orientation Changed as a Function of Thermal Treatment 151

5.6 Comparisons Between the As-pressed and Highly Annealed Specimens 152

5.7 The Progression of Thermal Treatment Affects as Determined by DSC and X-ray Diffraction 153

Chapter 6. CONCLUSIONS AND RECOMMENDATIONS 156

6.1 Confirmation of Earlier Studies 157

6.2 Expansion of Other Studies 159

6.3 Changes in the DSC Endotherm Peaks 159

6.4 Recommendations for Additional Work 162

6.5 Summary 165

References 166

LIST OF FIGURES

			Page
Figure	1.	Nematic ordering	9
Figure	2.	Two types of smectic ordering	10
Figure	3.	Cholesteric ordering	13
Figure	4.	Flat aromatic ring structures which tend to exhibit liquid crystallinity	23
Figure	5.	An example of a liquid crystalline structure with slightly dipolar side groups	24
Figure	6.	Tie molecules with a random coil type structure connecting folded chain crystallites	26
Figure	7.	Flat aromatic ring structures	27
Figure	8.	XYDAR^{R} SRT-300 fracture surface	33
Figure	9.	Formula diagrams for EKKCEL^{R} I-2000, and XYDAR^{R} SRT-300	37
Figure	10.	Actual random structure produced by the synthesis of XYDAR^{R} SRT-300	39
Figure	11.	Photomicrograph of the fracture surface of an injection molded part, showing the layered internal structure	44
Figure	12.	Diagram of the typical layered structure which occurs in XYDAR^{R} SRT-300 injection moldings	45
Figure	13.	DSC trace of as-pressed specimens	60

			Page
Figure	14.	DSC trace of an as-pressed specimen which was allowed to cool at 10°C/minute	61
Figure	15.	Diagram of the oven set-up for thermal treatment	64
Figure	16.	X-ray diffraction curve for specimen 14, which is in the experimental quenched condition, along with the estimated fully amorphous curve	75
Figure	17.	DSC trace for specimen 1; Condition: as-pressed	87
Figure	18.	DSC trace for specimen 7; Condition: as-pressed	88
Figure	19.	DSC trace for specimen 13; Condition: as-pressed	89
Figure	20.	DSC trace for specimen 2; Condition: quenched	90
Figure	21.	DSC trace for specimen 8; Condition: quenched	91
Figure	22.	DSC trace for specimen 14; Condition: quenched	92
Figure	23.	DSC trace for specimen 6; annealed at 300°C for 1 hour	93
Figure	24.	DSC trace for specimen 12; annealed at 300°C for 1 hour	94
Figure	25.	DSC trace for specimen 18; annealed at 300°C for 1 hour	95

			Page
Figure	26.	DSC trace for specimen 5; annealed at 300°C for 24 hours	96
Figure	27.	DSC trace for specimen 11; annealed at 300°C for 24 hours	97
Figure	28.	DSC trace for specimen 17; annealed at 300°C for 24 hours	98
Figure	29.	DSC trace for specimen 3; annealed at 360°C for 1 hour	99
Figure	30.	DSC trace for specimen 9; annealed at 360°C for 1 hour	100
Figure	31.	DSC trace for specimen 15; annealed at 360°C for 1 hour	101
Figure	32.	DSC trace for specimen 4; annealed at 360°C for 24 hours	102
Figure	33.	DSC trace for specimen 10; annealed at 360°C for 24 hours	103
Figure	34.	DSC trace for specimen 16; annealed at 360°C for 24 hours	104
Figure	35.	DSC trace for the initial heating of a second portion from specimen 10	116
Figure	36.	DSC trace for the second heating of a second portion from specimen 10	117
Figure	37.	DSC trace for the third heating of a second portion from specimen 10	118

			Page
Figure	38.	DSC trace for the initial heating of a second portion from specimen 11	121
Figure	39.	DSC trace for the second heating of a second portion from specimen 11	122
Figure	40.	DSC trace for the third heating of a second portion from specimen 11	123
Figure	41.	X-ray diffraction trace for as-pressed specimens	127
Figure	42.	X-ray diffraction trace for quenched specimens	128
Figure	43.	X-ray diffraction trace for specimens annealed at 300°C for 1 hour	129
Figure	44.	X-ray diffraction trace for specimens annealed at 300°C for 24 hours	130
Figure	45.	X-ray diffraction trace for specimens annealed at 360°C for 1 hour	131
Figure	46.	X-ray diffraction trace for specimens annealed at 360°C for 24 hours	132
Figure	47.	X-ray diffraction trace for an injection molded specimen in the as-received condition	133
Figure	48.	X-ray diffraction trace for an injection molded specimen in the quenched condition	134
Figure	49.	X-ray diffraction trace for an injection molded specimen annealed at 300°C for 1 hour	135

			Page
Figure	50.	X-ray diffraction trace for an injection molded specimen annealed at 300°C for 24 hours	136
Figure	51.	X-ray diffraction trace for an injection molded specimen annealed at 360°C for 24 hours	137
Figure	52.	Typical DSC trace for an injection molded specimen in the as-received condition	146

LIST OF TABLES

			Page
Table	1.	Variations in mechanical properties as a function of test specimen thickness	43
Table	2.	Various reported mechanical properties for the XYDAR^{R} SRT-300 resin system	48
Table	3.	Effects of molding parameters on tensile strength	49
Table	4.	Maximum temperature and exposure times for the quenching treatment	67
Table	5.	Summary of the DSC Results for the As-pressed Condition	81
Table	6.	Summary of the DSC Results for the Quenched Condition	82
Table	7.	Summary of the DSC Results for Specimens Annealed at 300°C for 1 Hour	83
Table	8.	Summary of the DSC Results for Specimens Annealed at 300°C for 24 Hours	84
Table	9.	Summary of the DSC Results for Specimens Annealed at 360°C for 1 Hour	85
Table	10.	Summary of the DSC Results for Specimens Annealed at 360°C for 24 Hours	86
Table	11.	Relative percent crystallinity and specific energies of the crystalline-solid to liquid-crystal transition for the various specimens	149

Chapter 1. INTRODUCTION

This study was initiated as an outgrowth of work which was in progress at Hexcel Corporation in 1985. At that time, Hexcel was working on processes for the impregnation of carbon fibers with high temperature thermoplastic matrices. One of the matrix materials under study was a liquid crystalline polymer marketed by Dart Manufacturing Company under the trade name XYDAR^{R}.(*) This trade name is used to describe a family of liquid crystalline polymers which are based on the same constituent monomers.(#) The specific resin Hexcel used was XYDAR^{R} SRT-300. This is a neat (unfilled) aromatic polyester material which is produced by the condensation polymerization of p,p-biphenol, terephthalic acid, and p-hydroxybenzoic acid, with a molar ratio of 1:1:2, respectively.(1)

One of the problems Hexcel encountered while using this system as a matrix resin was that molecules of the resin tended to align in the same direction as the fibers. This was undesirable because the resulting composite was exceptionally reinforced in the fiber direction but was soft, weak and brittle in the cross-fiber direction. This is

---

(*) The superscript character R will be used to represent the symbol for Registered Trade Mark which is ®.

(#) The formulation and rights to XYDAR^{R} were sold to Amoco in 1988. Amoco continues to market these materials under the XYDAR^{R} name.

because liquid crystalline polymers have mechanical properties which are lowest in the directions which are transverse to the molecular axis. The two primary purposes of the matrix in a composite material are to transfer load from fiber to fiber and to provide strength in the directions which are transverse to the direction of the fiber. Thus, having the molecules of the XYDAR^{R} matrix aligned with the reinforcing fibers produces a situation where the mechanical properties of the composite prepreg (#) are not maximized.

If the orientation of a significant portion of the matrix molecules could be changed so that they would no longer be aligned with the reinforcing fibers, the transverse strength of resulting composites would be improved. In order to determine if it is possible to alter the orientation of the matrix molecules in the prepreg material, it must first be determined whether the degree of crystallinity of the matrix material itself can be altered.

To this end, it has been the goal of this study to determine if the degree of crystallinity of the liquid crystalline polymer known as XYDAR^{R} SRT-300 can be altered using only thermal processing techniques. If the degree of

---

(#) Composite prepreg is a ready-to-mold material in which the reinforcing component is pre-impregnated with an appropriate resin system.

crystallinity can be altered, the overall properties of the material can be engineered to meet specific needs.

The theory that crystallinity can be changed through thermal treatment is an extension of the premise of United States Patent No. 3,974,250,[2] that states that a related material can be quick cooled from at, or near, the melt temperature to produce a form which is more amorphous than the as-polymerized material. If quick cooling is required to limit the level of crystallinity within a sample, it is reasonable to propose that the proper thermal processing at elevated temperatures would favor an increase in the degree of crystallinity.

The thermal processing approach is similar to the annealing of metals which are typically already crystalline in structure. Annealing does not increase the degree of crystallinity, but the size of individual crystals or grains is increased at the expense of smaller grains. In an analogous approach, it is postulated that for XYDAR^{R} SRT-300, the degree of crystallinity will be increased as the size of the crystalline domains increase and the amorphous regions are incorporated into the lower energy crystalline structure.

Wide angle X-ray diffraction and differential scanning calorimetry (DSC) are the techniques used in this study to assess changes in the degree of crystallinity. Since there

are no standards available, these techniques are not able to provide an absolute measure of the degree of crystallinity. Qualitative assessments of the relative degree of crystallinity are possible, and an evaluation of the feasibility of altering the extent of crystalline structure through thermal processing can be made.

Chapter 2. PARTIAL MOLECULAR ORDERING DURING PHASE TRANSFORMATIONS

Understanding a liquid crystalline material requires an understanding of some of the intermediate degrees of ordering which can occur in many organic materials as they transform from a solid to an isotropic liquid. This transitional ordering exists between the completely disordered isotropic liquid phase and the structured crystalline solid phase. The ordered transitional structures are referred to as "mesophases."

Mesophases can exhibit two basic kinds of partial molecular ordering. The first kind is known as disordered crystal mesophases. Materials exhibiting this type of ordering have a 3-dimensional crystal lattice that defines the molecular positions, but the molecules are not rotationally ordered. This means that the molecules are ordered in their positions in space but they are not ordered with respect to their orientation relative to each other. The second kind of partial molecular ordering includes materials which exhibit no fixed crystal lattice but do retain rotational order between molecules. The lack of a lattice structure allows these types of mesophases to be fluid, and they are known as ordered fluid mesophases. The type of partial molecular ordering a substance can exhibit is dependent on the molecular configuration. Translational

order can be achieved regardless of the shape of the molecules, while rotational order only has real significance when the molecules are not symmetrical.

2.1 Disordered Crystal Mesophases

Materials which produce disordered crystal mesophases tend to contain molecules which are predominantly spherical in shape and have energy barriers to rotational motion which are small compared to the lattice energy. As the energy of the system is increased, these materials transform from a conventional crystalline structure where the molecules have a regular rotational and spatial orientation relative to each other to a structure where the molecules retain their lattice position, but are no longer restricted to a particular orientation. When sufficient energy, usually in the form of heat, is input to the system, the lattice energy is overcome and the disordered crystal structure transforms to an isotropic liquid.[3]

2.2 Ordered Fluid Mesophases

Ordered fluid mesophases are more commonly known as "liquid crystals." As stated earlier, in order for a substance to be in an ordered fluid (liquid crystalline) state, it must have some degree of rotational order. Even though they have no 3-dimensional crystal lattice, some

liquid crystals can also exhibit a certain amount of translational order. It is the ability of liquid crystalline materials to exhibit liquid-like fluidity while maintaining some solid crystal-like (rotational) molecular order that gives them their unique properties. Because rotational order has meaning only if the molecules are not fully symmetric, liquid crystalline materials tend to be composed of elongated molecules. These elongated molecules have been described as being similar to short, rigid rods.[3,4,5] Most of the commercially available liquid crystalline polymers (LCP) contain aromatic groups which are joined in a linear structure. These molecules tend to be more like rigid ribbons than rigid rods. The typical molecular aspect ratio for these ribbons or rods has been reported as ranging from 4:1[3] to around 30:1.[5]

2.3 Ordering Within Liquid Crystals

Within the ordered fluid mesophase or liquid crystalline state, a further refinement of molecular ordering can be identified. There are three basic states of ordering possible within liquid crystals, with each state representing a different level or degree of ordering. The least ordered state is known as the nematic state. The term nematic is derived from the Greek word for thread and describes the thread-like morphologies seen in nematic

materials when they are viewed through polarized light. The structure of this state is depicted in Figure 1. It is characterized by having long-range rotational order, in that all the molecules are lined up with their principal axes pointing in the same general direction. The direction of the principal axis (↑n) is known as the director. For the nematic phase the orientation of the director is uniaxial and arbitrary in space. An additional feature of this state is that there is no center of mass. While the principal axes of the molecules are lined up along the director, they do not occupy any specific position in any other direction.

A more ordered state occurs when the molecules line up in the same direction, as with the nematic phase, but they also separate into distinct layers. This condition provides one degree of translational ordering. This level of ordering actually consists of a family of states which have different specific structures but are characterized by the molecules separating into layers. This ordering is known as the smectic state. The smectic state derives its name from the Greek word for soap. This is because the layering effects seen in smectic states is also observed in soap. The two most disordered smectic states are illustrated in Figure 2. In observing this figure, note that the spacing between the molecules remains random such that **only** one degree of translational ordering is obtained. The lack of

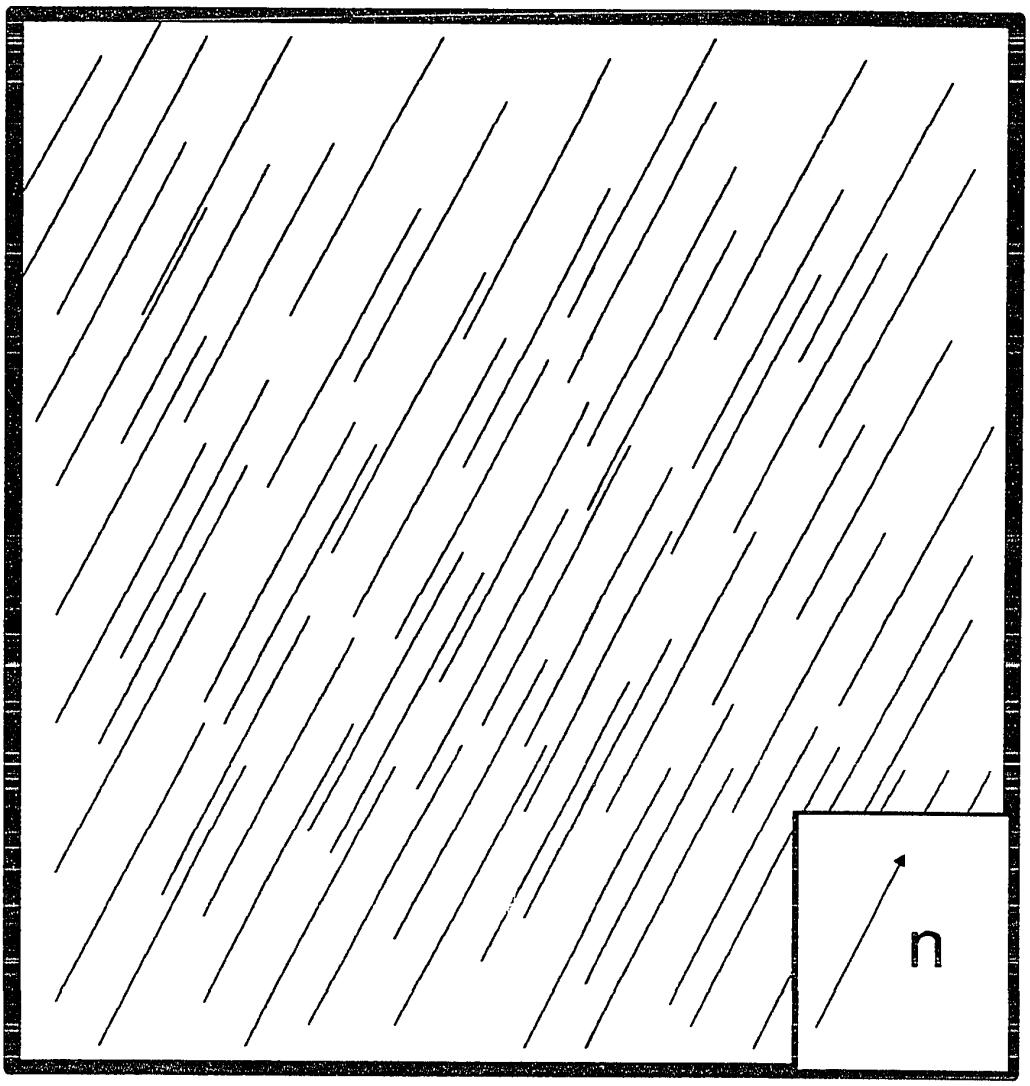

Figure 1. Nematic ordering.

(a)

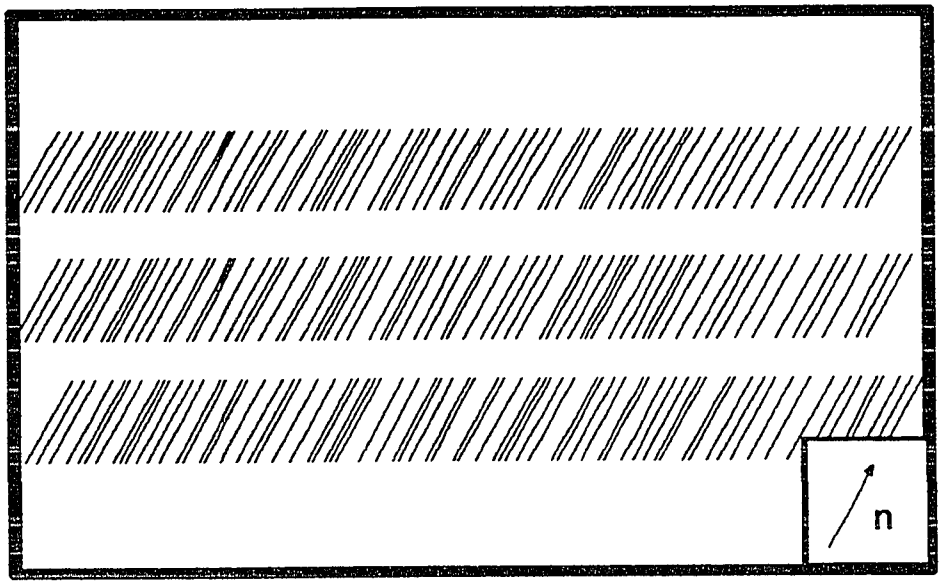

(b)

Figure 2. Two types of smectic ordering (a) smectic A ordering, (b) smectic C ordering.

translational ordering allows the layers to be individually fluid which allows them to slide past one another. While the layers are internally fluid, there is only a limited probability of inter-layer diffusion. The molecules in a layer can align themselves parallel to the layer normal as in Figure 2(a). This state is known as smectic A ordering. The molecules can also be uniformly aligned at some angle to the layer normal as depicted in Figure 2(b). This structure is known as smectic C ordering. The smectic C structure was proposed because X-ray scattering studies showed that the layers in this type of structure were significantly thinner than the molecular length of the chain molecules from which they are formed.[3] Another type of smectic ordering is known as smectic B. Results of X-ray scattering studies suggest that not only are the molecules in this structure organized into layers the same as smectic A and C but also show ordering within the layers. This results in smectic B having three degrees of order. Since smectic B has three degrees of order, it could be argued that this mesophase is crystalline rather than liquid crystalline. The properties of the smectic B mesophase do not match those expected from a structure which has full 3-dimensional order, and as a result it has been concluded that the structure is different from that found in a crystalline solid.[3] It is worth noting that the layers of smectic B ordering are no longer

fluid, and it has been postulated that smectic B ordering produces a plastic crystal.[3] In addition, it has been proposed that the ordering within the layers consists of groups of molecules which are arranged into cylindrical units which are in a hexagonal close packed arrangement.[6] An illustration of smectic B ordering has not been included because its exact nature remains controversial,[3,6] largely because the molecular rotations involved make it difficult to understand the exact nature of the type ordering within the layers.

While the smectic A, B and C mesophases referred to above are the mesophases most commonly referred to in the liquid crystalline literature, it is worth mentioning that several other smectic states have been identified.[3,6] All of these, with the exception of smectic D, have the shared characteristic of aligning themselves into layers. It has been proposed that smectic D order is a cubic arrangement of spherical groupings of molecules. There is still some debate about this issue.[6]

Figure 3 depicts a third basic state of liquid crystalline order, known as cholesteric ordering. This type of ordering derived its name from cholesterol since it is frequently found in derivatives of cholesterol. It is a special case of nematic ordering, and is often referred to as the twisted nematic state which occurs when the

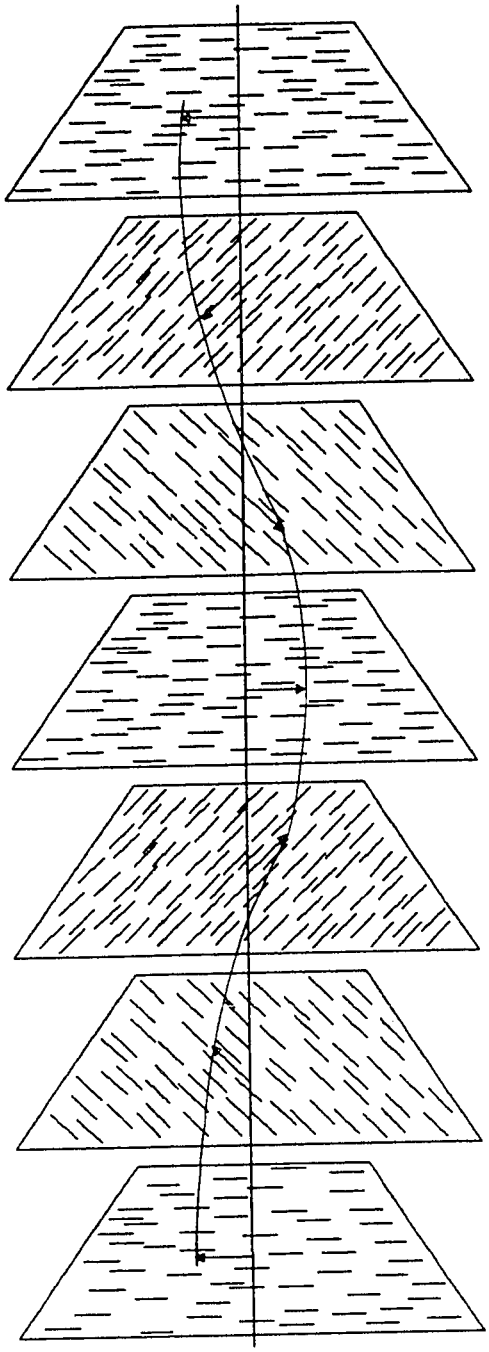

Figure 3. Cholesteric ordering.

constituent molecules are optically active. This state is different from the "regular" nematic state because it exhibits a continuous twist as one travels through the material perpendicular to the planes containing the directors. The twisting in the orientation of the directors is commonly described as forming a helix. It is important to note that the molecules themselves do not form the helix but rather it is the orientation of the molecules, as indicated by the directors, which form the helical pattern. The structure of the cholesteric helix is regular with the pitch P defined as the distance over which the directors ($\uparrow n$) make one complete turn around the axis which runs normal to the director planes. Scattered light cannot differentiate between directors which are pointing in opposite directions. The apparent spatial period L, is defined as half the pitch P.[7] When L is in the same size range as the wavelengths of visible light, there is strong Bragg scattering. If the wavelength of the scattered light is in the visible portion of the spectrum, the cholesteric substance will appear brightly colored.[3] This phenomenon is used in some types of liquid crystalline thermometers. Inside these types of thermometers, there are several similar cholesteric substances which differ only slightly from each other. Each one of the substances has a narrow range of temperature within which it is in the cholesteric state. Each substance

is placed behind a window which indicates the temperature at which it is cholesteric. When the thermometer reaches the temperature range where a particular substance is cholesteric, the brightly colored material can be seen through the window. When the substance is not at its cholesteric temperature, it appears dark in the window. Thus, the window with the bright color indicates the temperature.

2.4 Classification of Liquid Crystalline Materials

There are two major classifications of liquid crystalline materials: lyotropic and thermotropic. When a normally isotropic solvent is used to dissolve certain elongated molecules, an anisotropic solution may be produced. The resulting anisotropic molecular ordering of the solute in the solution produces what is referred to as a lyotropic liquid crystalline state. Substances that can undergo this kind of ordering in a solvent are referred to as lyotropic liquid crystalline materials. While lyotropic liquid crystalline materials require a solvent to exhibit this behavior, a solute-solute interaction is the principal interaction that produces the long range ordering. The solute-solvent interactions are only of secondary importance to the liquid crystalline structure. In other words, the liquid crystalline state achieved in lyotropic systems is a

function of the ability of the solute molecules to move relative to each other. The tobacco mosaic virus, isolated cholesterol, and the commercially important aramid fibers, such as Kevlar^{R}, are examples of solution-oriented liquid crystals.

On the other hand, thermotropic liquid crystalline materials do not require a solvent to produce a liquid crystalline state. These materials rely on changes in thermal energy to accomplish the transition from an isotropic liquid state to a liquid crystalline state. Thermotropic liquid crystals are typically organic substances which are comprised of ribbon-like or rod-like molecules. Most of the commercially available thermotropic liquid crystalline materials are copolyesters, copolyamides, or polyester-amides.(4)

2.5 Order Transformations Between Mesophases

When a liquid crystalline material is capable of exhibiting two or more of the mesophase states described earlier, it is said to be polymorphic. Both thermotropic and lyotropic liquid crystals can be polymorphic; however, they are not required to be polymorphic. In the case of lyotropic systems, the transition takes place as the amount of solute is increased in the solution. At low solute concentrations, when there are only a few molecules in solution, the

molecules are able to translate and rotate freely. This results in an isotropic solution. As the amount of solute is increased, the degree of ordering of the solute molecules also increases resulting in a lyotropic liquid crystalline solution. As the concentration of the solute is further increased, the resulting lyotropic solution can progress through the various mesophases with an associated increase in the level of order of those mesophases. As stated earlier, lyotropic liquid crystalline materials are not required to be polymorphic, and they may exhibit only one intermediate state of order as they transform from a low solute concentration, isotropic liquid, to a solute-only (no solvent) solid. In fact, all of the commercially important lyotropic liquid crystalline materials only exhibit the nematic mesophase.[5]

Some thermotropic liquid crystals also exhibit only one intermediate transformation between solid and isotropic liquid. There are many more thermotropic liquid crystals which can exhibit several different degrees of ordering as they transition from a solid to an isotropic liquid. As indicated earlier, these order transitions are driven by changes in temperature. As the temperature rises, the degree of ordering decreases until the material becomes an isotropic liquid. Since liquid crystals are often polar molecules, their ordering can be influenced by electric

fields. For example, substances which are comprised of polar molecules and have cholesteric ordering can be converted to nematic ordering with the application of an electrical field. This ability to alter the degree of ordering in a liquid crystalline material is the principal behind the current use of liquid crystals in thin screen displays.

This thesis focuses on a thermotropic liquid crystalline material; therefore, the discussion on the various transformations between ordered fluid mesophases will be based on the thermal transformations which take place as a result of changes in temperature.

Based on our knowledge of traditional phase transformations, we generally know that as the temperature of a material is increased the degree of molecular ordering within the material decreases. Using this as a guide, one can surmise that as the temperature of a thermotropic liquid crystalline material is increased, the phase transformations will progress from the most ordered mesophase to the least ordered mesophase and ultimately to an isotropic liquid. For example, in materials which exhibit both smectic A and C ordering along with nematic ordering the progression of mesophases with increasing temperature would be:

solid → smectic C → smectic A → nematic →
isotropic liquid [1]

As previously discussed, a material does not have to exhibit more than one mesophase. If a material does not possess one or more of the mesophases listed in [1], it can be deleted from the list. For example, if the material does not exhibit smectic A ordering but does have smectic C and nematic ordering the mesophase progressing with increasing temperature would be:

solid → smectic C → nematic → isotropic liquid [2]

For materials which have cholesteric and both types of smectic ordering, the progression would become:

solid → smectic C → smectic A → cholesteric → isotropic liquid [3]

If any mesophase is not exhibited by the material, it is simply deleted from the list. One case might be where only cholesteric ordering is present. This would result in the following transitions:

solid → cholesteric → isotropic liquid [4]

There are no known cases where a material will exhibit both cholesteric and nematic ordering without an externally

applied electric field.[3] As stated earlier, cholesteric ordering is a special case of nematic ordering that occurs when the molecules are optically active. Molecules are optically active when they cannot be superimposed on their mirror image; however, a racemic mixture of optically active molecules may occur. In this case there are exactly the same number of mirror image molecules as there are molecules with the original orientation within a given sample. In this situation, the resulting mixture will exhibit nematic ordering rather than cholesteric ordering.

2.6 Mesophase vs Phase Nomenclature

Up to this point, the liquid crystalline states which lie between solid and isotropic liquid phases have been referred to as "mesophases." This convention has been used despite the fact that the literature seems to use the terms mesophase and phase somewhat interchangeably, with the terminology varying between authors. Barrett, Nix and Tetelman state: "A phase is a homogeneous, physically distinct and mechanically separable portion of the material with a given chemical composition and structure."[8] Other references have also provided a similar description for the definition of a phase.[9,10] It has now been shown that the various crystalline mesophases exhibit both a specific structure in terms of the way the molecules are ordered, as

well as definite transitions which occur between one type of order and another. Furthermore, these transitional states can be thermodynamically stable, and when they are, they match the description of a phase presented above. In this context, the author believes that the term phase can be used in place of mesophase; however, there are some instances where a particular liquid crystalline state may not be thermodynamically stable or homogeneous thus precluding the use of the term phase to describe these liquid crystalline states. Since the term mesophase refers to a transitional state between solid and isotropic liquid, this report will continue to use the term interchangeably with the previously described liquid crystalline states. The preceding discussion was included to clarify some of the differences in terminology found in the literature.

2.7 The Molecular Structures of Liquid Crystalline Materials

Researchers have identified thousands of molecular structures which exhibit liquid crystalline behavior with more being identified each year. In reviewing the structures, some obvious characteristics emerge. Liquid crystalline behavior tends to occur in systems that contain molecules which have: (1) elongated and rectilinear flat segments such as aromatic rings, (2) a rigid molecular backbone, which contains many double bonds, (3) strong

dipoles along the molecular axis, or (4) weak dipolar groups at their ends.[11]

The molecular structure which is most common among liquid crystalline materials is the flat segment type in which the flat segment is produced by joining two aromatic rings directly or with a short chain linkage. Some examples of liquid crystalline materials which contain this type of structure are shown in Figure 4. No specific examples of a liquid crystalline material containing a rigid backbone and a high number of double bonds without aromatic groups could be found in the literature. It seems feasible that polymers with this kind of structure are possible in biological systems. The most common examples of structures which have strong dipoles along the molecular axis are soaps. Lyotropic solutions of soap and water are often formed. Figure 5 shows an example of a structure which contains weak dipolar side groups. This type of structure is important in biological systems.

Most of the commercial liquid crystalline polymers (LCP) are copolyesters, copolyamides or polyester-amides with aromatic molecular structures such as those shown in Figure 4, further structural discussions will be based on these configurations.

Figures 1 thru 3 depict the constituent molecules of liquid crystalline materials as straight or rigid rods. The

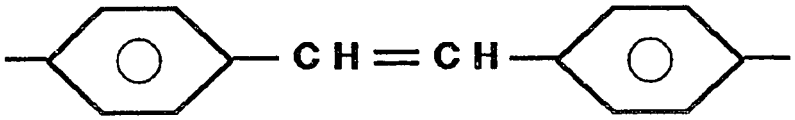

(a)

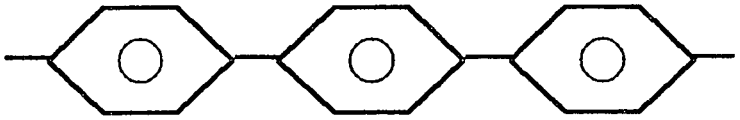

(b)

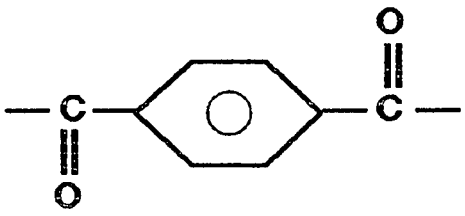

(c)

Figure 4. Flat aromatic ring structures which tend to exhibit liquid crystallinity.

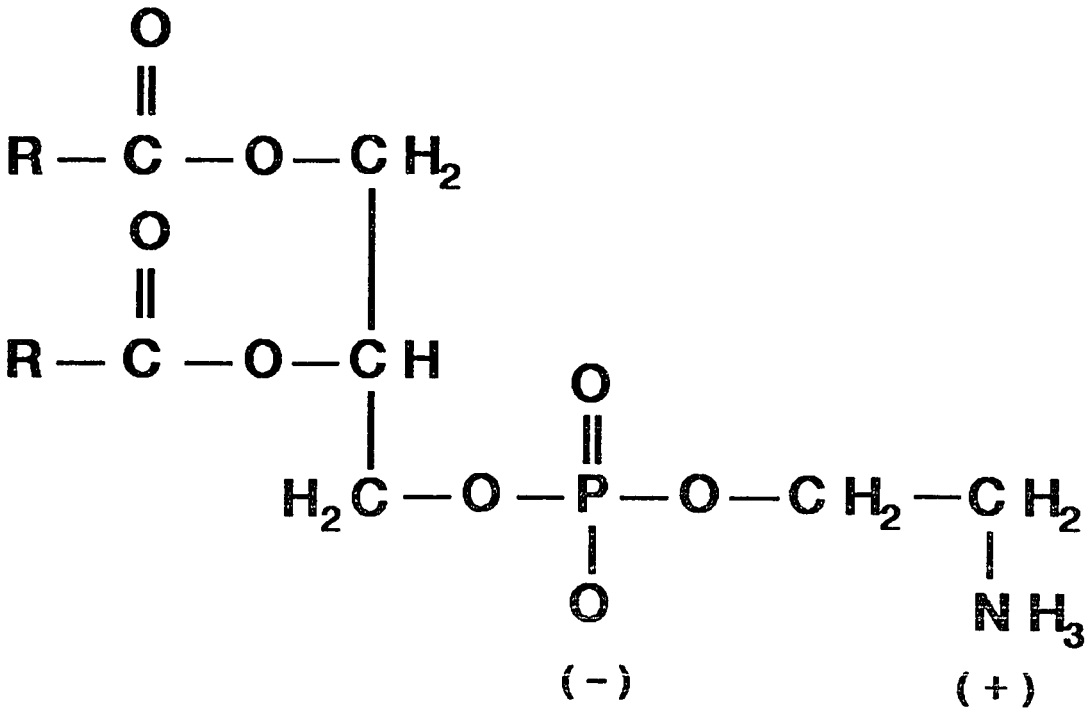

Figure 5. An example of a liquid crystalline structure with slightly dipolar side groups.

rigid rod model illustrates some very important features of these types of molecules. In accordance with the rigid rod model, liquid crystalline molecules tend to be elongated with high aspect ratios. This implies that the molecules tend to have very limited, or no branching and are fairly rigid. Other linear polymer chain molecules can exhibit the kinds of structures shown in Figure 6, where the tie molecules between the crystallites have a random coil structure and the crystallites have a folded chain structure. Molecules which exhibit liquid crystalline behavior must retain their linear configurations. Such molecules are fairly rigid, and are not free to move around and assume different shapes, with twists and kinks, in the same manner as chains of other thermoplastic polymers. While some limited movement is possible along the length of liquid crystalline molecules, the extent of such movement is much less than that allowed in typical linear chain molecules.

The rigid nature of liquid crystalline molecules is a result of the kinds of monomers which make up liquid crystalline polymers. Figure 7 shows some examples of the typical monomers which make up most of the structural LCPs. They tend to be linear and flat structures with the open bond sites oriented such that the polymerization reactions tend to build a linear chain. Furthermore, they have backbone links that are quite inflexible, and yield a

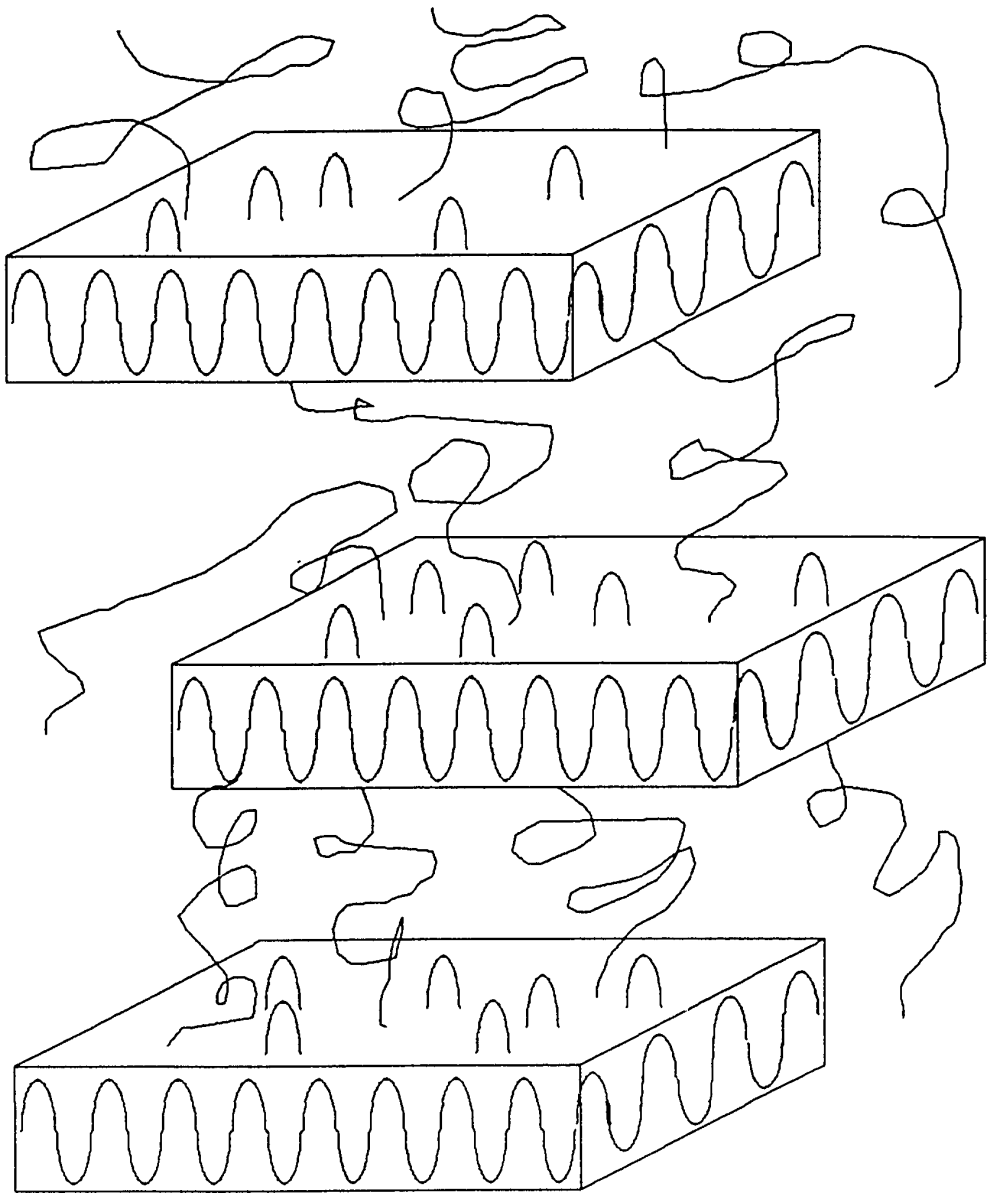

Figure 6. Tie molecules with a random coil type structure connecting folded chain crystallites.

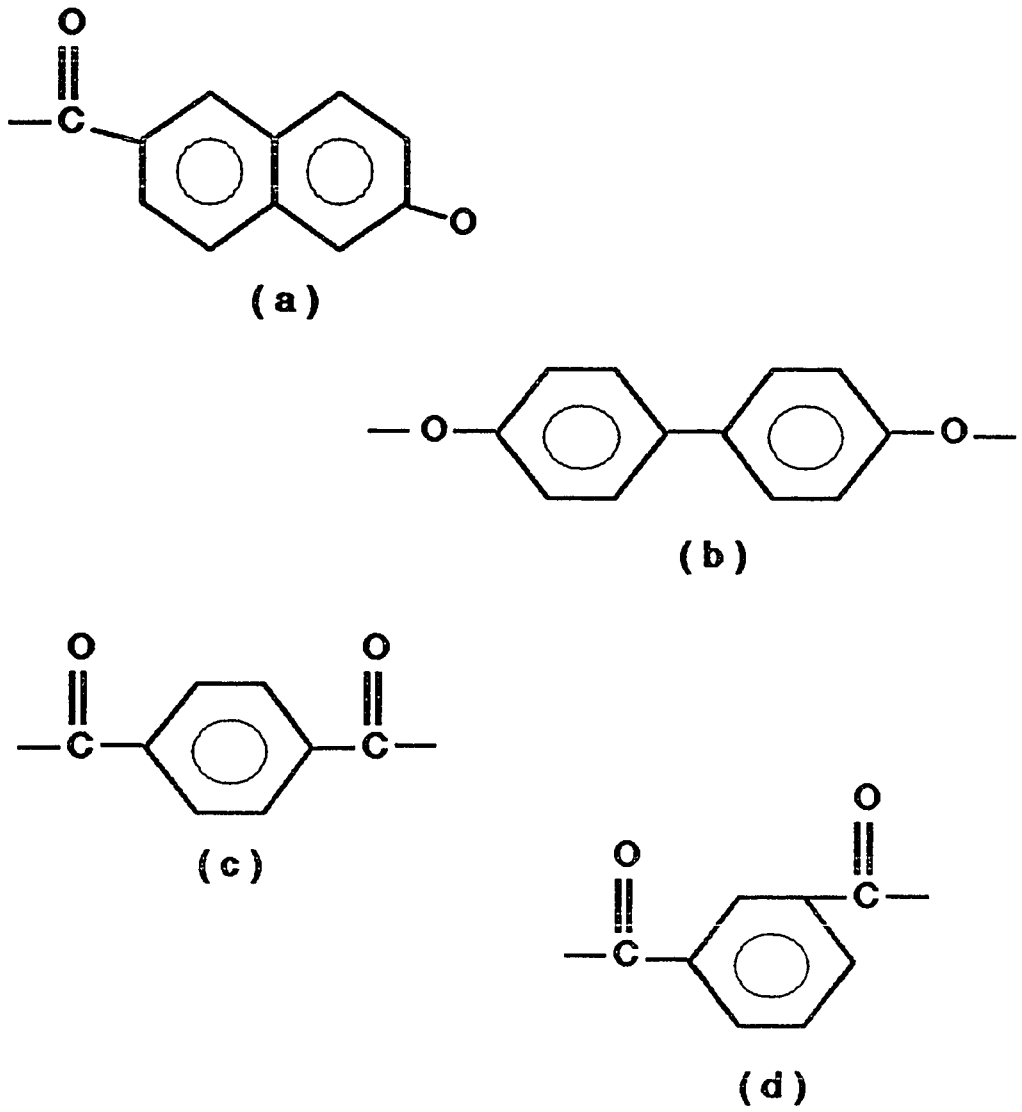

Figure 7. Flat aromatic ring structures, (a) hydroxy naptholic acid, (b) biphenol, (c) terephthalic acid, (d) isophthalic acid.

molecule that has minimal level flex or bend and does not fold or twist.

Chapter 3. XYDAR^{R} SRT-300 RESIN

XYDAR^{R} SRT-300 resin was chosen for this study because it was the matrix material that Hexcel Corporation was using for its impregnation program. The specific reasons for Hexcel's choice of this particular resin are not known; however, the author believes that it was chosen because it has the best mechanical properties in the XYDAR^{R} family and it is an unfilled resin system. The lack of a filler eliminates the possibility of filler-fiber interactions which could complicate impregnation of the carbon fibers.

3.1 The XYDAR^{R} Family of Resins

The XYDAR^{R} family of products currently marketed by Amoco consists of several resin systems which are based on three monomers: p,p-biphenol, terephthalic acid, and p-hydroxybenzoic acid. When these resins were originally marketed, by Dart Manufacturing Co., they included neat or unfilled, glass-filled, mineral-filled and a combination glass- and mineral-filled systems. While the unfilled systems deliver higher maximum mechanical properties than the filled resin systems, they are more difficult to process and they also produce a more orthotropic (#) injection molded product. The drop in properties for the filled

(#) Orthotropic is defined as the quality of having three mutually perpendicular planes of elastic symmetry.

systems is not behavior typical of thermoplastic resins, and the reasons for this nontypical behavior will be explored later in this chapter. Because of the problems described above, a market for the unfilled resins has never been fully developed, and Amoco is in the process of phasing out the unfilled resin systems. Amoco is currently marketing only glass-, mineral-, and combination glass- and mineral-filled systems. Unfilled systems are only available by special order.

At one time, there were two grades of neat resin: the SRT-300 grade and the SRT-500 grade. SRT-500 was introduced as a resin which was easier to injection mold than the original grade. SRT-500 does not decompose as quickly at processing temperatures, and it has a slightly lower melt temperature than the SRT-300 version. The difference between the two resin systems is the addition of a small amount of a proprietary substance in the SRT-500 resin.[12] A review of the patent literature,[13] indicates that the additive may be distearyl pentaerythritol diphosphite added at the rate of 0.250 parts per hundred. The temperatures for the peak endotherm reported in the patent match those reported for SRT-300 (no additive) and SRT-500 (with additive). It is not clear if the organic diphosphite mentioned above is indeed the one used due to the proprietary nature of the additive. There are several other types of phosphites listed in the

patent, and there are other patents[14,15] which describe other types of additives and/or monomer substitutions which alter the thermal and processing characteristics of the base resin.

3.1.1 Family Characteristics of XYDAR^{R} Resins

XYDAR^{R} resins have many interesting characteristics that make them stand out from other thermoplastic materials. The principal commercial advantage of these resins is their ability to retain their strength in high temperature environments. The heat deflection temperature at 1.8 MPa (264 psi)(*) for one of the XYDAR^{R} resins has been reported to be 355°C (671°F).[16] This is very high when compared to the typical <u>melt</u> temperature of 137°C (279°F) for polyethylene,[17] and 212°C (350°F) for poly(vinyl chloride),[17] which are both considered typical thermoplastic materials. The maximum heat deflection temperature is even considered high when compared to some of the high performance thermoplastics such as polyphenylene sulfide (Ryton^{TM}) which <u>melts</u> at 285°C (545°F),[18] and polyetheretherketone (PEEK) which <u>melts</u> at 343°C (650°F).[19]

(*) SI units are used in this thesis; however, most of the literature and experimental data were obtained in English units and converted to SI units. When such data appear in this thesis, the SI units will be followed by English units in parentheses.

While the heat resistance properties are very impressive, the most striking characteristic of these resins is a consequence of their liquid crystalline nature. As a nematic liquid crystalline material, the molecules of the resin tend to align themselves in the same direction. These molecules then group themselves into fiber like chains which are known as microfibrils. The smallest of these groupings is about 500 Angstroms in diameter. The smaller microfibrils subsequently group themselves into larger microfibrils which are approximately 0.5 microns in diameter. These 0.5 micron microfibrils pack together to create the largest microfibrils, which have diameters on the order of 5 microns. The largest size microfibrils then pack together in a more random fashion to form the material core.[5] It is the grouping of the microfibrils which provide the basis for the self reinforcing characteristics which are seen in XYDAR^{R} and other liquid crystalline polymers. The SEM micrograph shown in Figure 8, exhibits a fractured area in a resin pellet which was subjected to a hammer blow after being cooled to liquid nitrogen temperatures. The microfibril hierarchy can be seen as smaller microfibrils split off of larger ones. Also note that underneath the fractured layer is another group or domain of microfibrils which were not fractured. This area shows how the largest microfibrils pack together to form the material core.

Figure 8. XYDAR^{R} SRT-300 fracture surface.
This fracture surface was produced by striking a resin pellet, which was cooled to liquid nitrogen temperatures, with a hammer. The resulting fracture shows the microfibril hierarchy in the material's structure.

XYDAR^{R} resins are also considered important since they represent a group of materials which not only possess high temperature resistance, but can also be injection molded. Some earlier materials marketed under the name EKKCEL^{R} also exhibited high temperature resistance but they could not be injection molded. Parts made from EKKCEL^{R} had to be fabricated using compression molding. In comparison to injection molding, compression molding is a relatively slow and inefficient process. The number of applications for EKKCEL^{R} were limited by the requirement for compression molding. To alleviate these problems, an injection moldable version of EKKCEL^{R}, known as EKKCEL^{R} I-2000, was developed; however, this resin suffers from an irreversible transformation which occurs during initial heating.[20] EKKCEL^{R} I-2000 resin exhibits an endotherm at approximately 430°C during the first heating cycle. Cooling the material from a temperature slightly above the endotherm produces no significant transformations which would be indicative of a reversal of the transformation observed during the initial heat up. Reheating the material, in a second thermal cycle to a temperature above the initial endotherm did not produce any sign of the original transformation.[21] It can be concluded from this behavior that some kind of irreversible change takes place at 430°C during the initial heating cycle. The XYDAR^{R} resins developed from these earlier resins

can be thermally cycled to temperatures above the major endotherm temperature without any irreversible transitions occurring.

Other key properties possessed by XYDAR^{R} resins include a high degree of chemical resistance,[16,22] a high dielectric constant, dimensional stability which results in low mold shrinkage, and microwave transparency.

3.1.2 Current Uses for XYDAR^{R} Resins

The most predominant use of XYDAR^{R} resins takes advantage of the material's microwave transparency. Tupperware^{R} has been marketing a line of microwave cookware under the name Ultra 21^{R}. This cookware is marketed for its microwave characteristics and is also touted to be thermal oven safe. The high heat deflection temperature and melting point of XYDAR^{R} resins, enables the cookware to handle 285°C (550°F), the maximum cooking temperature of most home thermal ovens.

These resins are useful in high density electrical interconnects because of their low mold shrinkage behavior and low coefficient of thermal expansion. In addition, the high temperature resistance of the resins allow the interconnects to be directly soldered to wires without damaging the connectors. These resins are also being considered for use in automobile fuel systems and as tower

packing materials for the chemical processing industry because of their chemical resistance.

3.2 The Specific Structure and Properties of XYDAR^R SRT-300

In an effort to provide a background and a basis for understanding the nature of the material of this study, the general structure and properties of liquid crystalline materials were presented at the beginning of this report. The discussion was then limited to thermotropic liquid crystalline materials followed by a further reduction in scope to the XYDAR^R family of resins. The discussion is now narrowed to the specific resin studied, XYDAR^R SRT-300. The reader should now be able to relate the properties of the XYDAR^R SRT-300 resin to those of thermotropic liquid crystals in general.

3.2.1 The Chemical Structure of XYDAR^R SRT-300

As stated earlier, XYDAR^R resins are an outgrowth of earlier materials marketed under the name EKKCEL^R. As a result, XYDAR^R SRT-300 resin has a chemical formulation that is very similar to EKKCEL^R I-2000. Figure 9 shows the combined monomeric formulation for both EKKCEL^R I-2000 and XYDAR^R SRT-300. At first glance, it appears that these two materials are identical; however, a closer look shows that there are some structural differences between the two

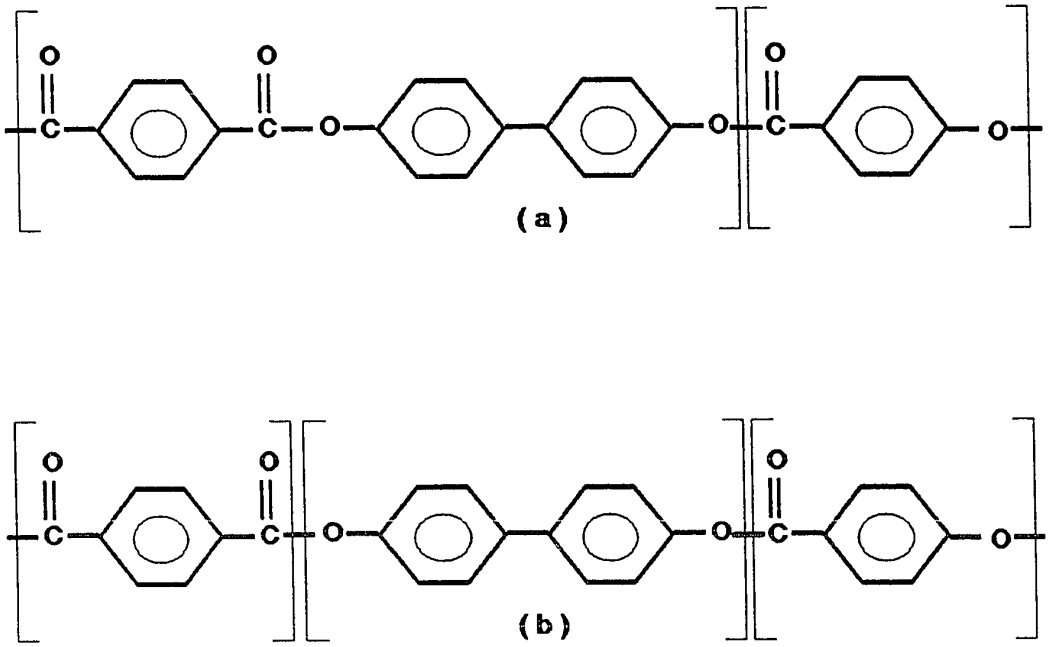

Figure 9. Formula diagrams for (a) EKKCEL^{R} I-2000, and (b) XYDAR^{R} SRT-300.

polymers. The first difference is evident in the way the monomeric units are grouped. EKKCEL^{R} I-2000 is produced by the polymerization of p-hydroxybenzoic acid (PHB) and biphenylene terphthalate (BPT) with a respective molar ratio of 2 to 1.[21] In the formulation diagram presented in Figure 9(a), the constituent monomer groupings are BPT and PHB. Even though Figure 9(b), the formulation structure for the SRT-300 resin, looks the same, it differs in that there are three monomeric units, p-hydroxybenzoic acid, terephthalic acid (TA), and p,p-biphenol (BP), from which it is synthesized. Another similarity between the two resins is the molar ratios of PHB, BP, and TA, which are 2 to 1 to 1, respectively. This results in a formulation where both polymers have the same ratio of constituent structural units. The critical difference between the two resins is in the way the structural units are organized. EKKCEL^{R} I-2000 starts out with a structure which is equivalent to a structure where the p,p-biphenol and terephthalic acid have been previously combined to produce BPT. The biphenyl groups must always be connected to a terephthalate group on at least one side. In the case of the SRT-300, the biphenyl group is free to react with TA or PHB in a random manner. The random configuration for the molecular backbone has been deduced from X-ray diffraction studies.[22,23] This is shown in Figure 10, which gives a schematic representation

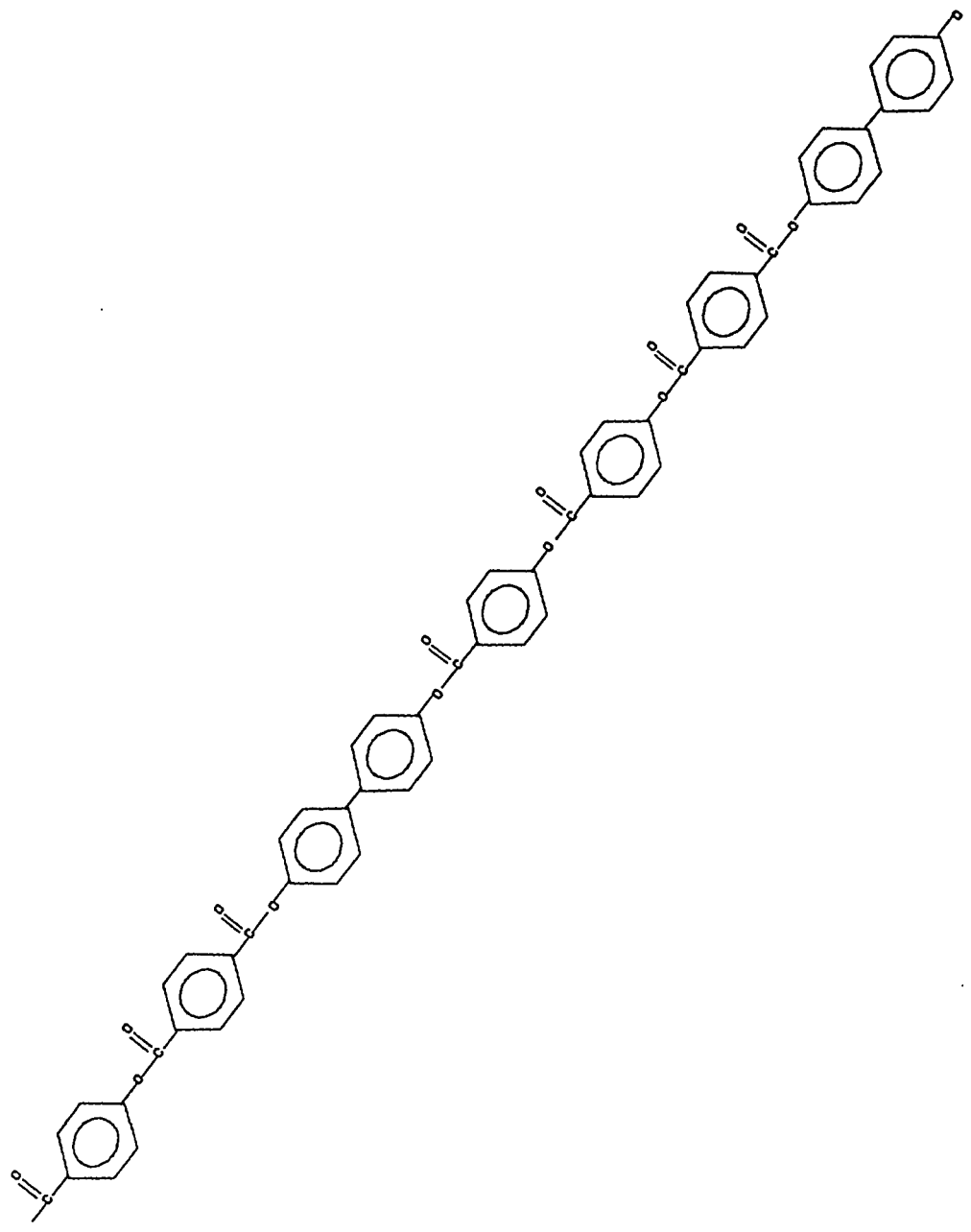

Figure 10. Actual random structure produced by the synthesis of XYDAR® SRT-300.

of the structure resulting from the copolymerization reaction that is used to produce the XYDAR^{R} SRT-300 resin. It is modeled after a similar figure presented by Blackwell et al.,[22] and is intended to show the random way in which structural units combine to form the molecular structure.

When the chemical synthesis procedure used to prepare XYDAR^{R} SRT-300 resin is examined, it is somewhat surprising to see that a random backbone develops. SRT-300 resin is produced in an acidolysis condensation reaction of an acetylated mixture of the monomers BP, TA, and PHB. An excess of acetic anhydride is used to assure that the acetylation of the phenolic hydroxyl groups occurs.[23] The result is a copolymer in which the mer units are connected through ester linkages. If a periodic block type structure is to be produced, there must be some kind of preferential bonding between reacting monomer groups. Preferential bonding occurs when the activity of one of the reacting groups is higher than the activity of other reacting groups in the mixture. In the case of XYDAR^{R} SRT-300, it seems likely that the monomers would have different reactivities since the terephthalic acid is insoluble in the mixture in the early stages of the reaction.[22] The structure of the linking sites between the monomer units in the final polymer are such that they have approximately the same surrounding structure after the reaction takes place. Each of the ester

linkages is connected to an aromatic ring on both sides of the linkage. As a result, there are no significant differences between the final reacting sites. This uniform reaction site condition is likely to exist just after the formation of oligomers; thus, the transesterification reactions between the oligomers may be the mechanism that produces the random structural sequence seen in the final polymer.(22)

The molecular weight is another important factor in the structure of the resin. It is important because the general rule states that larger molecules require more energy to initiate and sustain motion than smaller molecules. The need for more energy translates into higher thermal transformation temperatures. In the case of rigid rod liquid crystalline polymers, the molecular weight is directly related to the length of the molecule, and it has a direct effect on the transition temperatures. The number average molecular weight of the commercial version of XYDAR^{R} SRT-300 is approximately 25,000 grams per mole, and the physical properties reported in following sections are based on that molecular weight.

3.2.2 Reported Mechanical Properties for XYDAR^{R} SRT-300

The mechanical properties for this resin are difficult to report because the values obtained depend on the manner

in which the test specimens are fabricated and the thickness of each specimen.[1] This is a consequence of the degree of molecular orientation imparted to the test specimens from the molding operation. The degree of orientation accounts for the orthotropic properties of the material. A striking example of how specimen thickness effects the mechanical properties is presented by Duska.[1] Table 1 summarizes some of Duska's results pertaining to mechanical properties as a function of specimen thickness. The values presented in Table 1 show a 67 percent increase in the apparent room temperature tensile strength when the specimen thickness is reduced from 3.175 mm (0.125 in.) to 0.794 mm (0.031 in.). Duska states the reasons for this behavior are apparent when examining the internal structure of the specimens. Figure 11 shows the layered structure at the fracture surface of an injection molded XYDAR^{R} SRT-300 part. Figure 12 diagrams how injection molded parts are segregated into a symmetrical, layered structure. The layered structure consists of two main regions: the skin and the core which can both be further divided into two additional areas. Examining the cross section of a part starting at the surface, the first 0.025 mm (0.001 in) consists of the outer skin which contains molecules that are aligned parallel to the flow direction, and have a quenched appearance. Below the outer skin is the inner skin. This layer is approximately 0.18 mm

Table 1. Variations in mechanical properties as a function of test specimen thickness (after Ref. 1)

Property	Specimen thickness, mm (in) 3.175 (1/8)	1.587 (1/16)	0.794 (1/32)
Tensile Strength, MPa (psi)			
Unfilled	109.2 (15840)	152.6 (22140)	182.6 (26500)
Glass-filled	98.8 (14340)	111.2 (16130)	113.6 (16480)
Mineral-filled	79.0 (11460)	88.9 (12900)	96.5 (14000)
Tensile modulus, GPa (Msi)			
Unfilled	19.7 (2.86)	16.8 (2.43)	20.0 (2.90)
Glass-filled	15.5 (2.25)	15.3 (2.22)	18.4 (2.68)
Mineral-filled	13.2 (1.92)	13.6 (1.97)	16.5 (2.40)
Flexural strength, MPa (psi)			
Unfilled	135.7 (19680)	163.9 (23780)	203.8 (29570)
Glass-filled	135.8 (19700)	139.3 (20210)	150.6 (21840)
Mineral-filled	105.1 (15250)	117.6 (17060)	124.2 (18020)
Flexural modulus, GPa (Msi)			
Unfilled	12.5 (1.81)	13.6 (1.98)	21.4 (3.11)
Glass-filled	12.3 (1.78)	14.7 (2.13)	14.9 (2.16)
Mineral-filled	10.8 (1.57)	12.3 (1.78)	12.4 (1.80)

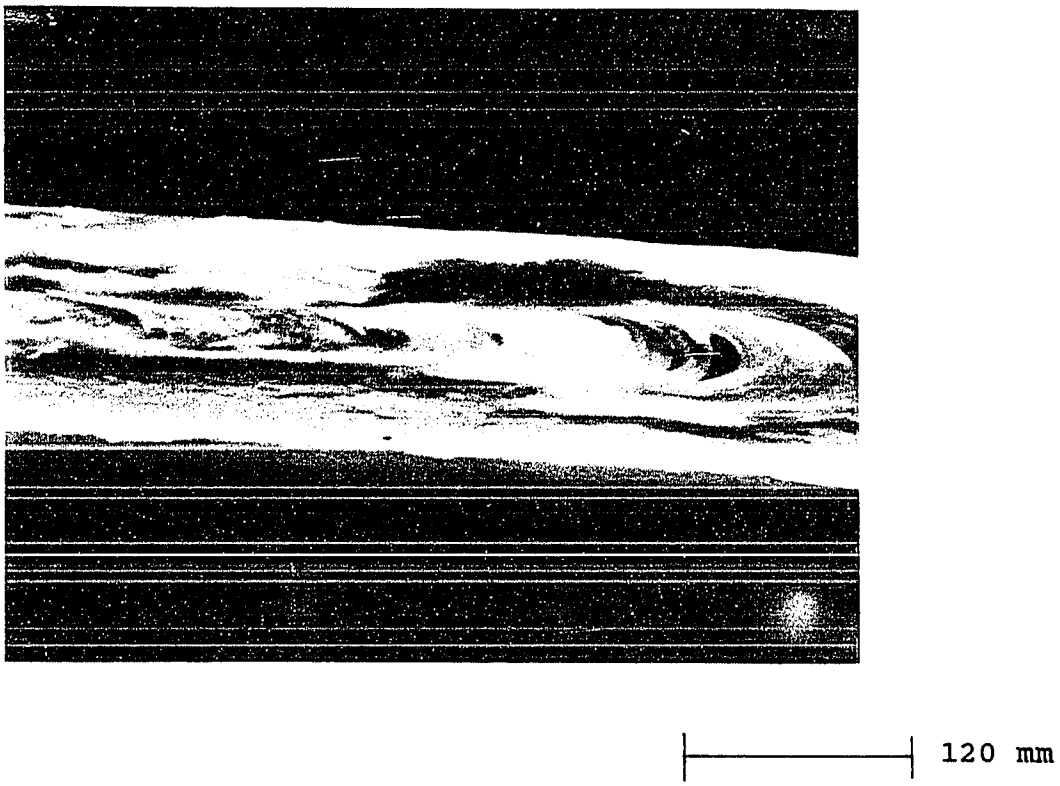

Figure 11. Photomicrograph of the fracture surface of an injection molded part, showing the layered internal structure.

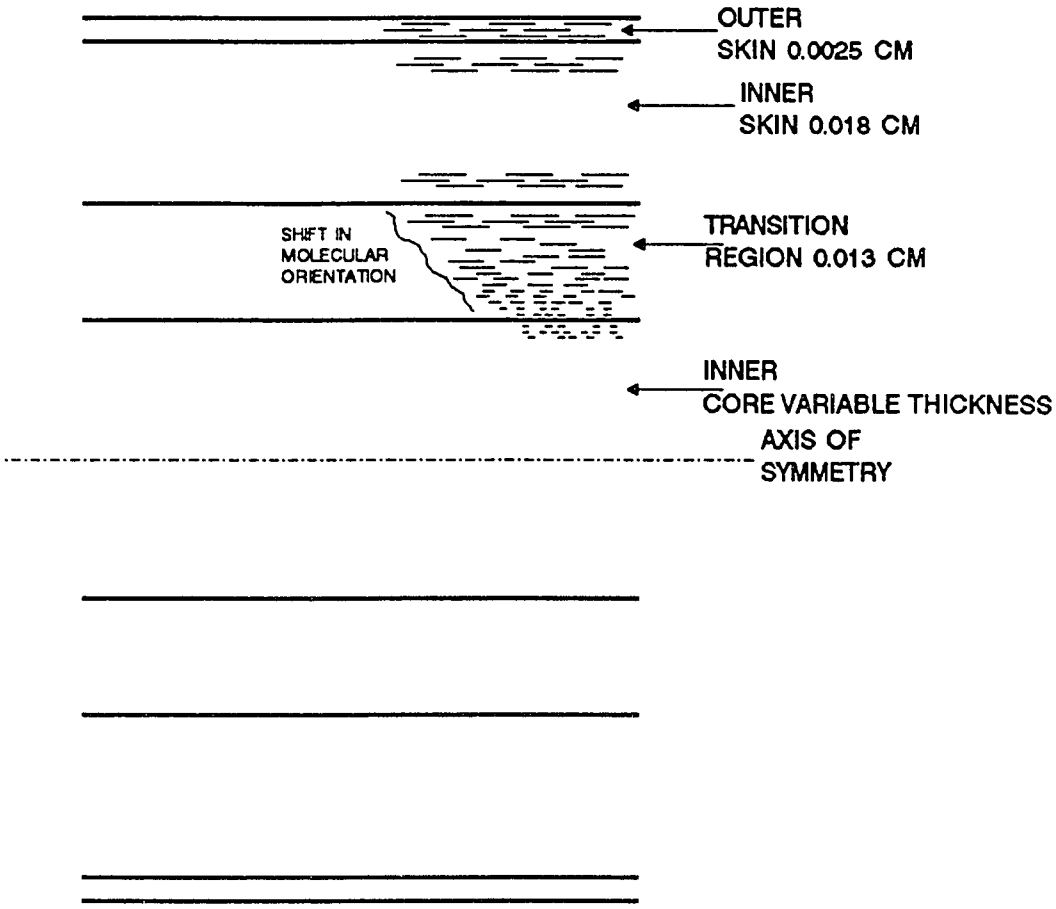

Figure 12. Diagram of the typical layered structure which occurs in XYDAR® SRT-300 injection moldings.

(.007 in) thick and has the same general molecular orientation as the outer skin with a quenched appearance.

The core region consists of the transition layer and the inner core. The transition layer is approximately 0.13 mm (0.005 in) thick, and is unique because the molecular orientation rotates 90 degrees from one side of the layer to the other. At the interface with the inner skin, the transition layer molecules are aligned parallel to the flow direction. At the interface with the inner core, the transition layer molecules are oriented perpendicular to the flow direction. The molecules in the middle of this layer are oriented to produce a continuous transition between the two extremes. As a result of the molecular rotation within the transition layer, it exhibits quasi-isotropic properties. The outer skin, inner skin, and transition region account for approximately 0.33 mm (0.013 in) of the total part thickness on each side of the inner core. The remainder of the thickness consists of the inner core. In this layer, the molecules are aligned perpendicular to the outer skin and exhibit an annealed appearance.[1] The inner core thickness depends on the thickness of the part; thus, as the part gets thinner, the percentage of the overall thickness which is inner core also drops. The skin thickness is primarily a function of molding parameters, and is not typically affected by the part thickness. Most of the axial

strength is contained in the skin region; thus, when the thickness decreases, the percentage of the overall thickness which is skin is raised and the apparent strength is increased.

The thickness effect could account for some of the variations in mechanical properties reported in other references.[16,24] Table 2 lists some of these properties by reference. The differences are not considered large but they are important because they illustrate that the material properties are sensitive to process history. The theme of process sensitivity is further reinforced by Duska[1] when he studied the effects of various processing conditions on the tensile strength of the resin. The results of his work in this field are summarized in Table 3.

Table 3 also includes Duska's results for filled versions of the resin. The filler content for the resin systems reported was 50 percent. One system was filled with glass while the other system was mineral filled. In both cases, the filled versions produce specimens with lower mechanical properties than the neat resin. To understand how these fillers affect the material properties, it is important to note that the values shown in Tables 1 through 3 are for tests run in the axial direction. The applied stresses are parallel to the molding flow direction. Since most of the axial strength is supplied by the skin

Table 2. Various Reported Mechanical Properties for the XYDAR^{R} SRT-300 resin system.

Property @ 23°C	Values From Reference 16	Reference 24
Tensile Strength		
MPa	115.8	137.9
psi	16800	20000
Tensile Modulus		
GPa	9.65	17.2
Msi	1.4	2.5
Flexural Strength		
MPa	131.0	131.0
psi	19000	19000
Flexural Modulus		
GPa	11.0	13.7
Msi	1.6	2.0

Table 3. Effects of Molding Parameters On Tensile Strength, (after Ref. 1).

Injection Pressure (MPa)	Injection Speed (cc/sec.)	Mold Temp. (°C)	Tensile Strength (MPa) Neat Resin	Glass Filled Resin	Mineral Filled Resin
93.07	34.4	149	195.7	115.4	98.6
139.95	34.4	149	182.6	109.0	91.8
93.07	77.0	149	190.7	120.4	90.3
139.95	77.0	149	171.5	114.4	95.8
93.07	34.4	260	184.3	115.8	96.3
139.95	34.4	260	155.9	108.8	93.0
93.07	77.0	260	161.3	114.7	93.8
139.95	77.0	260	161.0	109.3	91.4

regions, which are highly oriented along the specimen's axis, it is reasonable to assume that anything which would interfere with the level of orientation in the skin would reduce the maximum properties of the material. Adding fillers to the neat resin interferes with the orientation of the resin molecules, thus reducing the maximum mechanical properties. The reduction in mechanical properties is accompanied by a reduction in the molecular orientation, making the part more isotropic, which is a condition which is usually desired in injection molded parts.

3.3 Thermal Transformations Which Occur in XYDAR^{R} SRT-300

Three thermally induced transformations have been reported between room temperature and 480°C where the material begins to rapidly decompose.[23] The decomposition is a result of the breaking of the ester linkages which bind the polymer together. The first transformation has been reported to occur around 100°C, and corresponds to a solid state crystal-crystal transition. This transformation appears to be a change in the size of the pseudo unit cells which have been proposed to be orthorhombic with the "c" axis being the length of an average dimer.[23] The next transformation occurs around 427°C and is associated with the transformation from a crystalline-solid to a nematic-liquid-crystal. This is followed by the nematic-liquid-

crystal to isotropic-liquid, or the "true melt" transition which has been reported at about 472°C. All of these transitions were observed as endotherms by differential scanning calorimetry. All the transitions are reported to be reversible with the following caveats. Cooling from 450°C at 10°C per minute results in a 40°C supercooling before the nematic liquid crystal reverts to a crystalline solid. Quenching the material from the nematic state results in a structure that does not exhibit the solid state crystal-crystal transformation at 100°C. Subsequent reheating of the quenched material to a temperature below 260°C does not cause the return of the crystal-crystal transformation. In order for the 100°C crystal-crystal transformation to return, the material must be annealed at temperatures between 260°C and 350°C.[23] This behavior along with X-ray diffraction results, has prompted Field[23] to describe the quenched solid as a disordered version of the crystalline solid form which occurs at temperatures above 100°C. It appears that below 260°C the thermal energy is not sufficient to allow the quenched structure to convert to the low temperature crystalline solid form. Annealing at temperatures above 260°C causes the meta-stable quenched structure to convert to the stable ordered structure which occurs above the solid state crystal-crystal transition. Once the stable high temperature form is returned, it can

revert to the low temperature crystalline solid structure below 100°C.

Chapter 4. RESEARCH METHODS FOR ALTERING THE DEGREE OF CRYSTALLINITY

The research methodology used can be broken down into three categories: development of procedures for obtaining suitable test specimens, thermal treatment of the test specimens, and the analysis of the test specimens following thermal treatment.

4.1 Preparation of Suitable Specimens

The XYDAR^{R} SRT-300 resin used in this study was supplied in two forms: injection molded plates and resin pellets. The plates were primarily leftover material from the injection molding of tensile specimens for some of the work described in References 5 and 25.

The plates consisted mainly of rejected parts and flashings from the injection molding of tensile specimens. As mentioned in Section 3.1.1, injection molded parts have many different types of crystalline structures within a single part. Because of this, the molded plates were not considered suitable for the major portion of this study. Their primary purpose was to provide information on how actual injection molded parts might react to heat treatment relative to the specimens produced from resin pellets.

The resin pellets were obtained from Hexcel Corporation. Pellets are the resin form typically used by injection molding houses. The pellets are basically spherical in shape with an approximate diameter of 4.75 mm (0.187 in); unfortunately, in this configuration the resin does not lend itself to the types of investigation techniques used in this study.

A disk approximately 2.54 cm (1 in) in diameter would be a more appropriate configuration for study. Injection molding a specimen disk of this type was not feasible because the type of equipment that is needed to process XYDAR^{R} was not available to the author. In addition, the different crystalline structures produced within an injection molded part was a concern. In order to avoid the injection molding problems, attempts were made to pressure mold several pellets together in a laminating press. The mold consisted of a thick-walled hollow cylinder with an inside diameter of 2.54 cm (1.0 in). Pressure was applied through two floating pistons which were inserted into each end of the cylinder. The resin pellet charge was placed in the cylinder between the two pistons and the assembly was then placed into a preheated laminating press. Platen pressure was applied to the resin through the pistons which were protruding from the mold. The temperature of the mold was monitored by a thermocouple placed in hole drilled in

the mold wall. Despite several attempts using several different combinations of temperature, time, and pressure, this method failed to produce a uniform molded disk. The disks produced by this method had several problems. The primary problem was that the pellets did not fully fuse together to produce a reasonably uniform part. The pressure molding process only applied static pressure on the pellets with no provision for applying a shear force. Shearing the pellets tends to break up the crystalline domains present in the microstructure. This appears to be a requirement for welding or fusing the pellets into a uniform part. Injection molding provides this shearing action in two ways: the pellets are sheared in the barrel section of the molding equipment by the screw which pushes the resin through the barrel. A shearing action is also created by the friction between the mold and the resin as the resin flows through the cavities of the mold. The other problems with pressure molding were related to the set-up. Even though the press platens and the mold were preheated, the heating rate once the resin charge was placed in the mold was relatively slow. XYDAR^{R} SRT-300 tends to decompose in air at temperatures above 430°C. Since the pressure molding was conducted in a laminating press, the environment around the mold could not be controlled. All of these processing problems resulted in

specimens which were not welded and/or specimens which were discolored, indicating decomposition.

The lessons learned from the initial attempts at specimen preparation were: (1) in order to break up the crystalline domains, the pellets had to experience some level of plastic flow; (2) the material had to be heated to the processing temperature as quickly as possible; and (3) the exposure to air at elevated temperatures had to be minimized.

Based on these lessons, an alternate processing method was developed. Once again, a laminating press was used, but this time a mold was not used. The resin pellets were spread across the surface of the lamination press and pressed (flattened) into thin plates.

The resin pellets were dried prior to processing in a forced air oven at 150°C (300°F) for 16 hours. This was done at the manufacturer's recommendation. While XYDAR^{R} SRT-300 is not hygroscopic, an 8 hour dry time at 150°C is required to remove surface moisture.[24] The presence of water at the processing temperatures can cause decomposition of the ester linkages.[4] After drying, the pellets were placed between two pieces of KAPTON^{R} release film. The pellets were spread across the surface such that they were not in contact with each other. The KAPTON^{R} film and resin pellets were then placed between two 0.63 cm (0.25 in) stainless steel caul

plates, and this assembly was placed between the platens of a high temperature, high pressure laminating press. A clamping force of 8896 N (2000 lbf) on a 13.33 cm (5.25 in) diameter ram was applied while heating the platens from room temperature to 315°C (600°F). The heating rate was programmed at 14°C (25°F) per minute, but the actual heat up rate was approximately 9°C (16°F) per minute. The temperature was monitored with four platen controlling thermocouples. Once the average temperature of the four thermocouples reached 315°C (600°F), the temperature of the platens was allowed to stabilize for approximately three and one half minutes. After this time, the four thermocouples were within 2.8°C (5°F) of each other. The temperature controller was reset to 371°C (700°F) with a programmed rise rate of 14°C (25°F) per minute. The rise rate was limited by the equipment to 9°C (16°F) per minute. The temperature of 371°C (700°F) was chosen for the pressing operation because it represents the maximum temperature capability of the KAPTON^{R} film. KAPTON^{R} has the highest working temperature of any readily available release film. The 371°C (700°F) temperature is also below 430°C where the XYDAR^{R} SRT-300 resin begins to rapidly decompose in air. Once the average of the four thermocouples was 371°C (700°F), the load was increased to 533760 N (120,000 lbf) on a 13.33 cm (5.25 in) diameter ram. At this loading force,

the platens were completely closed and it was determined that any further load increase would be unproductive. Approximately one minute after applying the maximum load, the heat to the platens was turned off and the platens were cooled by passing compressed air through the cooling channels. This resulted in an average cooling rate of 1°C (1.8°F) per minute as the temperature dropped from 371°C (700°F) to 290°C (555°F).

The resulting specimens were between 0.13 mm (0.005 in) and 0.18 mm (0.007 in) thick. Single pellets produced plates which were between 13 mm (0.5 in) and 19 mm (0.75 in) in diameter. In some cases, the pellets were close enough to flow together, fuse and produce larger plates. In most cases, the pellets had good fusion, and even though some weld lines were still visible, the pellets appeared to be fully welded.

Table 3 shows that the properties of XYDAR^{R} SRT-300 are process dependent. This is a result of the varying degrees of orientation produced by different processing techniques. In order to study how thermal processing affects resin crystallinity, a specimen with a molecular structure as close as possible to virgin material is desired. Any residual stress or thermal history effects could cause a change in the energy required to produce a change in the crystalline structure. In order to establish the condition

of the specimens after pressing, some of the plates were examined using the DSC. The details of DSC testing are discussed in Section 4.4. One of the DSC traces for an as-pressed specimen is presented in Figure 13. It indicates that the pressing process did produce some change in the molecular condition of the material. There are three endothermic peaks in Figure 13. The first has an onset temperature of 116.0°C with the maximum occurring a 127.4°C. The literature reports that this endotherm occurs at around 100°C.[23] None of the as-pressed specimens tested in this study showed this endotherm occurring at 100°C. All the as-pressed specimens exhibited an onset temperature between 110°C and 116°C, and the peak temperature was around 125°C. The second endotherm has been reported as having a peak temperature between 421°C [16,24] and 427°C.[23] The peak temperature for this endotherm is shown in Figure 13 as occurring at 423.8°C, which is within the range reported in the literature. The size of this endotherm is also significant; Field et al.[23] report it to be around 10.5 J/g. This is somewhat lower than the 13.6 J/g shown in Figure 13. This could be an indication of residual stresses in the specimen caused by plastic flow during the pressing operation. The position and energy of the last endotherm of Figure 13 correlates very well with the literature.[23] In addition, Figure 14 shows the super cooling effect seen when

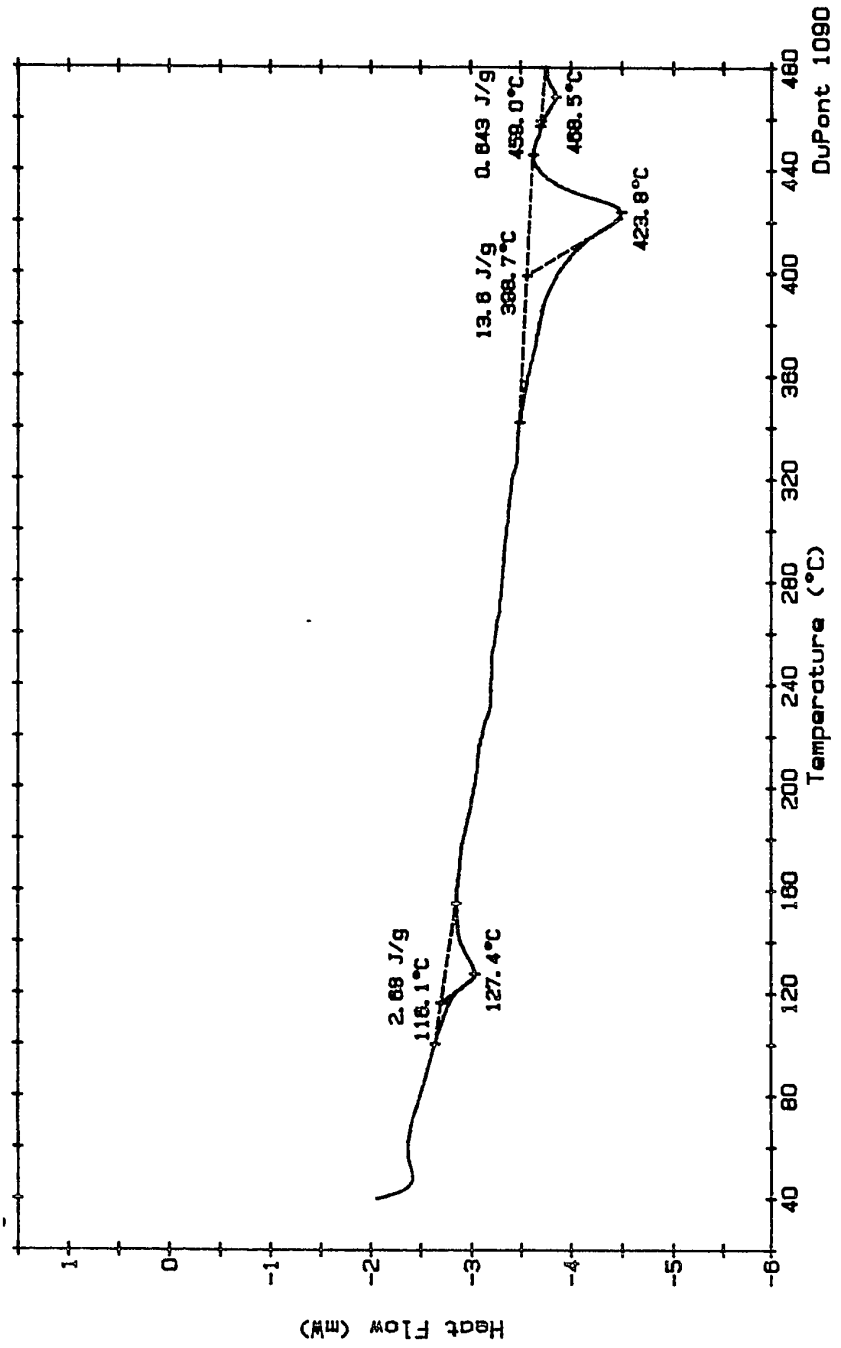

Figure 13. DSC trace of as-pressed specimens.

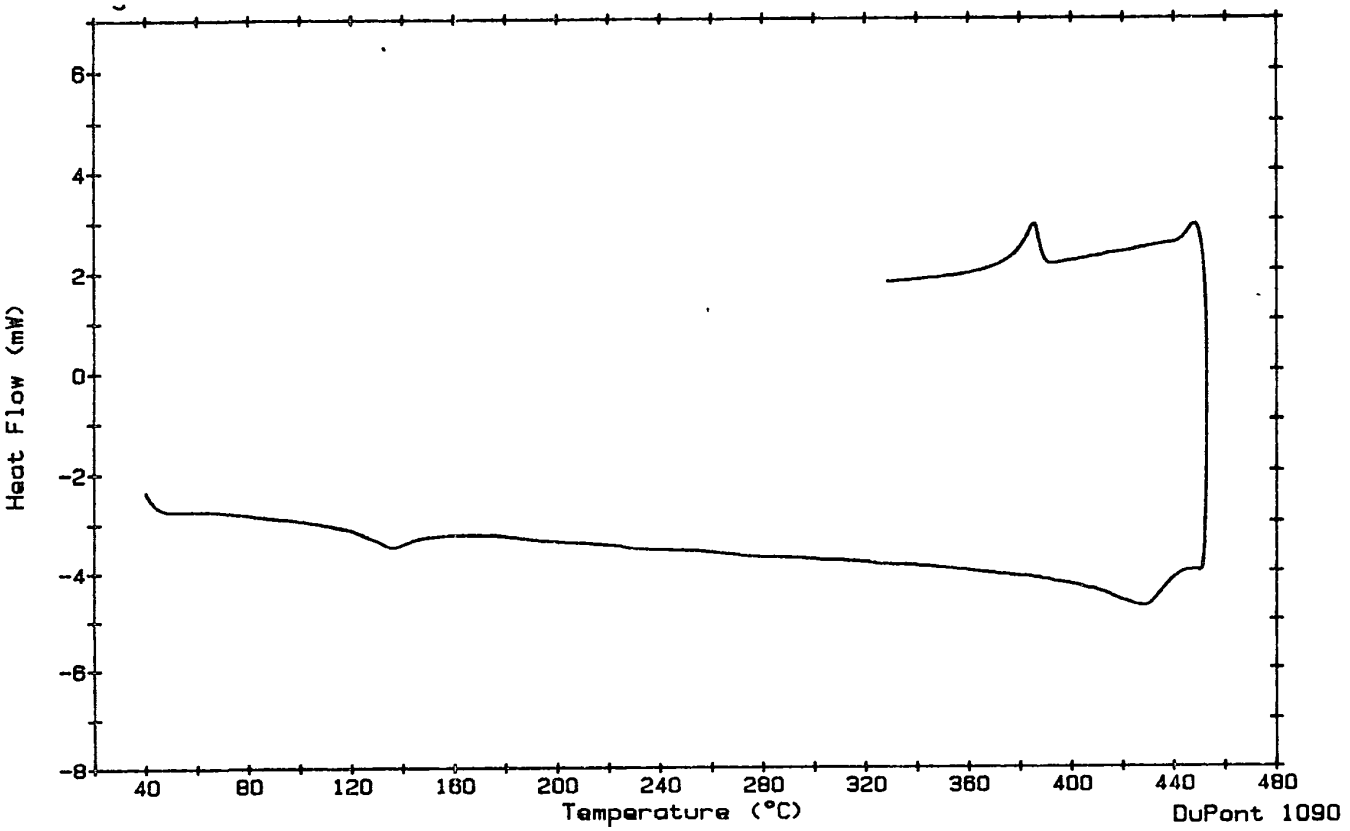

Figure 14. DSC trace of an as-pressed specimen which was allowed to cool at 10°C/minute; thus showing the recrystallization exotherm and associated supercooling.

XYDAR^{R} SRT-300 is cooled at a rate of 10°C per minute. It is very similar to the DSC traces reported.[16,23,24]

4.2 Thermal Treatment

After the condition of the pressed test specimens was established, they were ready for thermal treatment. The heat treatment was performed in two phases. The first phase was the quenching phase where the specimens were heated to temperatures between 427°C and 430°C (800°F and 807°F), and then quick quenched in liquid nitrogen. The second phase consisted of annealing the specimens in nitrogen for different times and temperatures. The times used were 1 hour and 24 hours, while the temperatures were 300°C and 360°C ± 5°C (572°F and 680°F ± 9°F).

4.2.1 Quench Treatment

The goal of the quench treatment was to minimize the amount of crystallinity in the specimens. Ideally, this would be accomplished by raising the temperature above the liquid-crystal to isotropic-liquid transition (clearing) temperature, approximately 472°C. This was not practical because the material decomposes very quickly at these temperatures, and in the time required to remove the specimens from the oven the material would have suffered irreversible damage. In addition, one of the goals of this

study was to determine if the crystallinity of injection molded parts and prepreg material could be altered. Heating to the clearing temperature would likely destroy the part or change the resin content of the prepreg. In light of this, a goal temperature of 430°C was chosen for the quench treatment as it was just above the peak temperature of the second endotherm.

4.2.1.1 Oven Set-up

The heating process was carried out in a forced air oven. Figure 15 shows a diagram of the oven set-up. The specimen chamber consisted of a Pyrex container which was 10 cm in diameter and 5 cm high for a volume of approximately 390 cm^3. The top of the Pyrex chamber was covered with a 6.35 mm (0.25 in) thick piece of aluminum plate with two holes drilled through it. One of the holes was to provide access for the nitrogen cover gas and the chamber thermocouple. The remaining hole served as a vent for the nitrogen, so that pressure would not build up and cause the cover to float off the chamber. Nitrogen gas was brought into the chamber, at a flow rate of 1.15 liters per minute, via 6.35 mm (0.25 in) diameter stainless steal tubing. The tubing was brought into the oven through an access port in the top wall of the oven. The tubing also acted as a conduit for the chamber thermocouple. Care was taken to insure that

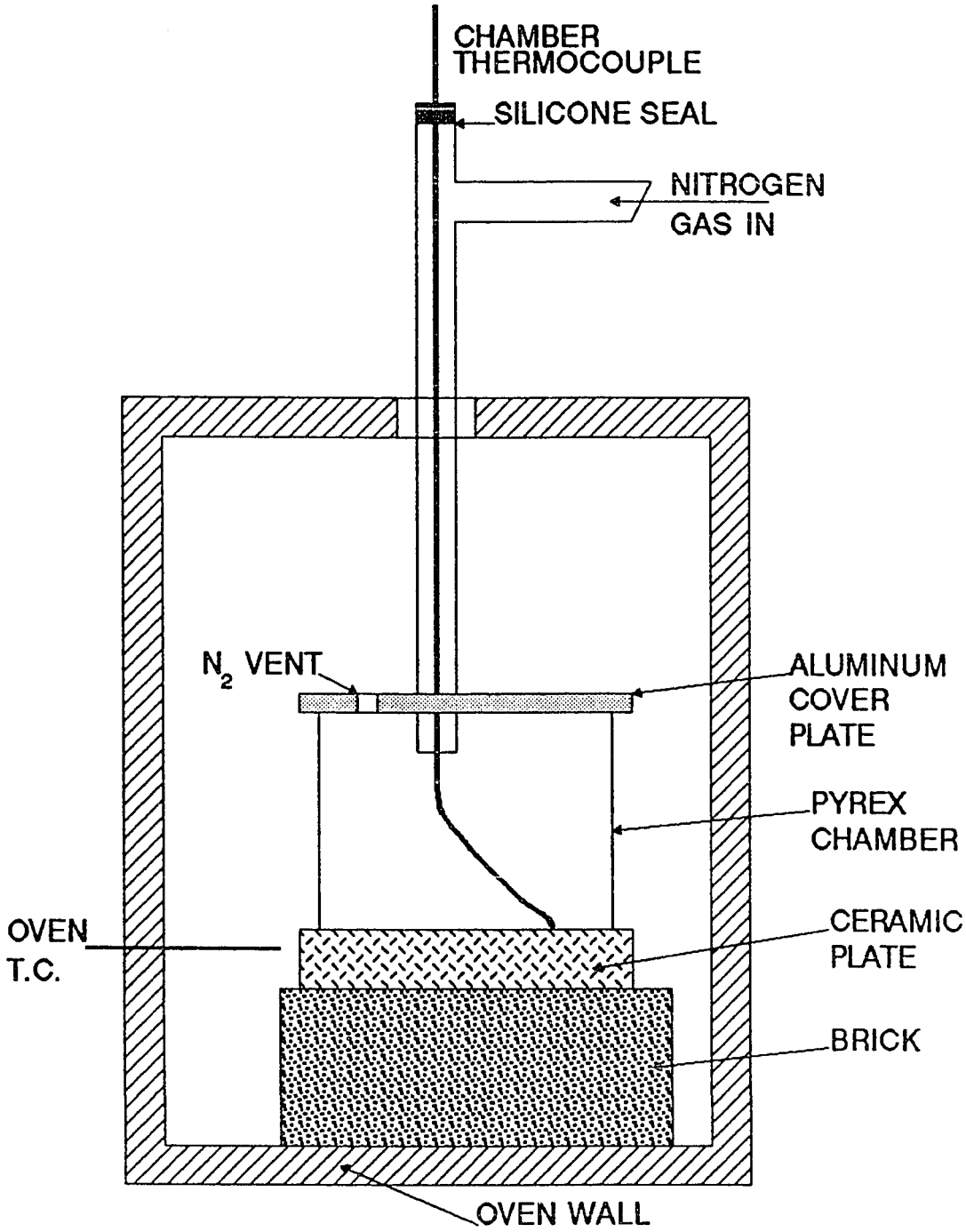

Figure 15. Diagram of the oven set-up for thermal treatment (not to scale).

the thermocouple wire was long enough to touch the bottom of the Pyrex chamber outside of the concentrated nitrogen flow area. This reduced the chance that the nitrogen would cool the thermocouple and cause an erroneous chamber temperature measurement. The area where the thermocouple entered the stainless steel tubing was sealed with silicon sealant to eliminate the aspiration of air into the nitrogen gas flow.

Since the oven was a forced air oven, it had a regular temperature fluctuation of about 9°C (16°F) as the heater controller cycled on and off. In order to monitor the oven temperature adjacent to the chamber, an additional thermocouple was placed in the oven close to the brick. This thermocouple is described in Figure 15 as the oven thermocouple. Both the oven and the chamber thermocouples were Type K and were calibrated using the ice water, boiling water technique. Using this technique, they were determined to be accurate within 0.5°C (1°F). Strictly speaking, calibration using this technique is not sufficient for the heat treating temperatures used. A calibrated thermal source should have been used to calibrate the thermocouples for the heat treating temperatures; however, a calibrated source was not available for that temperature range. The water method did show that the thermocouples were properly welded, which made it very unlikely that there would be a significant error in the temperature data.

The purpose of the brick was to act as a thermal dampening devise which reduced the temperature fluctuations experienced by the Pyrex chamber, and subsequently the resin specimen.

4.2.1.2 Quench Treatment Procedure

The oven containing the brick was preheated and allowed to soak for 2 hours at 461°C ± 4°C (862°F ± 8°F). During heat up and soak, the oven temperature was monitored by the oven thermocouple. Prior to any processing, the XYDAR^{R} SRT-300 specimens were dried at 150°C for a minimum of eight hours. After drying, the specimens were placed in the Pyrex chamber, with an aluminum cover plate on the top, and a ceramic plate on the bottom. The Pyrex chamber, aluminum cover plate and ceramic plate were not preheated. This was done to give the chamber time to be purged with nitrogen before the temperature of the chamber exceeded 400°C. The assembly consisting of the aluminum plate, the Pyrex chamber containing the specimens, and the ceramic plate was placed in the preheated oven. The stainless steel nitrogen purge line and chamber thermocouple were inserted into the chamber through the hole in the aluminum cover plate as quickly as possible. The oven door was closed and the temperature of the chamber was monitored using the chamber thermocouple until the chamber bottom reached the desired temperature

Table 4. Maximum temperatures and exposure times for the quenching treatment.

Run Number	Specimen Type	Maximum Temperature	Time To Temperature
1	Pressed pellets	430°C (807°F)	510 sec.
2	Pressed pellets	430°C (807°F)	540 sec.
3	Molded Plates	434°C (813°F)	510 sec.

range. Table 4 lists the maximum temperature obtained and the time required to reach maximum temperature. Once the maximum temperature was reached, the chamber was quickly removed from the oven and the specimens were dumped into a dewar containing liquid nitrogen. After five minutes, the specimens were removed from the liquid nitrogen and returned to the 150°C oven for drying.

4.2.2 Annealing

After the quenching operation, the specimens were annealed. Because of the limited number of specimens available, the number of times and temperatures studied was limited to two each. The upper annealing temperature of 360°C was chosen because annealing XYDAR^{R} SRT-300 at or near this temperature had been reported in the literature.[22,23] Because this temperature had been used in other studies it was felt that the chances of degrading the resin at this temperature would be minimal. The lower anneal temperature of 300°C was chosen because it had not been reported in the literature and was above the minimum reported annealing temperature of 260°C.[23] The annealing time reported in the literature for the 360°C anneal is one hour. The 24 hour anneal time was used at the suggestion of J.J. Rusek.[26] He has used this extended annealing time in his work on "physicochemical annealing" of liquid crystals.[5]

4.2.2.1 Annealing Treatment Procedure

The equipment used for the annealing treatment was the same as that used for the quench treatment. The nitrogen flow rate remained at 1.15 liters/min. The procedure was slightly modified because the lower temperatures reduced the concerns of specimen decomposition. For the annealing cycles, the ceramic plate and Pyrex chamber were preheated with the brick. This was done to reduce the amount of time required to bring the resin specimens into thermal equilibrium with the oven. The aluminum cover plate was not preheated in an attempt to promote safety by reducing the chance of burns occurring during the installation of the nitrogen gas line and chamber thermocouple.

As with the quench cycles the oven temperature was monitored during heat up and thermal soak using the oven thermocouple. For the 360°C anneal cycles, the oven was preheated to 359 ± 3°C (679 ± 5°F), and for the 300°C anneal cycles the preheat temperature was 297 ± 3.3°C (567 ± 6°F). Once the desired preheat temperature was obtained, the oven and its contents were allowed to thermally soak for a minimum of two hours.

Before being placed in the Pyrex chamber, the resin specimens were dried at 150°C for a minimum of eight hours. Once the specimens were in the Pyrex chamber the cover plate was quickly placed on top of the chamber and the nitrogen

gas line inserted. At this point monitoring of the specimen temperature was done with the chamber thermocouple. Extremely tight temperature control is not possible in an industrial oven so a temperature tolerance of ± 2.8°C (± 5°F) was established. This tolerance was based on the control characteristics of the oven. It is tighter than the air temperature cycles monitored by the oven thermocouple since it was obtained by using the dampening effects of the brick which was allowed to thermally soak in the preheated oven. After the oven door was closed, the time required for the chamber thermocouple to reach the bottom of the annealing temperature tolerance band was determined. Once the temperature of the chamber thermocouple was within the tolerance band, the annealing time was initiated. When the total time for the anneal cycle was reached, the oven's heating elements were turned off and the specimens were allowed to cool in the Pyrex chamber with the oven fan running. The cooling rate was monitored for the first ten minutes to assure that it was below 10°C per minute. The maximum cooling rate observed for all of the anneal cycles, occurred between the first and second minute after the heat was turned off. This rate varied from 6.6°C (12°F) per minute to 5.6°C (10°F) per minute. The specimens were allowed to cool in the chamber under nitrogen purge until the temperature was below 150°C (300°F). At this point the

specimens were removed from the heat treating oven and allowed to cool to room temperature in an aluminum weighing pan. Since the specimens were so thin, it took less than a minute for them to cool to room temperature. The specimens were then placed in a plastic container until the x-ray diffraction studies could be performed.

4.3 X-ray Diffraction

The X-ray diffraction work was performed on a hybrid system which consisted of a power supply and tube control system produced by General Electric. The goniometer stage and associated hardware were also made by General Electric. The detector, detector control system, and goniometer position controls were manufactured by DIANO Corporation. The DIANO system was connected to a printer so that the set-up conditions, angle 2-theta, and associated intensity could be printed directly as the system's output.

The X-rays were produced by a copper tube with an operating current of 20 mA and an accelerating voltage of 40 KV. A nickel filter was used to limit the X-rays to Cu K_α having a wavelength of 1.54 Angstroms.

The alignment of the goniometer was checked using a quartz standard which has the (100) diffraction peak occurring at a 2-theta angle of 26.61° when using Cu K_α radiation. A step scan between 26.58° and 26.70° with 0.01°

steps and a two second count time was used to determine the peak diffraction angle in this region. The scan showed the peak angle to be at 26.66°, which results in an apparent error of 0.05°. The alignment error was not considered significant and was ignored, because the heat treated specimens were not perfectly flat and the X-ray diffraction studies were not being used to determine lattice spacings.

X-ray diffraction studies were performed on three pressed specimens and one injection molded specimen for each heat treatment condition. The one exception was the 1 hour at 360°C condition that did not have an injection molded specimen. Each of the specimens was scanned in the step scan mode with 2-theta ranging from 13° to 60°, using a step size of 0.2°, and a scan time of one second per step. The range of 2-theta angles used for this study was patterned after Reference 23, which used scan angles between 10° and 60°. The area between 10° and 13° was scanned in some of the initial set-up test runs and there was no significant change in the intensity observed in this three degree region. A review of the reference also showed no significant changes in intensity between these two angles and it was determined that the actual analysis scans would start at 13°. Upon completion of the scans, the intensity data were reviewed and it was determined for the purpose of this investigation that there were no significant peaks beyond 40°. This turned

out to be a surprise because the literature indicates that there is a very large peak around 42°.[23,24] None of the specimens tested showed any sign of this peak.

Since the data showed that the diffraction intensity was basically flat beyond 40°, the data beyond 41.6° were not plotted and did not receive any further attention. The remaining diffraction data were plotted with the aid of a commercial PC based spreadsheet program, Quattro Pro^{R}. The X-ray equipment used did not have any electronic data storage or transfer capabilities so the angle and associated intensity data were manually transferred from the diffractometer printout into the Quattro Pro^{R} spreadsheet. The data were then converted by the program into a graphical representation which is similar to the traditional diffraction plots obtained from X-ray diffraction equipment. In addition, the data were numerically integrated to determine the area under the intensity curve and the area under an estimated amorphous intensity curve. The purpose of this activity was to estimate the relative degree of crystallinity between the various specimens. This information was used as an indication of the differences between the various specimens; thus, several simplifying assumptions were made in determining the area under the curves.

Because there were no reference specimens with known degrees of crystallinity available, the shape of the amorphous curve was estimated. The method used to estimate the shape of the completely amorphous diffraction curve was the primary simplification in the relative crystallinity estimates. The shape of the amorphous diffraction curve was derived from the diffraction curve for specimen 14 which was a quenched specimen. The X-ray diffraction curve for specimen 14 was chosen because it appeared to be more amorphous than the other quenched specimen, specimen 2. Specimen 8, also a quenched specimen was not included in the estimation for reasons which will be described in the next chapter. Even though specimen 14 had been quenched it still retained some crystalline structure. This is evidenced in Figure 16 by the double peaks which appear between 2-theta angles of 18° and 24°. As a result, some estimation of the contribution of peak overlap to the intensity in this region was required. To do this, the curve was plotted and a line was drawn from the tangent of where the intensity starts to rise for the first peak to half the intensity of the minimum between the two peaks. In a similar fashion, a line is also drawn from half the intensity of the minimum between the two peaks and the tangent of where the intensity returns to background levels at the trailing edge of the second peak. Using the half intensity at the curve minimum was strictly

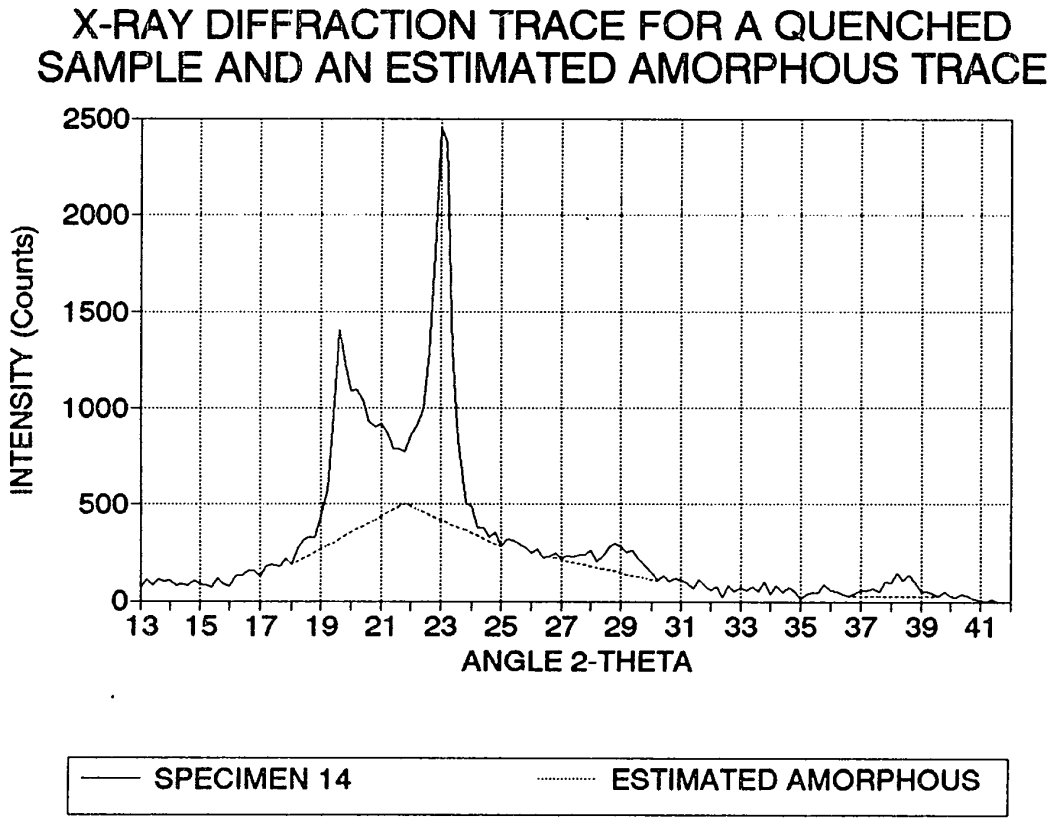

Figure 16. X-ray diffraction curve for Specimen 14 which is in the experimental quenched condition, along with the estimated fully amorphous curve.

an eyeball estimate; however, it did have the advantage of producing an amorphous peak which had an intensity roughly twice that of the surrounding intensities, and it was below the between-peak minimum obtained on the specimen which qualitatively appeared to be the most crystalline.

This is a major simplification because it does not fully take into account the amount of intensity contributed by the overlap of the two crystalline peaks in the quenched specimen. It also results in estimating the shape of the amorphous peak as two straight lines. This is not the case as the amorphous trace should produce a smooth curve throughout this region. Assuming that the area is defined by straight line underestimates the area under the amorphous curve. This may or may not be counteracted by the peak overlap estimate.

The second major simplification occurs in the method used to calculate the area under the diffraction curves. The area under the diffraction curves was estimated by assuming that the curves were composed of a series of rectangles. Each rectangle was 0.2° wide with a length equal to the X-ray intensity at the corresponding angle 2-theta. Depending on the rate of change of intensity in a particular region the rectangle method will over or under estimate the area of the curve. The area determination for all the curves had the same type of errors. The technique was sufficient

because it was used to determine relative and not absolute crystallinity. Other simplifications included; ignoring the possible effects of specimen thickness, loss characteristics of the detectors, and the loss characteristics of the diffraction set-up as a whole.

4.4 Differential Scanning Calorimetry Analysis

Differential scanning calorimetry (DSC) was performed using a DuPont 1090B Thermal Analysis Controller connected to a DuPont 910 DSC test cell. DSC analysis was performed on each of the pressed pellet specimens which had been X-rayed. Due to the possibility of varying types of structure, DSC analysis was not performed on the injection molded plates. Prior to analysis the specimens were again dried at 150°C (300°F) for a minimum of eight hours. The specimens used for the DSC analysis were cut from heat treated specimens using a #3 cork bore. The #3 cork bore was chosen because the resulting specimen disks are the same diameter as the DSC sample pan.

Once the DSC specimens were cut they were weighed and placed in the sample pan. Five holes were punched into the pan lid using a dental pick to allow the escape of any decomposition gasses that could distort the sample pan. Distortion of the sample pan can result in a change in the

amount of pan surface in contact with the DSC sample cell, which is a condition that can lead to erroneous data.

In all cases, the reference cell contained an empty sample pan with a lid. The nitrogen flow rate was approximately 90 ml per minute. The pretest purge time was a minimum of five minutes and the heating rate was 20°C per minute.

Prior to the start of the test series, a calibration run was performed using the calibration software that comes with the system. Two calibration runs were performed. The first calibration run was to determine the cell constant for the system using aluminum sample pans and a heating rate of 20°/min. This calibration run used indium as the calibration specimen and produced a cell constant of 1.048. Since indium melts at 156.6°C, a temperature well below the temperatures required in this study, it was not suitable for thermocouple calibration. The thermocouple calibration run used zinc as the calibration specimen. Zinc and aluminum form a low temperature eutectic so the aluminum sample pans were replaced by copper sample pans for this calibration run. Because the aluminum and copper sample pans have different thermal characteristics, the zinc calibration run could not be used to determine the cell constant for the XYDAR^{R} specimens. Zinc has a melting temperature of 419.58°C. At a heating rate of 20°C per minute, the calibration run showed

that the onset temperature for the melting peak of the zinc calibration specimen was 420.5°C. This indicates a thermocouple error of about 0.9°C. At 420°C, this represents about a 0.2 percent error, which is considered very good for thermocouple systems. This temperature error is small relative to the variations in peak temperatures observed between similar XYDAR^{R} specimens; therefore, a temperature correction factor was not incorporated into any of the figures or tables which illustrate the DSC runs.

Chapter 5. EXPERIMENTAL RESULTS AND DISCUSSION

5.1 Specific Differential Scanning Calorimetry Results

Tables 5 through 10 summarize the results of the DSC traces shown in Figures 17 through 34. The tables provide a summary of the onset temperature, peak temperature and specific energy for each endotherm seen in the DSC traces. Each table has been compiled individually so that specimens that have received the same thermal treatment are grouped together. The as-pressed specimens are grouped together, the quenched specimens are grouped together, the specimens which were annealed at 300°C for 1 hour are grouped together, and so on.

5.1.1 As-pressed Specimens

The DSC traces for the as-pressed specimens that were X-rayed appear in Figures 17, 18, and 19. They consist of specimens 1, 7, and 13, respectively. As expected, the as-pressed specimens exhibit three endotherms. For the three specimens tested, the first endotherm has an onset temperature which ranged between 108.1°C and 115.5°C, a peak temperature which ranged from 123.8°C to 131.8°C and a specific energy which ranged from 2.32 J/g to 3.97 J/g. These values match the previous traces presented in Figures 13 and 14 very closely, and like those traces, the initial

Table 5. Summary of the DSC Results for the As-pressed Condition

Specimen Condition: As-pressed

Crystalline-Solid to Crystalline-Solid Transition

Specimen	Onset Temp. (°C)	Peak Temp. (°C)	Endotherm Energy (J/g)
Run 1	110.4	123.8	2.32
Run 7	108.1	124.6	2.56
Run 13	115.5	131.8	3.97

Crystalline-Solid to Liquid-Crystal Transition

Specimen	Onset Temp. (°C)	Peak Temp. (°C)	Endotherm Energy (J/g)
Run 1	394.9	425.4	13.1
Run 7	411.7	428.7	11.7
Run 13	405.8	426.9	12.7

Liquid-Crystal to Isotropic-Liquid Transition

Specimen	Onset Temp. (°C)	Peak Temp. (°C)	Endotherm Energy (J/g)
Run 1	459.8	468.8	0.542
Run 7	461.5	469.3	0.615
Run 13	458.3	466.1	0.609

Table 6. Summary of the DSC Results for the Quenched Condition

Specimen Condition: Quenched

Crystalline-Solid to Crystalline-Solid Transition

Specimen	Onset Temp. (°C)	Peak Temp. (°C)	Endotherm Energy (J/g)
Run 2	112.8	142.9	0.684
Run 8	Did not produce an endotherm for this transition		
Run 14	Did not produce an endotherm for this transition		

Crystalline-Solid to Liquid-Crystal Transition

Specimen	Onset Temp. (°C)	Peak Temp. (°C)	Endotherm Energy (J/g)
Run 2	423.4	433.1	9.16
Run 8	379.1	417.6	8.33
Run 14	428.9	438.1	7.64

Liquid-Crystal to Isotropic-Liquid Transition

Specimen	Onset Temp. (°C)	Peak Temp. (°C)	Endotherm Energy (J/g)
Run 2	465.4	471.2	0.460
Run 8	457.9	464.9	0.792
Run 14	461.8	469.7	0.689

Table 7. Summary of the DSC Results for Specimens Annealed at 300°C for 1 Hour

Specimen Condition: Annealed 300°C for 1 hour

Crystalline-Solid to Crystalline-Solid Transition

Specimen	Onset Temp. (°C)	Peak Temp. (°C)	Endotherm Energy (J/g)
Run 6	106.2	117.2	0.836
Run 12	Did not produce an endotherm for this transition		
Run 18	Did not produce an endotherm for this transition		

Crystalline-Solid to Liquid-Crystal Transition

Specimen	Peak doublet, total Endotherm Energy across both peaks (J/g)
Run 6	6.91
Run 12	7.57
Run 18	8.10

Specimen	First Peak Peak Temperature (°C)	Second Peak Peak Temperature (°C)
Run 6	411.2	442.9
Run 12	417.0	442.0
Run 18	418.1	No Peak

Liquid-Crystal to Isotropic-Liquid Transition

Specimen	Onset Temp. (°C)	Peak Temp. (°C)	Endotherm Energy (J/g)
Run 6	466.3	472.2	0.396
Run 12	466.6	471.5	0.445
Run 18	459.7	469.9	0.856

Table 8. Summary of the DSC Results for Specimens Annealed at 300°C for 24 Hours.

Specimen Condition: Annealed at 300°C for 24 hours

Crystalline-Solid to Crystalline-Solid Transition

Specimen	Onset Temp. (°C)	Peak Temp. (°C)	Endotherm Energy (J/g)
Run 5	107.2	118.5	1.43
Run 11	106.9	123.0	1.25
Run 17	105.0	123.4	0.938

Crystalline-Solid to Liquid-Crystal Transition

Specimen	Peak doublet, total Endotherm Energy across both peaks (J/g)
Run 5	11.4
Run 11	11.2
Run 17	9.29

Specimen	First Peak Peak Temperature (°C)	Second Peak Peak Temperature (°C)
Run 5	409.2	437.7
Run 11	413.3	442.3
Run 17	420.6	446.8

Liquid-Crystal to Isotropic-Liquid Transition

Specimen	Onset Temp. (°C)	Peak Temp. (°C)	Endotherm Energy (J/g)
Run 5	464.5	472.2	0.513
Run 11	465.8	471.0	0.440
Run 17	466.4	473.3	0.456

Table 9. Summary of the DSC Results for Specimens Annealed at 360°C for 1 Hour

Specimen Condition: Annealed at 360°C for 1 hour

Crystalline-Solid to Crystalline-Solid Transition

Specimen	Onset Temp. (°C)	Peak Temp. (°C)	Endotherm Energy (J/g)
Run 3	101.0	122.0	1.54
Run 9	106.2	122.8	1.60
Run 15	109.8	125.0	3.72

Crystalline-Solid to Liquid-Crystal Transition

Specimen	Peak doublet, total Endotherm Energy across both peaks (J/g)
Run 3	11.2
Run 9	11.3
Run 15	11.6

Specimen	First Peak Peak Temperature (°C)	Second Peak Peak Temperature (°C)
Run 3	No Peak	443.0
Run 9	430.2	444.0
Run 15	412.8	442.7

Liquid-Crystal to Isotropic-Liquid Transition

Specimen	Onset Temp. (°C)	Peak Temp. (°C)	Endotherm Energy (J/g)
Run 3	470.5	474.5	0.186
Run 9	470.2	475.6	0.255
Run 15	465.9	471.7	0.500

Table 10. Summary of the DSC Results for Specimens Annealed at 360°C for 24 Hours

Specimen Condition: Annealed at 360°C for 24 hours

Crystalline-Solid to Crystalline-Solid Transition

Specimen	Onset Temp. (°C)	Peak Temp. (°C)	Endotherm Energy (J/g)
Run 4	100.3	122.4	1.96
Run 10	106.0	124.3	0.805
Run 16	104.3	121.9	1.12

Crystalline-Solid to Liquid-Crystal Transition

Specimen	Onset Temp. (°C)	Peak Temp. (°C)	Endotherm Energy (J/g)
Run 4	437.2	450.9	11.6
Run 10	439.0	446.7	11.4
Run 16	438.4	447.0	12.1

Liquid-Crystal to Isotropic-Liquid Transition

Specimen	Onset Temp. (°C)	Peak Temp. (°C)	Endotherm Energy (J/g)
Run 4	472.6	476.2	-- (**)
Run 10	467.7	474.7	0.581
Run 16	467.7	474.3	0.348

(**) The energy of the transition was not determined because the transition was not complete at the end of the DSC run

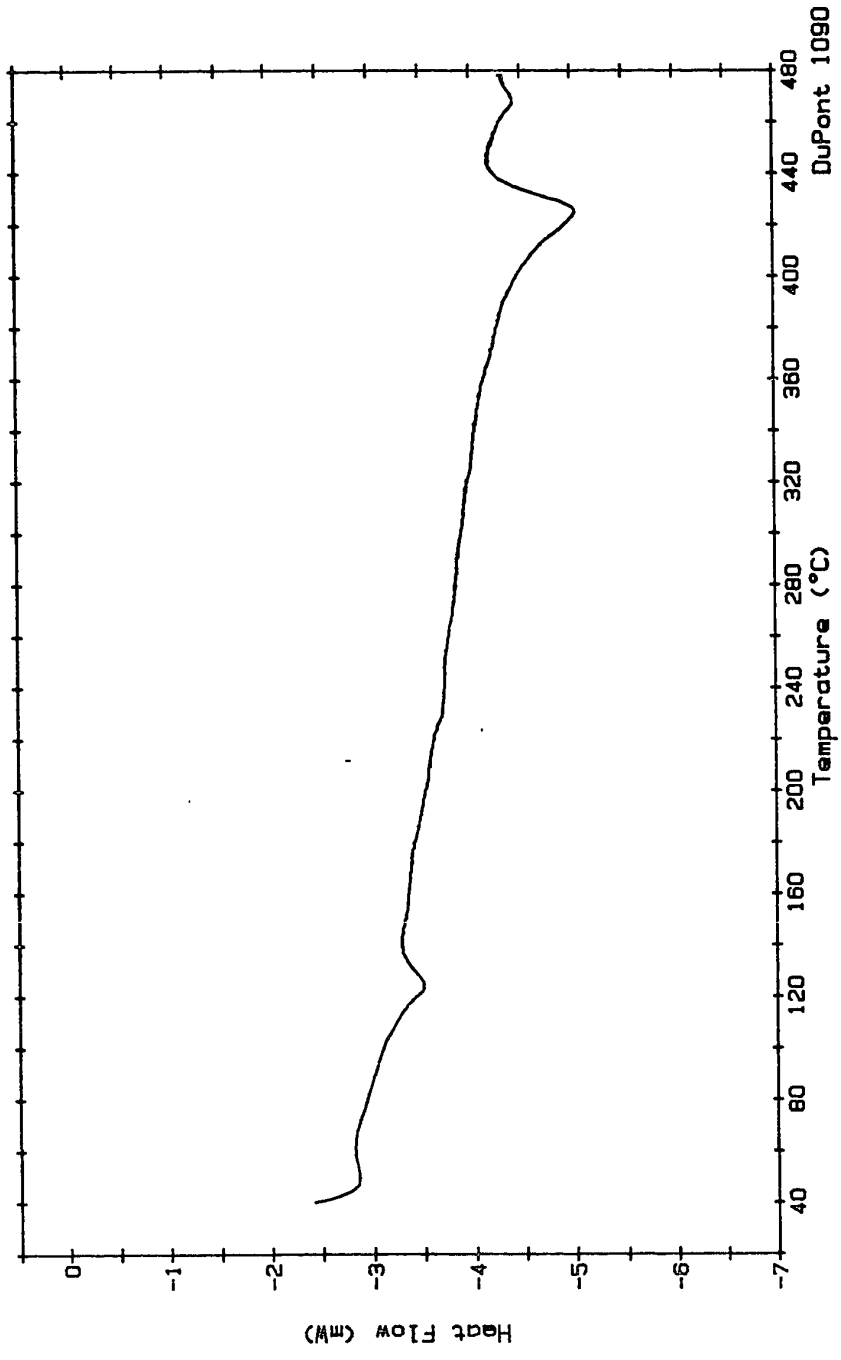

Figure 17. DSC trace for Specimen 1; Condition: as-pressed.

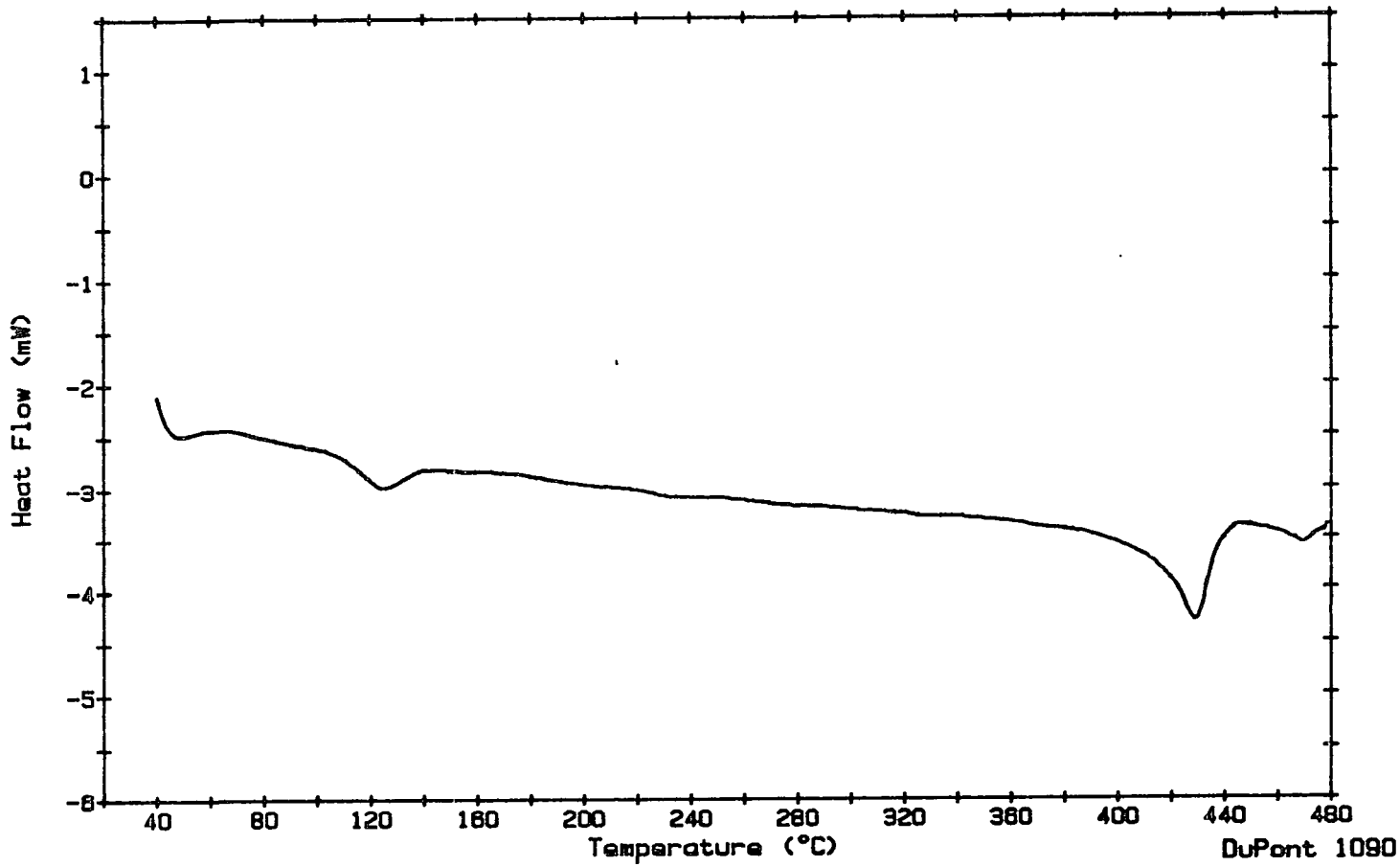

Figure 18. DSC trace for Specimen 7; Condition: as-pressed.

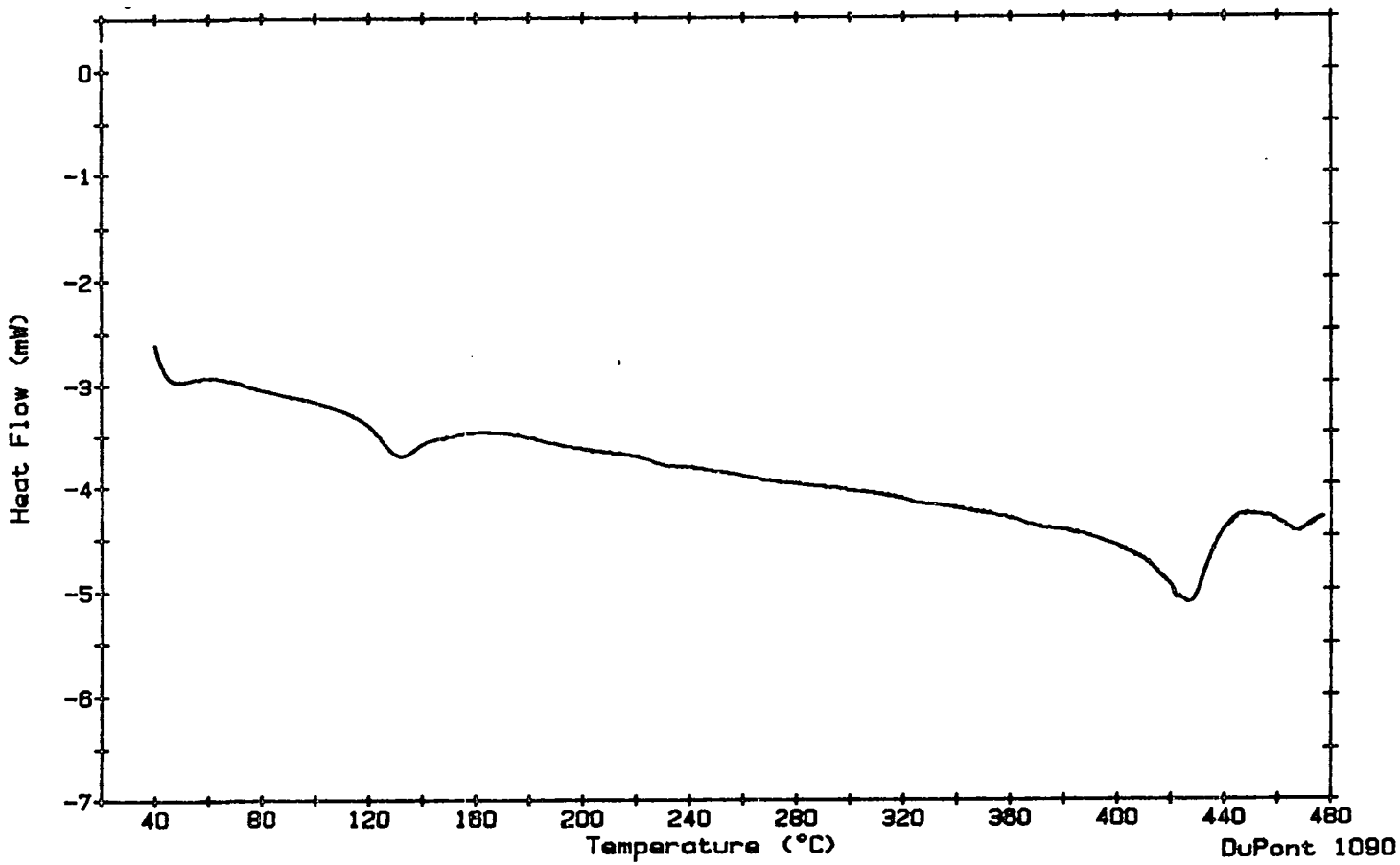

Figure 19. DSC trace for Specimen 13; Condition: as-pressed.

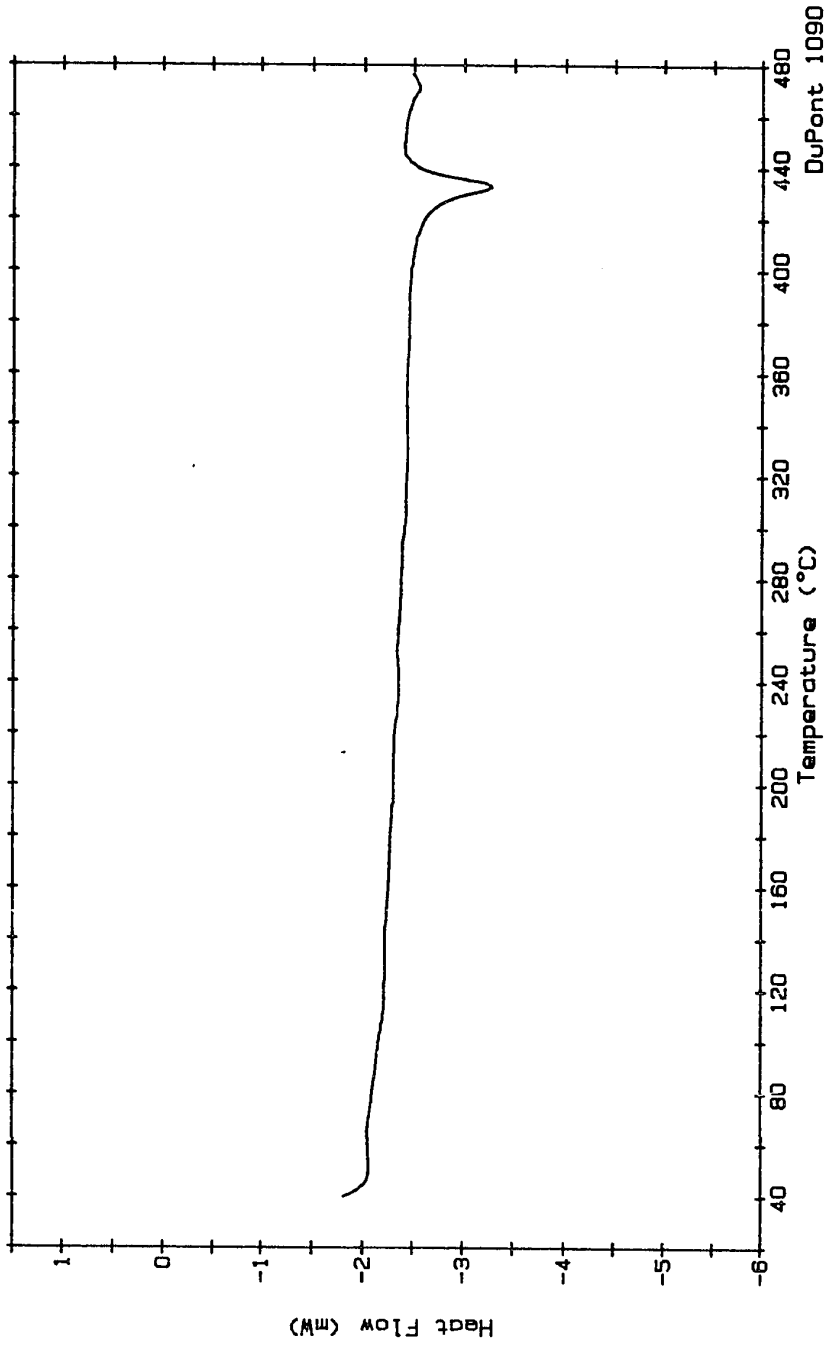

Figure 20. DSC trace for Specimen 2; Condition: quenched.

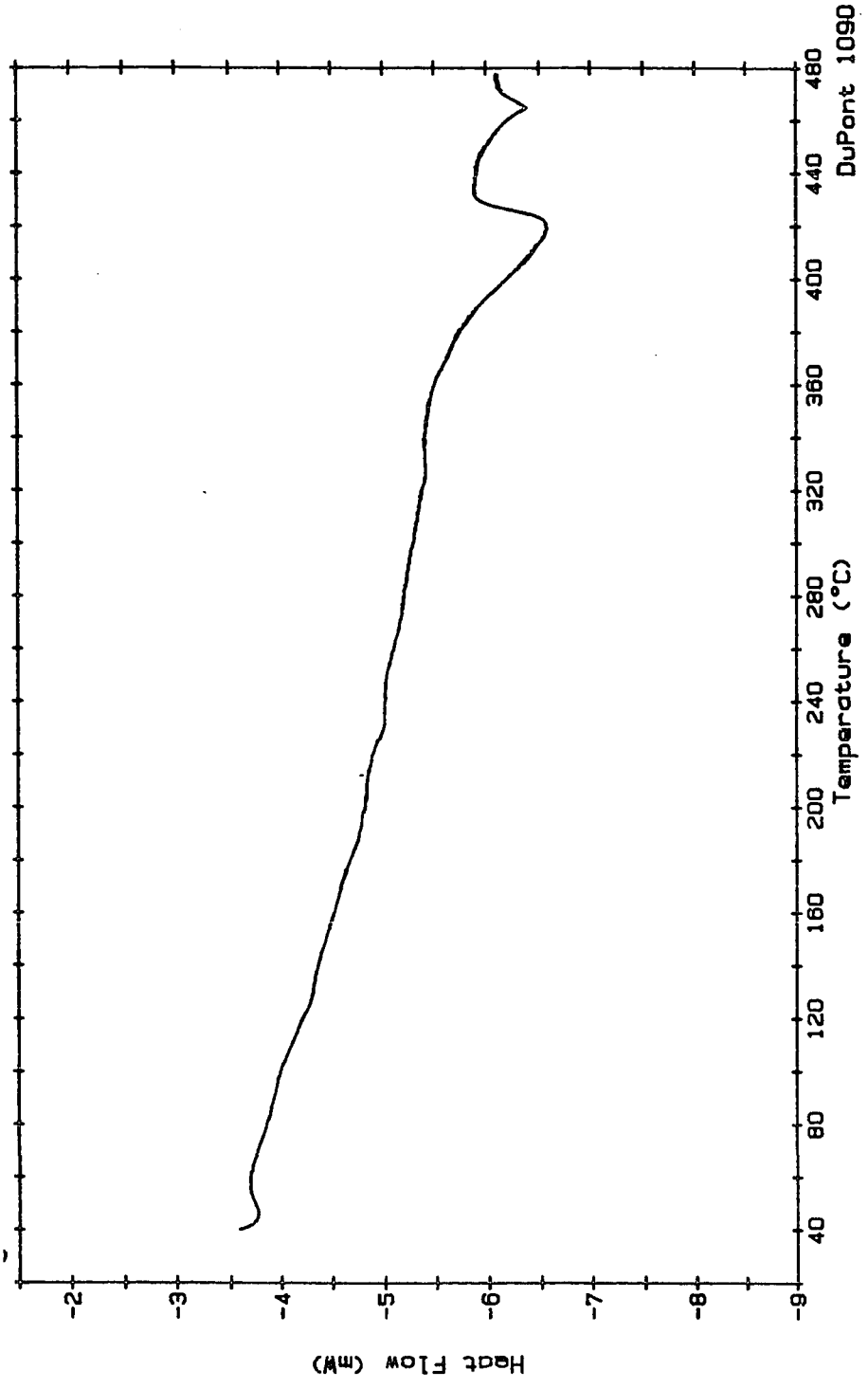

Figure 21. DSC trace for Specimen 8; Condition: quenched.

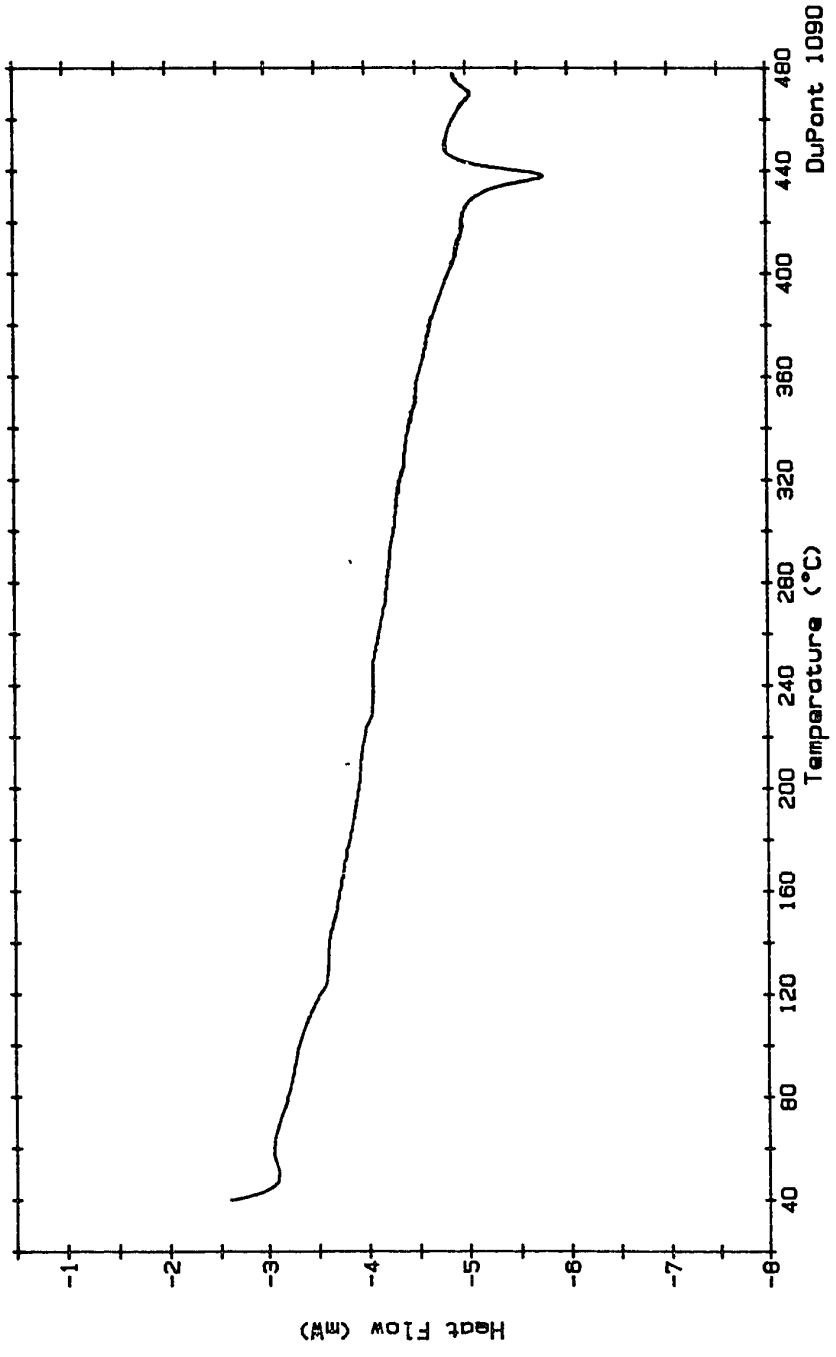

Figure 22. DSC trace for Specimen 14; Condition: quenched.

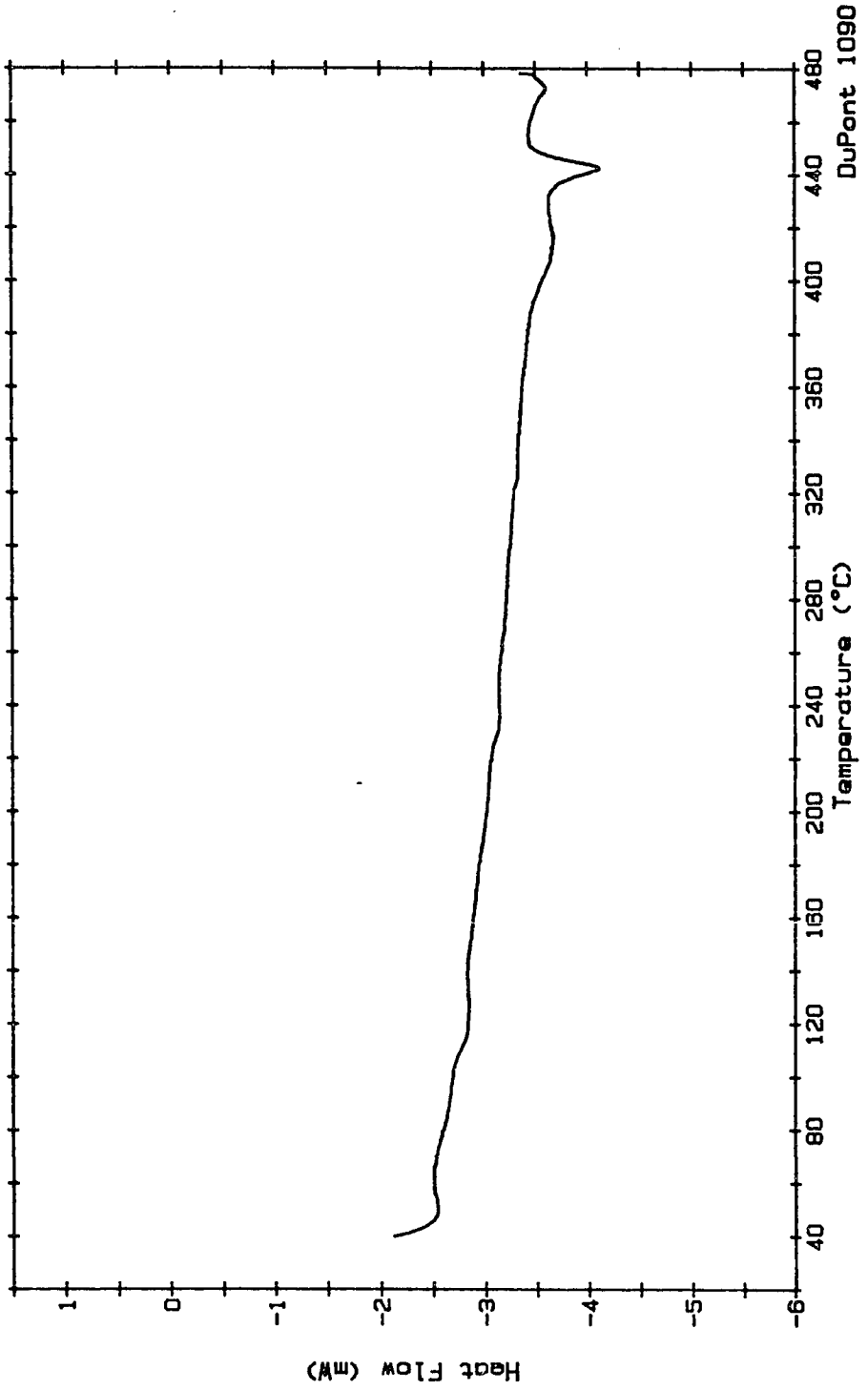

Figure 23. DSC trace for Specimen 6; Condition: annealed at 300°C for 1 hour.

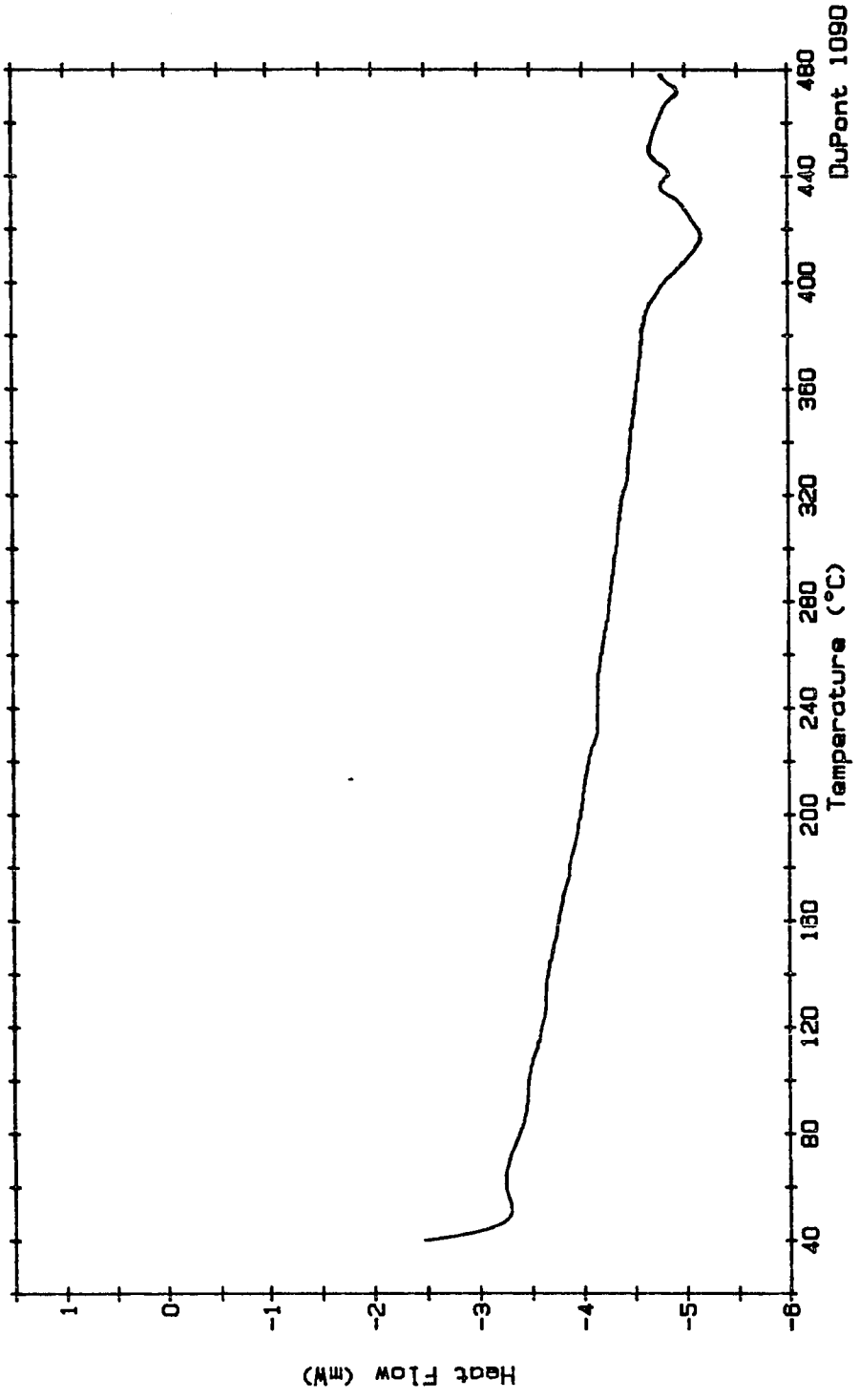

Figure 24. DSC trace for Specimen 12; Condition: annealed at 300°C for 1 hour.

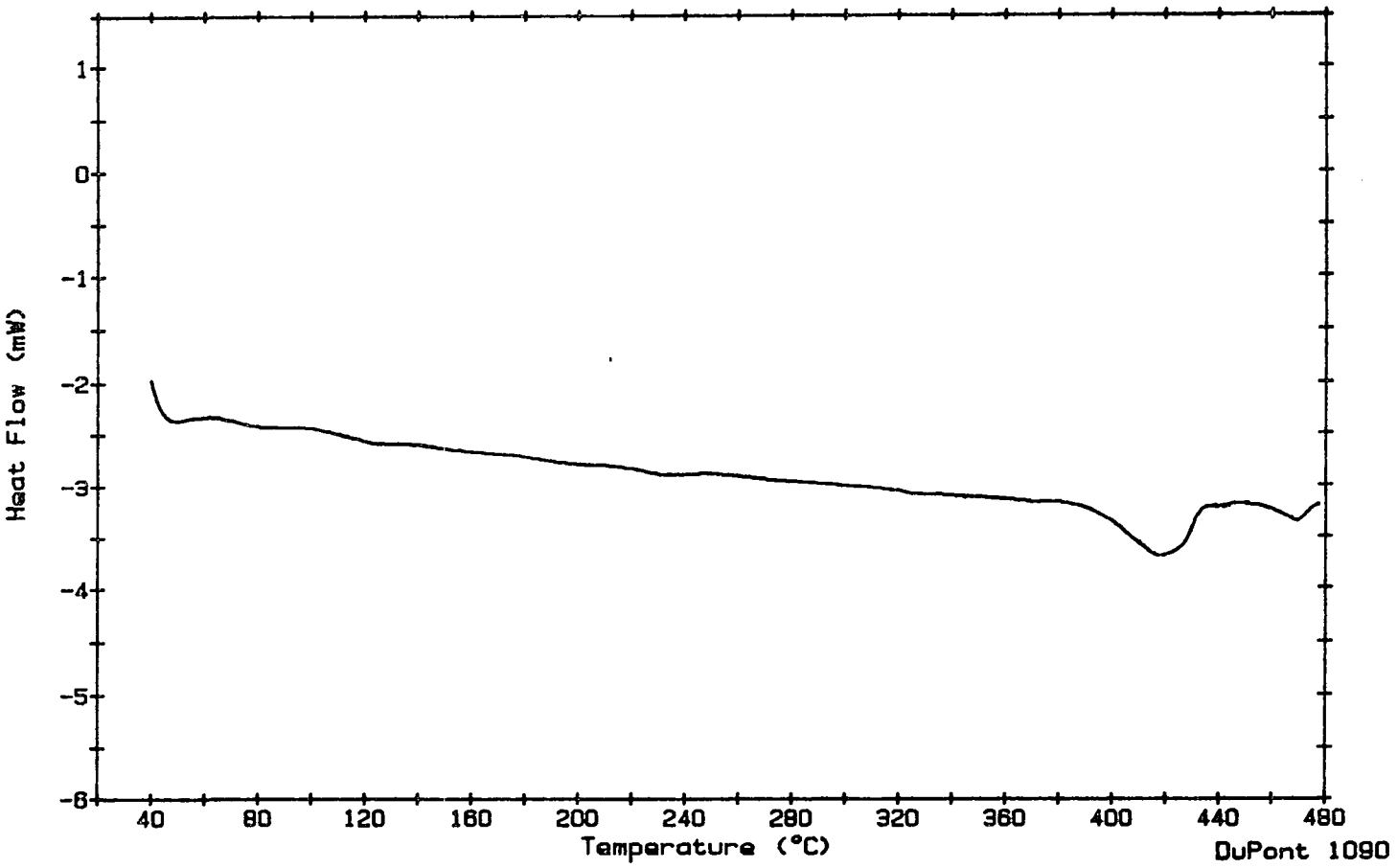

Figure 25. DSC trace for Specimen 18; Condition: annealed at 300°C for 1 hour.

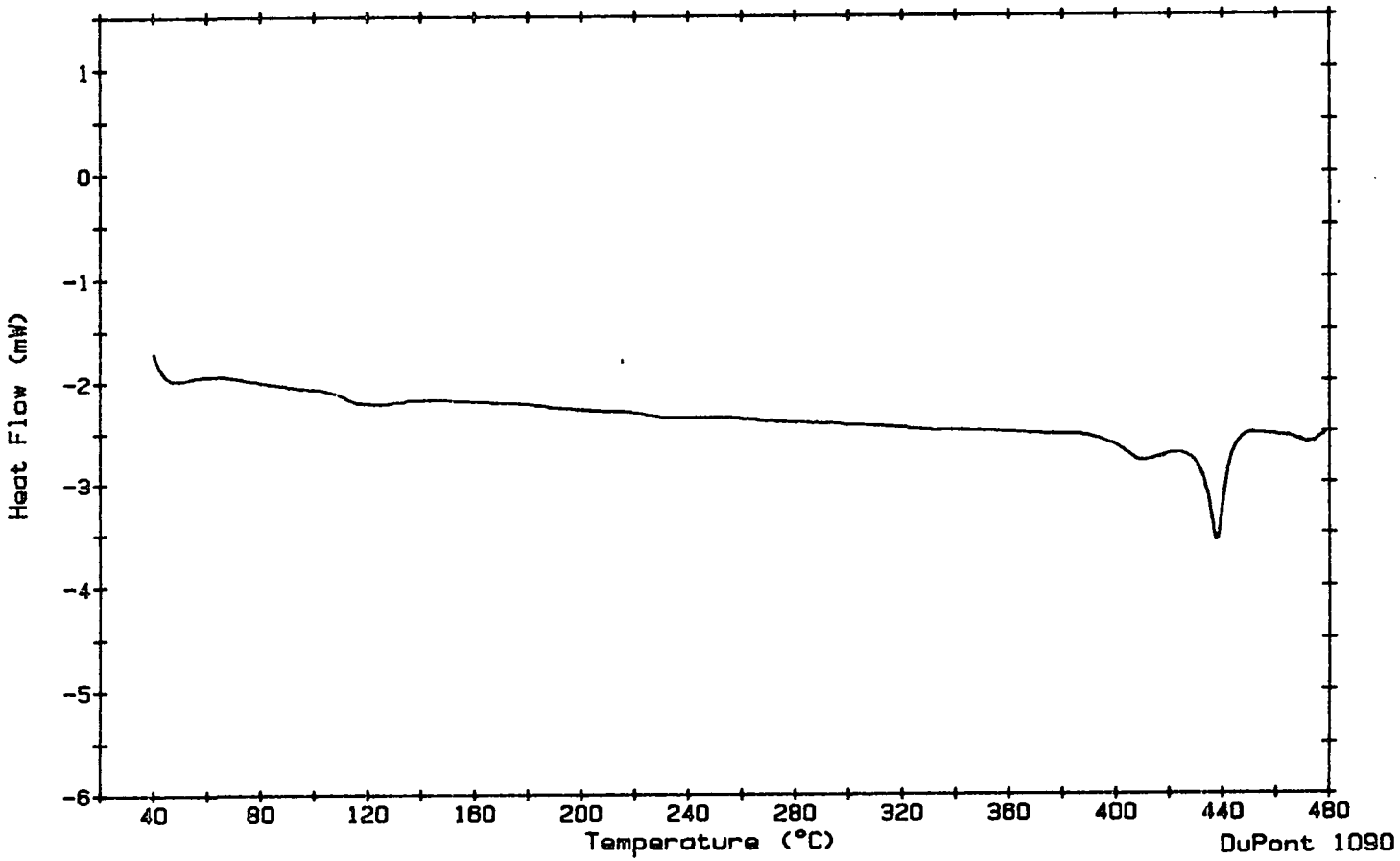

Figure 26. DSC trace for Specimen 5; Condition: annealed at 300°C for 24 hours.

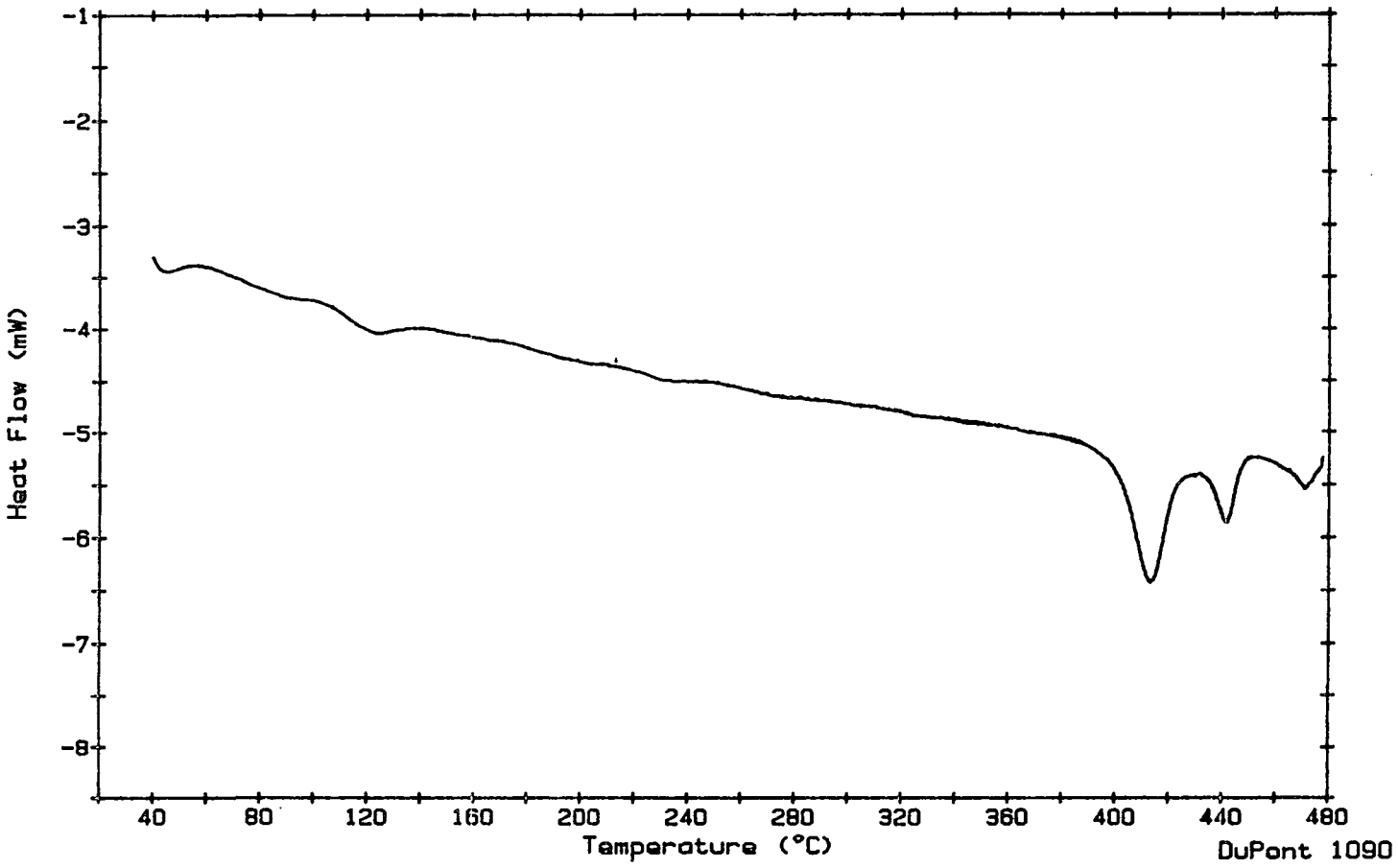

Figure 27. DSC trace for Specimen 11; Condition: annealed at 300°C for 24 hours.

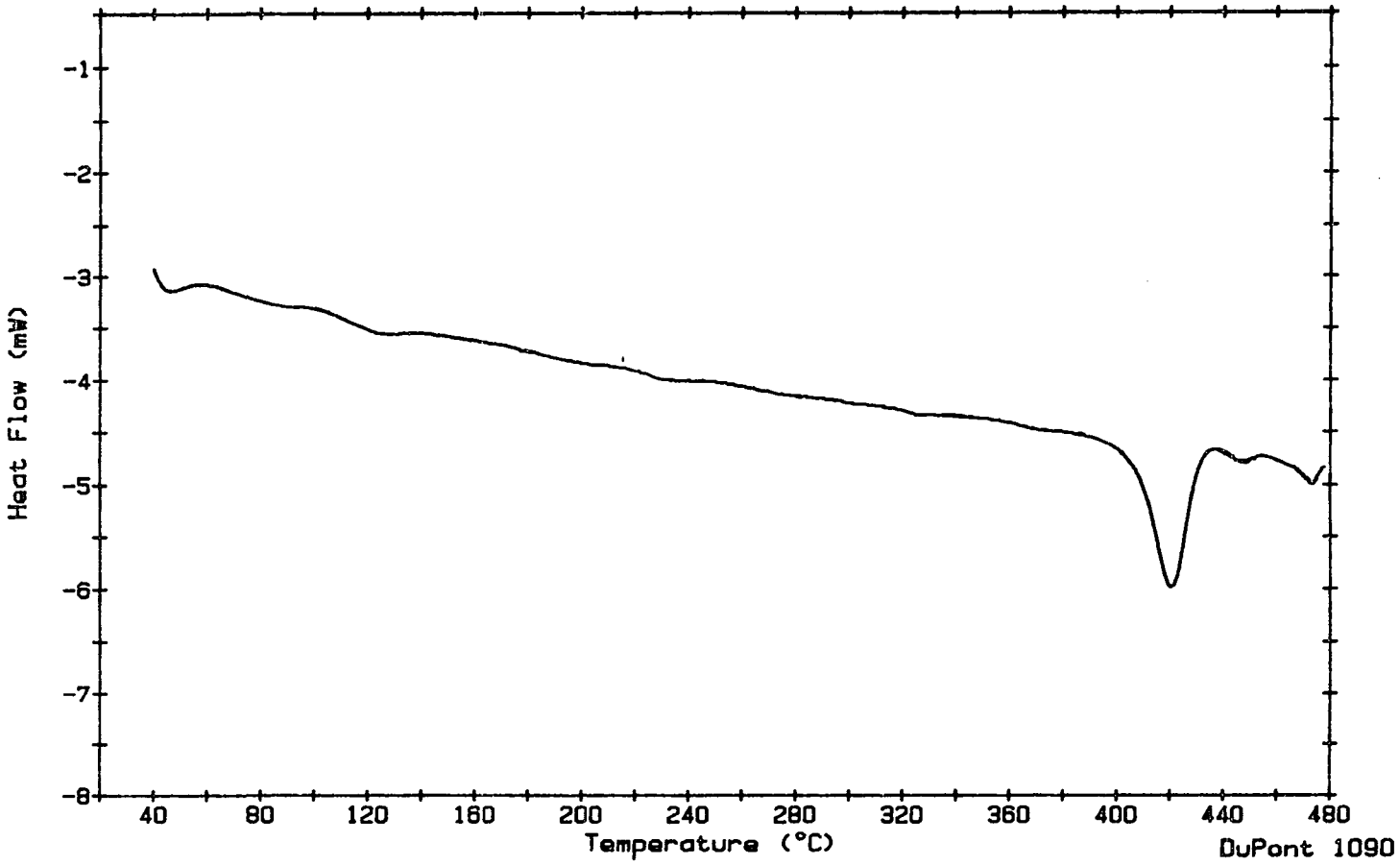

Figure 28. DSC trace for Specimen 17; Condition: annealed at 300°C for 24 hours.

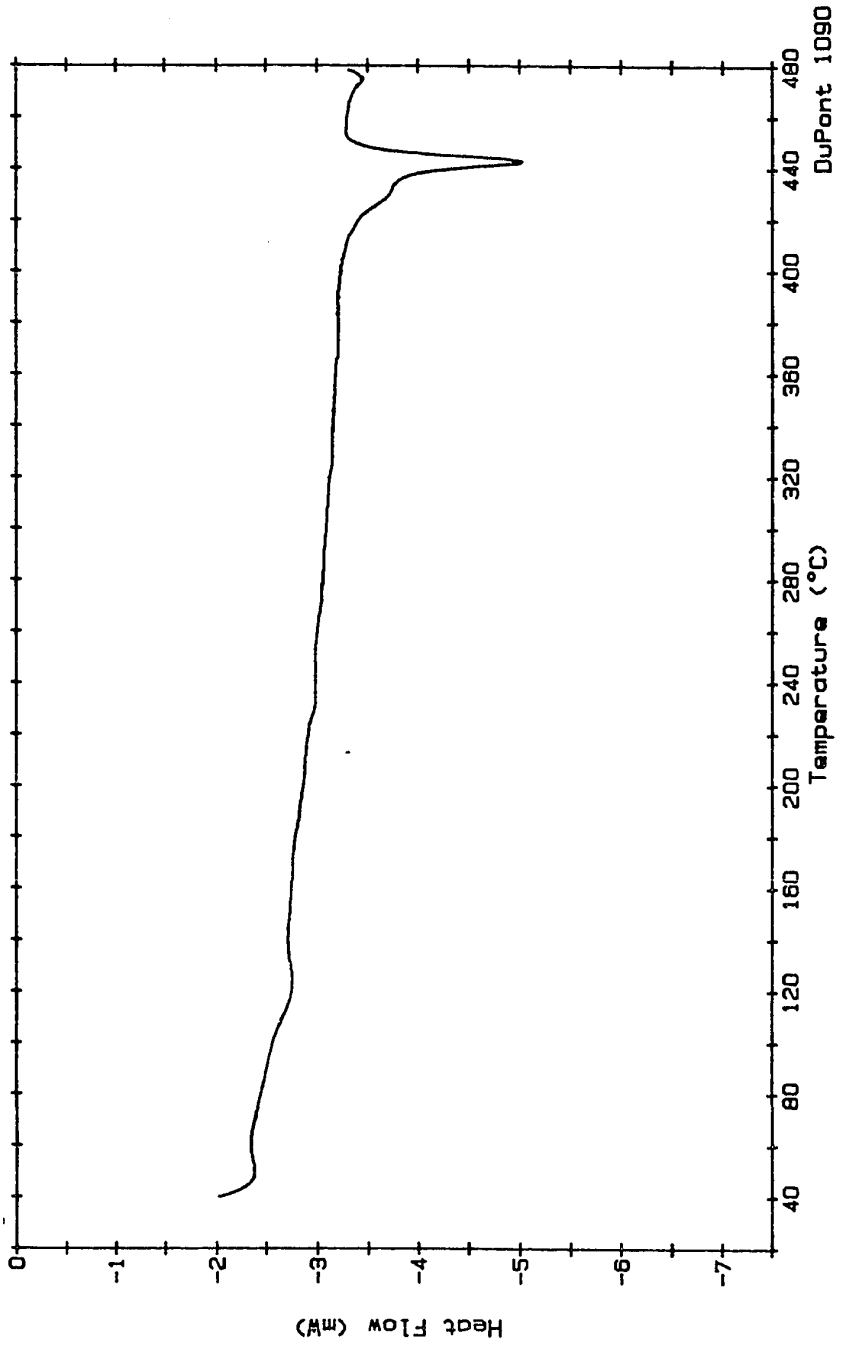

Figure 29. DSC trace for Specimen 3; Condition: annealed at 360°C for 1 hour.

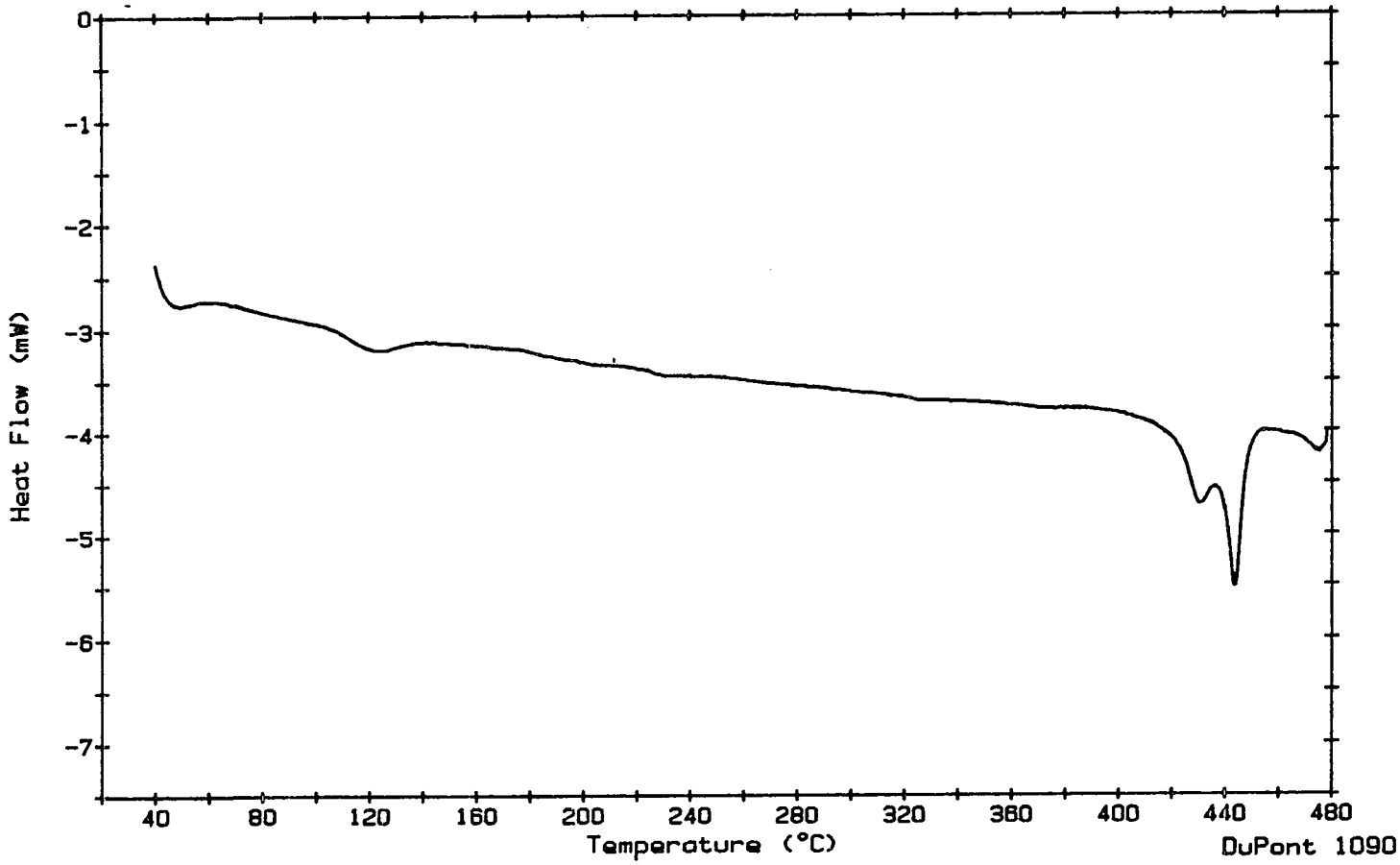

Figure 30. DSC trace for Specimen 9; Condition: annealed at 360°C for 1 hour.

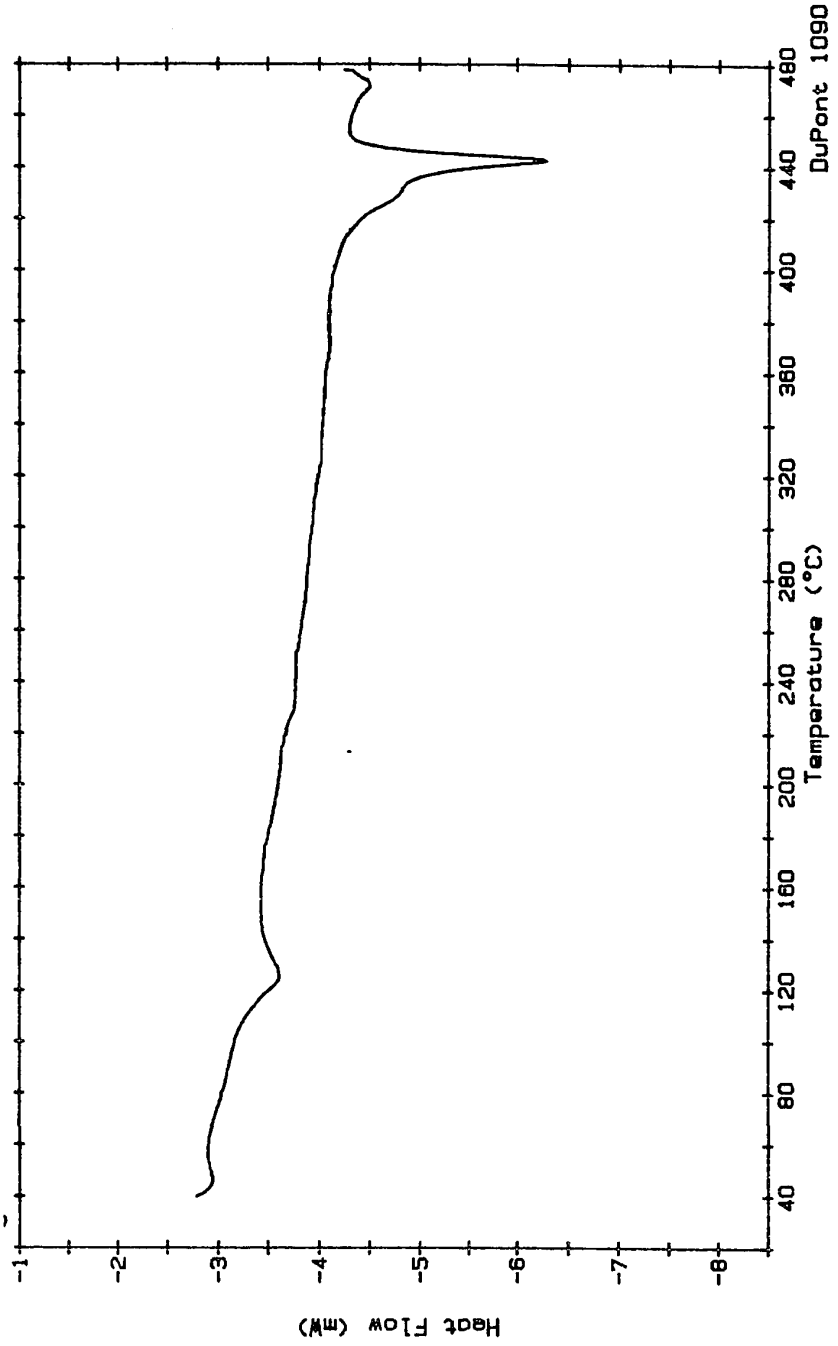

Figure 31. DSC trace for Specimen 15; Condition, annealed at 360°C for 1 hour.

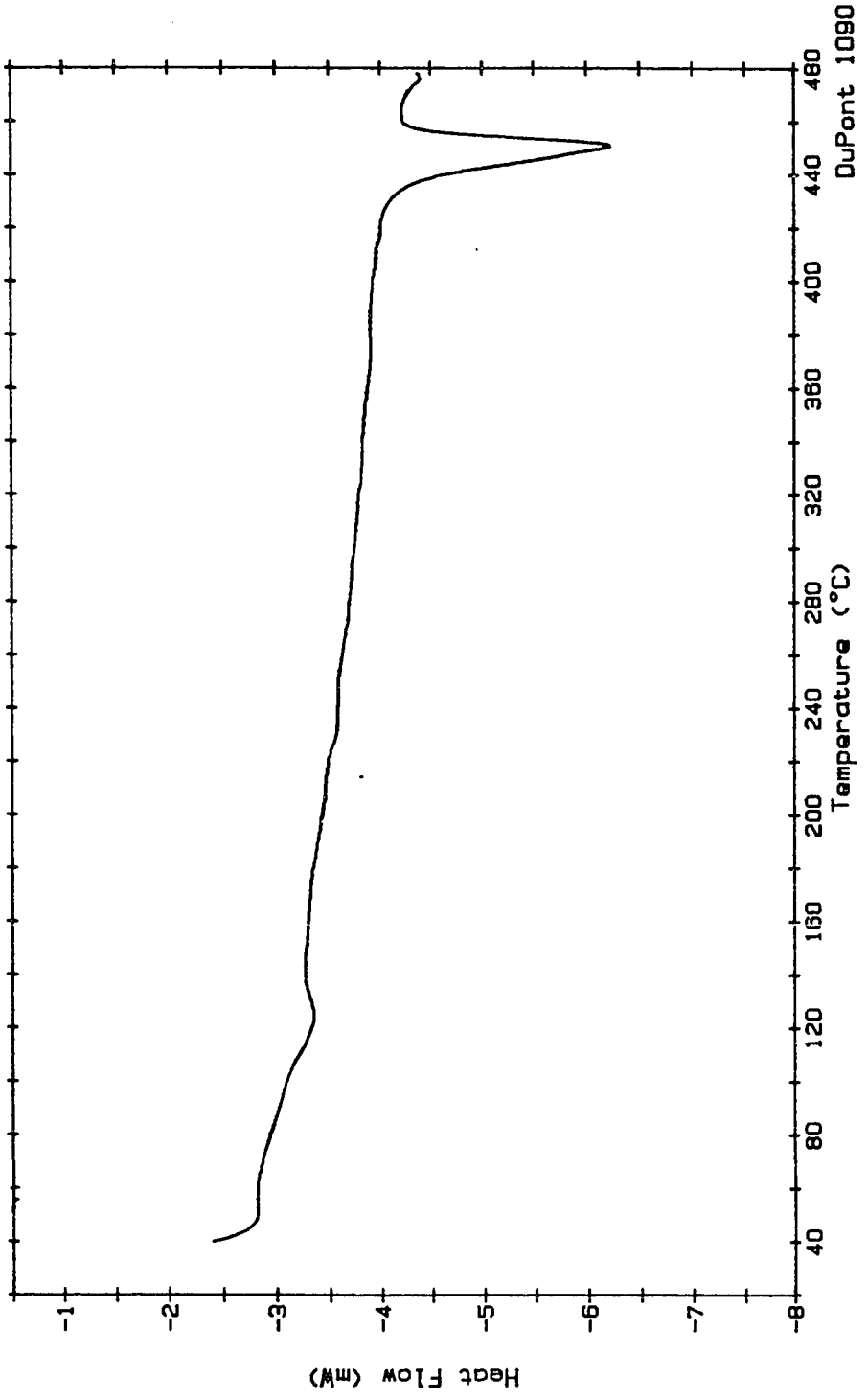

Figure 32. DSC trace for Specimen 4; Condition: annealed at 360°C for 24 hours.

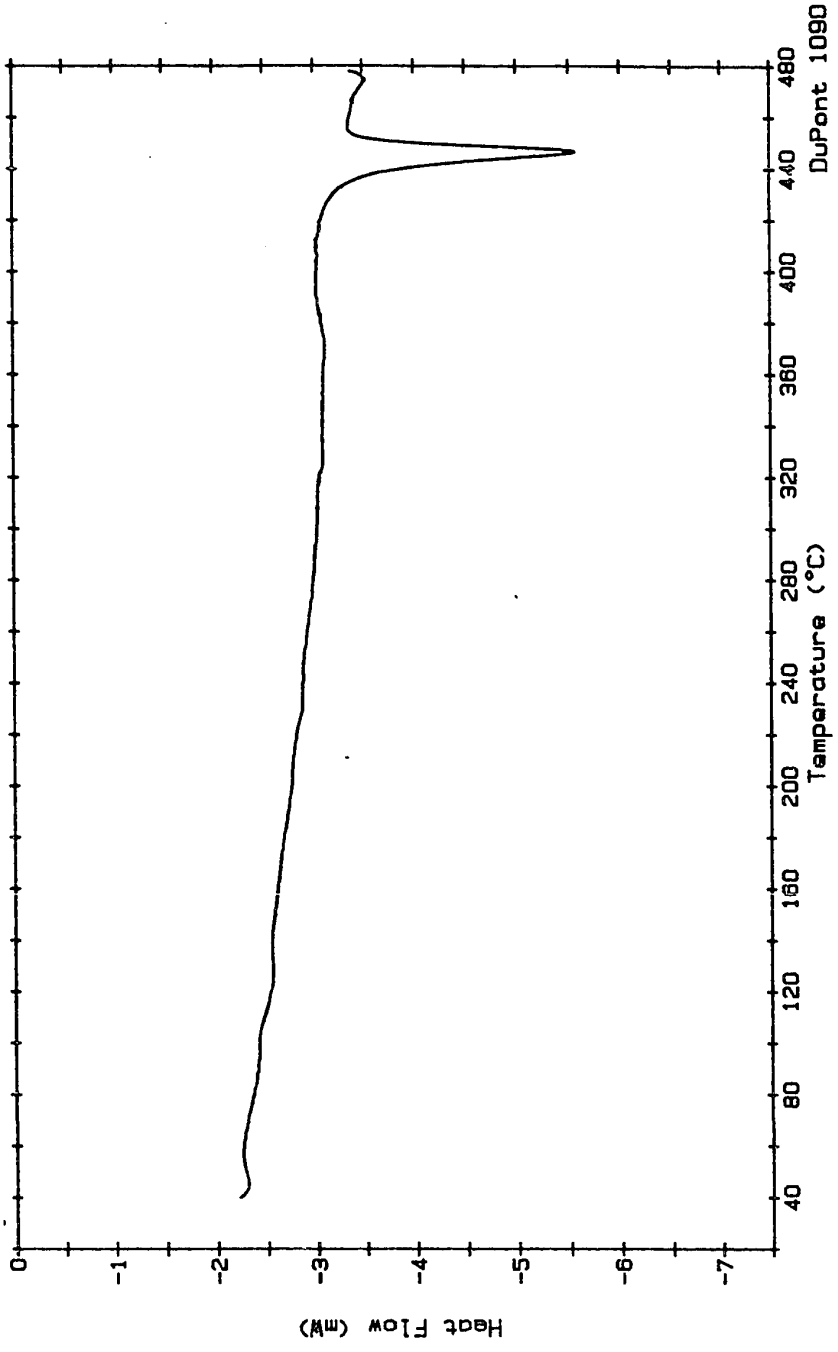

Figure 33. DSC trace for Specimen 10; Condition: annealed at 360°C for 24 hours.

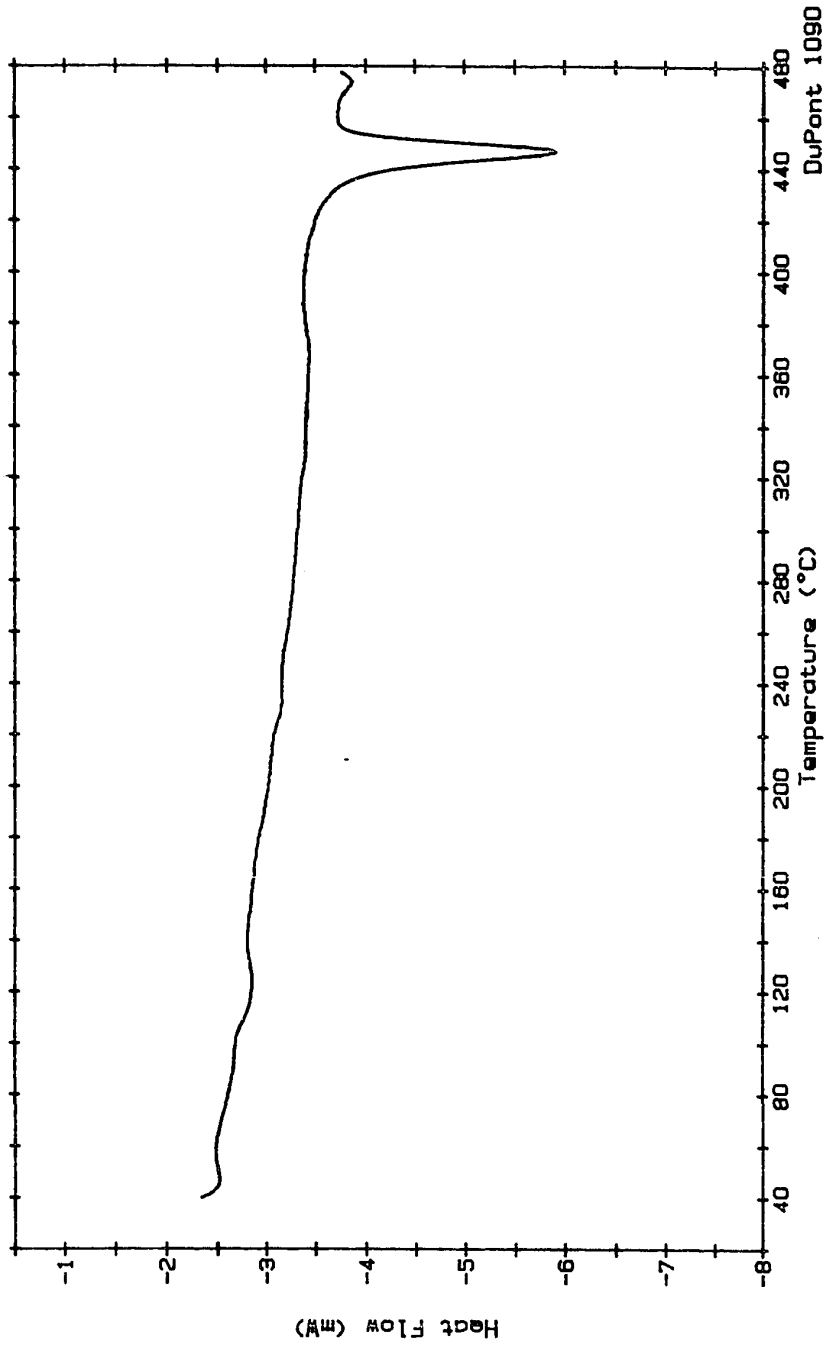

Figure 34. DSC trace for Specimen 16; Condition: annealed at 360°C for 24 hours.

endotherm occurred at a higher temperature than reported in Reference 23. The specific energy of the endotherm also appears to be slightly higher than the approximately 2 J/g reported in the same reference.

The second endotherm had a peak temperature which ranged between 425.4°C and 428.7°C. This matches the traces shown in Figures 13 and 14. The specific energy for the second endotherm averaged 12.5 J/g. This fits into the specific energy range of 17 J/g to 10.5 J/g which has been reported.[23] For all the specimens tested, the second endotherm was very broad with the difference between the onset temperature and the peak temperature averaging 22.9°C. This large difference can be interpreted as an indication that a fairly large degree of structural nonuniformity exists within the as-pressed specimens. When chemical reactions are not a factor, a reduction in the width of the transition peak can be interpreted as an indication that internal structure of the material is becoming more uniform.

The average specific energy of the third endotherm, which is the liquid-crystal to isotropic-liquid transition, matched closely with the literature value at .589 J/g.

5.1.2 Quenched Specimens

The DSC traces for quenched specimens 2, 8, and 14 appear in Figures 20, 21, and 22. While specimens 8 and 14

did not show a low temperature endotherm, specimen 2 does appear to have a small one. The endotherm was very broad with a difference between the onset and peak temperatures of about 30°C. The specific energy of this peak was also very low at 0.684°C. Because the peaks were very broad and the specific energy very low, it could be argued that it is really not a peak. If the peak had occurred in a different temperature region, it probably would not be considered a peak; however, the endotherm does appear to be in the same temperature range as the low temperature endotherms seen in the as-pressed specimens. As a result, it was determined to be small but real.

Specimen 8 does not appear to have the same transition temperature for the second endotherm as the other two specimens. It appears that this specimen is suffering from some degree of decomposition. Visually it is much darker in color than the other specimens, and the X-ray diffraction trace for this specimen is very different from the other two quenched specimens. This will be shown later in Section 5.3. This was the only specimen which appeared to be very different from the others. The cause of the decomposition can only be theorized. It is possible that the degradation is a result of exposure to oxygen during the pressing operation. Even though precautions were taken to minimize the exposure to air, a specimen which was positioned near

the edge of the caul plates may have been exposed to too much air. Since this specimen appears to be different from the other two, further discussion of the quenched results will be based on the remaining two specimens. For these specimens, the peak temperature of the crystalline-solid to liquid-crystal transition is around 435°C. This is slightly higher than the as-pressed specimens and it could be an indication that the quenched specimens have a more uniform structure than the as-pressed specimens.

It is important to note that in this case the term "uniform" denotes a specimen which has the same kind of structure throughout the specimen, but it does not mean that the structure is ordered. For example, a totally amorphous specimen would be described as very uniform, but by definition it would not be very structured. Additional data that support the contention that the quenched specimens are more uniform than the as-pressed specimens is that the difference between the onset temperature and the peak temperature has been reduced to about 10°C. At the same time, the specific energy of the endotherm for the quenched specimens has dropped so that it varies from 9.16 J/g to 7.64 J/g. The drop in specific energy is an indication that the material has a less ordered structure in the quenched state. The narrowing of the peaks indicate that the quenched specimens are more uniform than the as-pressed specimens.

The liquid-crystal to isotropic-liquid transformations appear to be about the same for the quenched specimens as for the as-pressed specimens.

5.1.3 Specimens Annealed at 300°C for 1 Hour

The specimens 6, 12, and 18 were annealed at 300°C for 1 hour. Their respective DSC traces are shown in Figures 23, 24, and 25. As with the previous group of specimens, two of the three specimens do not exhibit a low temperature endotherm while one specimen (specimen 6) does show a small one. The specific energy of this endotherm was only 0.836 J/g, and the difference between onset and peak temperatures was 11°C. Once again it is debatable as to whether or not the endotherm is real, but if the endotherm in specimen 2 is considered real, this one must also be considered real.

The most striking detail of these traces occurs at the solid-crystal to liquid-crystal transition. The single peak seen in the quenched and as-pressed specimens appears to be splitting into two peaks. The peak temperature for the first part of the peak ranges from 411.2°C to 418.1°C, and the peak temperature for the second part of the peak ranges from 442.0°C to 442.9°C. While Table 7 does not list a second peak for specimen 18, close examination of Figure 25 shows that there is an indication that the second endotherm for this specimen is also starting to split.

There is also some variation in size of the split peaks. In Figure 23, the second peak is the larger peak while in Figure 24 and 25 the first peak is larger. Because the software for the DSC equipment does not have the ability to deconvolute the peaks, the specific energies for each half of the split peaks could not be obtained. The total energy for the endotherm (both peaks) was determined and is reported in Table 7. One interesting observation is that the total specific energy for these annealed specimens is about the same as the quenched specimens which indicates that there may be only a limited change in the level of crystallinity using the 300°C for 1 hour anneal cycle.

In addition, the onset and peak temperatures for the liquid-crystal to isotropic-liquid have shifted upward by about 5°C from the as-pressed specimens, while the specific energy for the transition stays about the same. This could be a result of increased molecular weight. It is known that for a given polymer the higher the molecular weight, the higher the transition temperatures will be.

5.1.4 Specimens Annealed at 300°C for 24 Hours

The next group of specimens was annealed at 300°C for 24 hours. This group consists of specimens 5, 11, and 17. The corresponding DSC traces are shown in Figures 26, 27, and 28. The time and temperature combination here appears to

be sufficient to cause the return of the crystalline-solid to crystalline-solid transition. The average specific energy obtained for the three specimens for this endotherm is around 1.21 J/g; however, this does represent about a two hundred and forty percent decrease in the specific energy from the as-pressed condition. This may indicate that there are fewer molecules which have been transformed to the low temperature crystalline-solid structure than were present in the as-pressed specimens. This could be viewed as a sign that the material still has not become fully annealed. This is only a supposition since there is no direct data to support this argument.

As with the previous specimens, the second endotherm has two endotherm peaks; however, the peaks have become much more defined with the total specific energy of the combined peaks increasing to an average value of 10.63 J/g. Individual values range from a low of 9.29 J/g to a high of 11.4 J/g. This seems to indicate that a significant amount of ordering is occurring. The peak temperatures for the first peak and second peak of this endotherm remain about the same as for the specimens annealed for one hour at 300°C. Two of the specimens, numbers 11 and 17, display a first peak that is much larger than the second. This situation is reversed for specimen number 5, which has a relatively large and sharp second peak with the first peak

appearing to be about the same size or smaller than the corresponding peaks in the specimens annealed for 1 hour at 300°C.

The endotherm for the liquid-crystal to isotropic-liquid also appears to occur at about the same temperature as for the specimens annealed for 1 hour at 300°C. There may be some sharpening of the peak, but too few specimens were tested to prove this claim.

5.1.5 Specimens Annealed at 360°C for 1 Hour

Figures 29, 30 and 31 are from specimens 3, 9, and 15. These specimens were annealed at 360°C for 1 hour. Annealing under these conditions does not appear to alter the first endotherm significantly from the 300°C for 24 hour condition. While specimen 15 did show a large endotherm with a specific energy of 3.72 J/g, the other specimens did not exhibit this behavior. In addition, a relatively large endotherm of this kind was not seen in any of the specimens which were annealed for 24 hours at 360°C. This tends to suggest that the large initial endotherm observed with specimen 15 is a localized phenomenon.

Once again, the second endotherm shows the most interesting data. As with the two previous anneal cycles, there are two peaks to the endotherm; however, in this case it appears that the first peak is moving up in temperature

and is starting to combine with the second peak. Although Table 5 does not report a peak temperature for the first peak of specimen 3, examination of Figure 29 reveals that it has moved up in temperature and is a shoulder of the second peak in the same manner as the first peak of specimen 15 did in Figure 31. In Figure 31, the first peak remains defined enough to determine a peak temperature of 430.2°C. In Figure 30, the first peak also appears to be shifting toward the second peak but still has enough individual character to produce a well defined peak with a peak temperature of 412.8°C. The peak temperature of the second peak appears stable at around 445°C. The specific energy of the crystalline-solid to liquid-crystal endotherm was slightly increased over the 300°C anneal cycles to 11.4 J/g.

The specific energies of the liquid-crystal to isotropic-liquid transition reported in Table 9 are generally lower than reported for the previous anneal cycles. This appears to be due to a shift in the endotherm to a slightly higher temperature which results in the endotherm not being complete by the end of the DSC run. Specimen 15, which had a slightly low temperature endotherm, supplied specific energy values comparable to earlier tests. The final temperature for the DSC runs was not raised because of a concern about the decomposition of the specimen at temperatures above 480°C. If a specimen had bubbled out

of the sample pan during decomposition, it would have contaminated the DSC cell and caused a shift in the baseline making direct comparison between specimens more difficult.

5.1.6 Specimens Annealed at 360°C for 24 Hours

The DSC traces for the longest and highest temperature anneal cycles of this study are shown in Figures 32, 33, and 34. The figures correspond to specimens 4, 10, and 16, respectively. These specimens were annealed at 360°C for 24 hours. The longer anneal time does not appear to have any real effect on the crystalline-solid to crystalline-solid endotherm. The onset and peak temperatures are basically the same as for the specimens annealed for 1 hour at 360°C. With the exception of specimen 15, which appears to be out of family, the specimens annealed for 1 hour and 24 hours have almost the same specific energy.

The longer time at temperature has resulted in the elimination of the double peak in the second endotherm. For all three specimens, a single peak is observed. These peaks are very sharp compared to the other endotherms seen in this study. The average difference between the onset temperature and the peak temperature is only 10°C, with the smallest difference being only 7.7°C. Despite the sharpness of the peaks, the average specific energy has increased to 11.7 J/g. The peak temperature for the second endotherm has

also moved up slightly from the one hour anneal time to 448.2°C.

The final endotherm also appears to have moved up two to three degrees. Once again, the increase in temperature resulted in incomplete data being reported for the specific energy of at least two of the specimens. Concern about possible specimen decomposition made it impossible to test at a high enough temperature to allow the peaks to be fully defined.

5.2 General DSC Results

An overall review of the DSC data indicates several things. The most obvious of these is that there appear to be two different groups of molecules which undergo the crystalline-solid to liquid-crystal transition at different temperatures. This is indicated by the double peak which is seen in three of the four annealed specimen groups. It appears that this is a result of the anneal cycles since the splitting of the endotherm is not seen in the as-pressed or quenched specimens. One explanation for this phenomenon is that the molecules are changing structure in some way. This could be in the form of chain extension, cross-linking of some of the chains, or decomposition of the chains. All of these possible sources of change have one thing in common they should be irreversible. This would result in the DSC

traces of subsequent heating cycles showing only the higher temperature peak, or the return of the double peak for the endotherm with a slow shift toward the higher temperature peak. In order to test this theory, additional DSC runs were performed where some specimens were heated above the crystalline-solid to liquid-crystal transition temperature but below the transition to isotropic-liquid. The upper temperature of 450°C was imposed to reduce the chances of specimen decomposition through repeated heating cycles.

Figures 35 through 37 show how the DSC trace changes for material taken from specimen 10. Recall that this specimen had been annealed at 360°C for 24 hours. Figure 35 is for the first heating cycle; it is very similar to Figure 33 which was obtained from another portion of specimen 10. There is a single sharp peak for the crystalline-solid to liquid-crystal endotherm with the peak temperature being around 445°C. After heating, the specimen was allowed to cool at a rate of 10°C per minute down to 300°C. This was done to see how the associated crystallization exotherm behaved. As with the case shown in Figure 14, the material supercooled before the exotherm was seen. For this thermal cycle, the amount of supercooling was roughly 55°C.

Figure 36 shows the DSC trace for the second cycle of the same specimen. In the second, cycle the peak temperature for the endotherm dropped to around 422°C. This

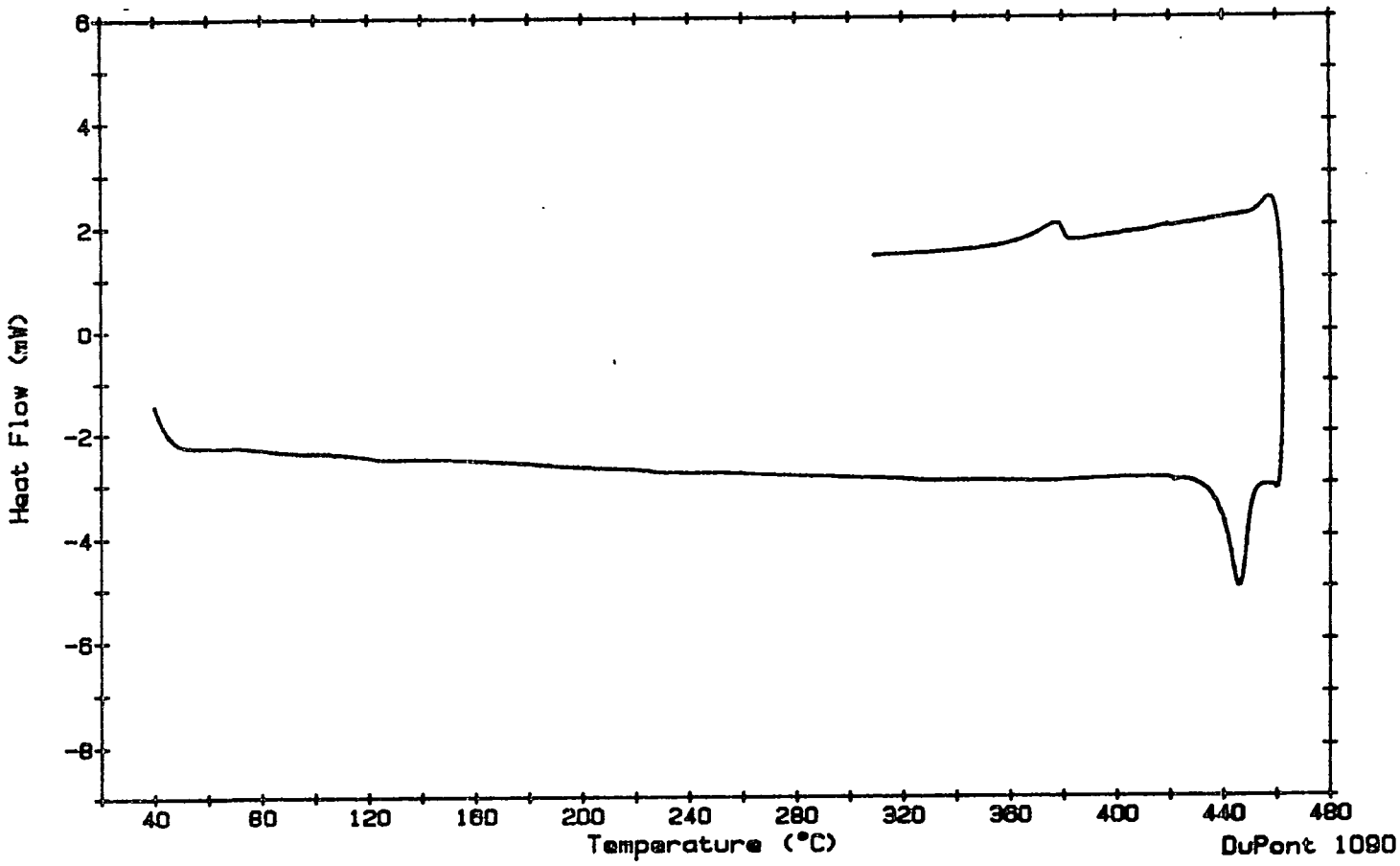

Figure 35. DSC trace for the initial heating of a second portion from specimen 10.

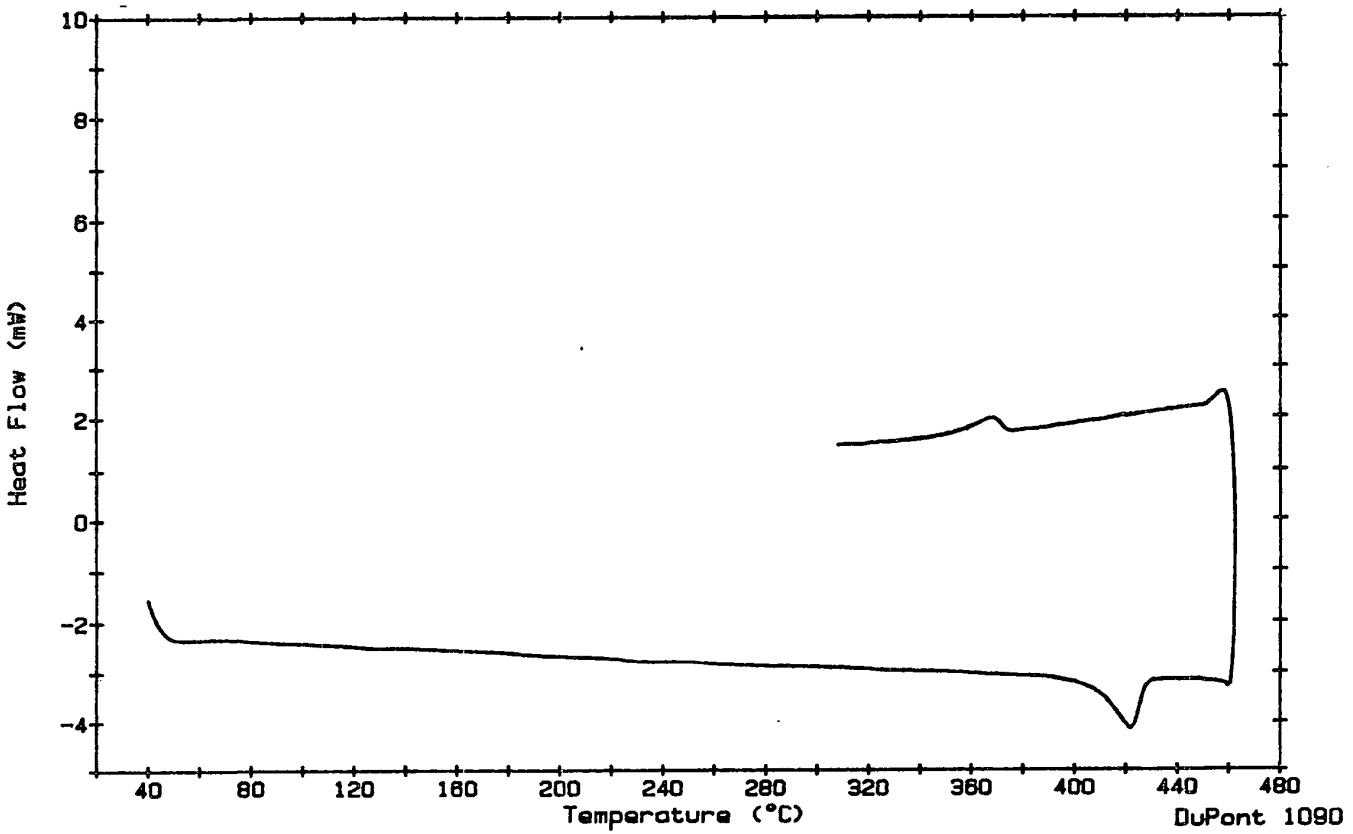

Figure 36. DSC trace for the second heating of a second portion from specimen 10.

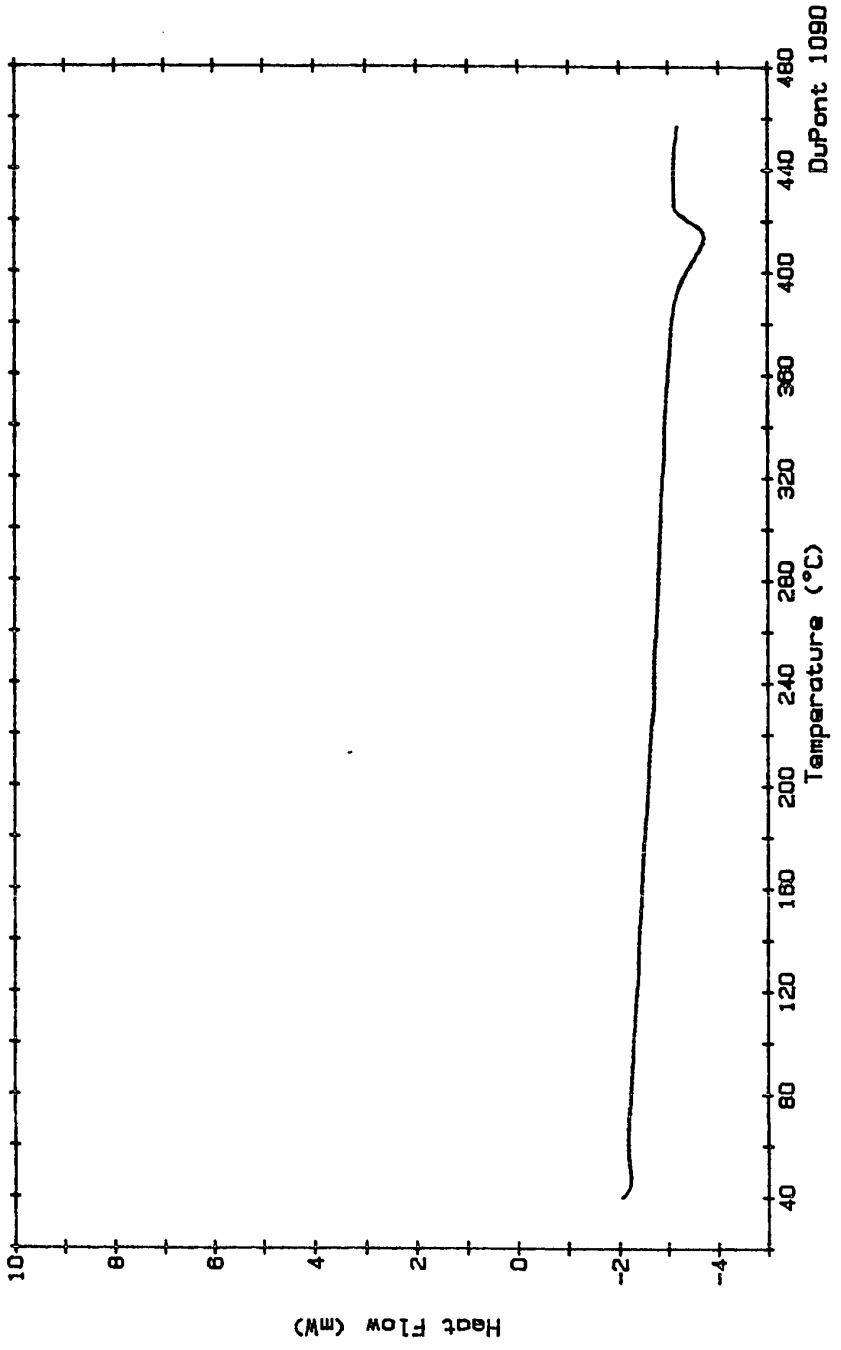

Figure 37. DSC trace for the third heating of a second portion from specimen 10.

is very similar to the range of temperatures observed in the as-pressed material. In addition, the peak is wider than the first thermal cycle. The temperature for the crystallization exotherm has been lowered by a few degrees and the amount of supercooling has dropped to nearly 30°C.

The third thermal cycle, shown in Figure 37, produces a further drop in the peak temperature of the endotherm to around 414°C. This is roughly the same temperature as the first peak for the specimens annealed at 300°C.

When all other things are equal, an increase in the molecular weight of a polymer will result in an associated increase in the melting temperature of that polymer. In the case of liquid crystalline materials, the true melting point is associated with the liquid-crystal to isotropic-liquid transition. An increase in molecular weight would be an ideal explanation for the increase in the crystalline-solid to liquid-crystal transition temperature which occurred as the anneal times and temperatures were increased; however, an increase in molecular weight would have resulted in a permanent increase in the crystalline-solid to liquid-crystal transition temperature. Figures 35, 36 and 37 show that the change in the transition temperature is not permanent. The transition temperature drops with thermal cycling, indicating that the molecular weight has not

significantly increased. This is supported by Figures 38, 39, and 40 which show the DSC traces for material taken from specimen 11, which was annealed at 300°C for 24 hours. Figure 38 is the initial heating cycle with the two peaks for the second endotherm clearly defined. On the second heating cycle, shown in Figure 39, only one peak is observed for the endotherm and its peak temperature is between the two initial peak temperatures. As with the previous example, the third heating cycle, shown in Figure 40, further reduces the peak temperature of the endotherm and increases the width of the peak.

This behavior is a strong indication that the high temperature peak is not produced by material which has gone through some type of chemical transformation. If an increase in molecular weight, cross linking, decomposition, or some other kind of chemical change in the molecular structure was responsible for the splitting of the endotherm, the increase in transition temperature and appearance of the high temperature peak would not be reversible.

Another interesting aspect of the DSC data is that the total specific energy for the split peaks correlates very closely with the specific energy for the single peak that was produced by specimens which were annealed at 360°C for 24 hours. While there was a slight trend toward higher specific energies for the higher energy anneal cycles, three

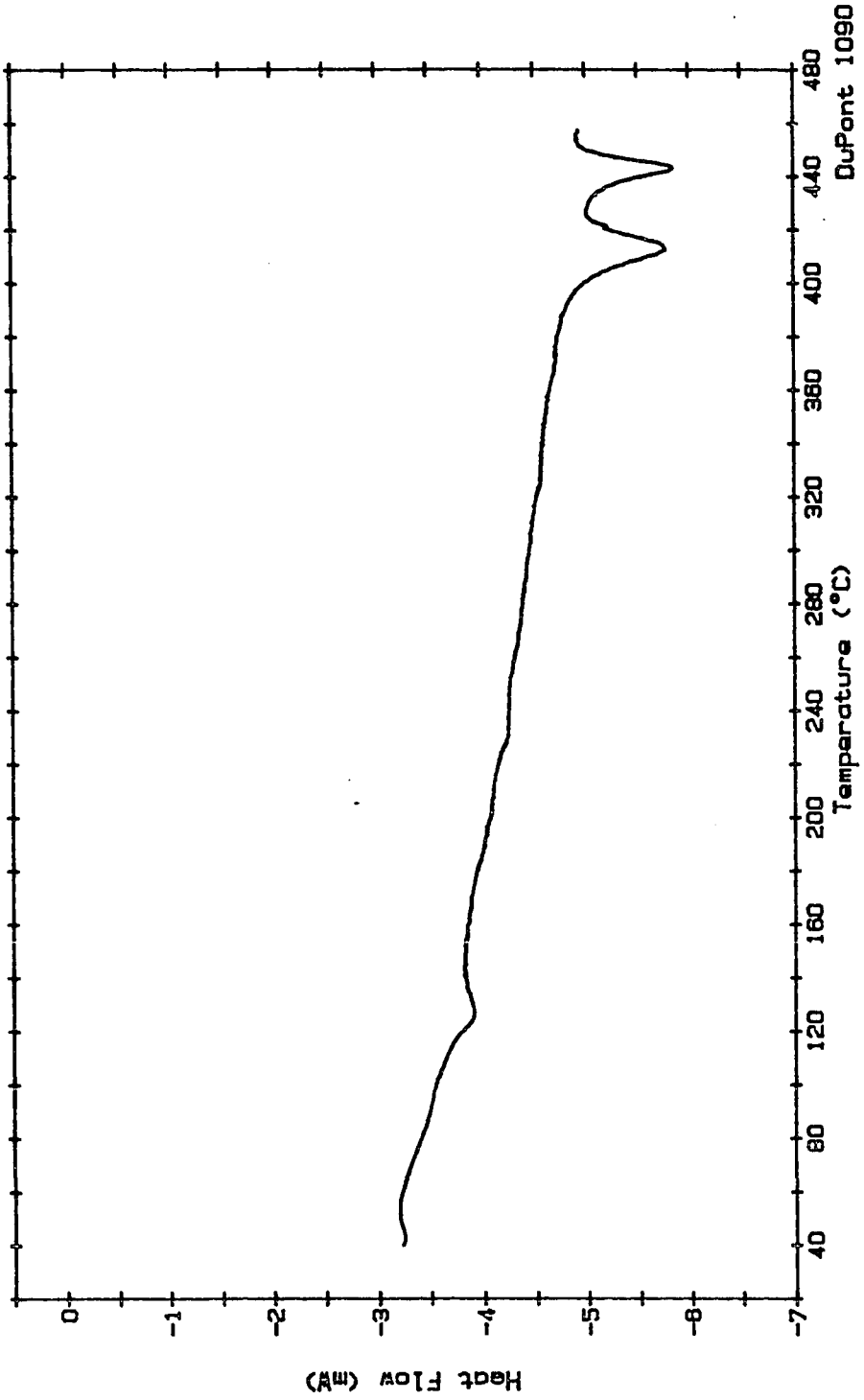

Figure 38. DSC trace for the initial heating of a second portion from specimen 11.

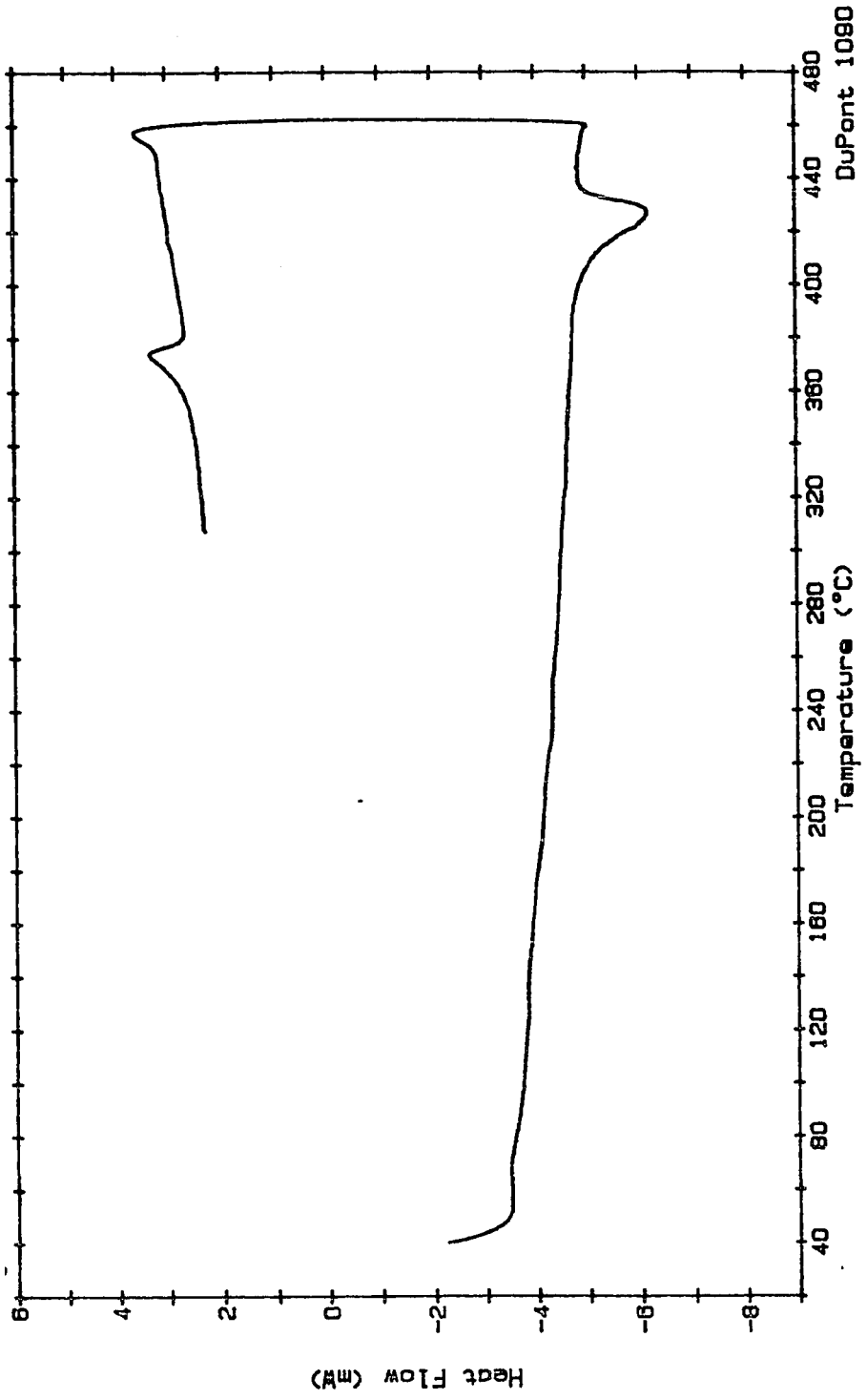

Figure 39. DSC trace for the second heating of a second portion from specimen 11.

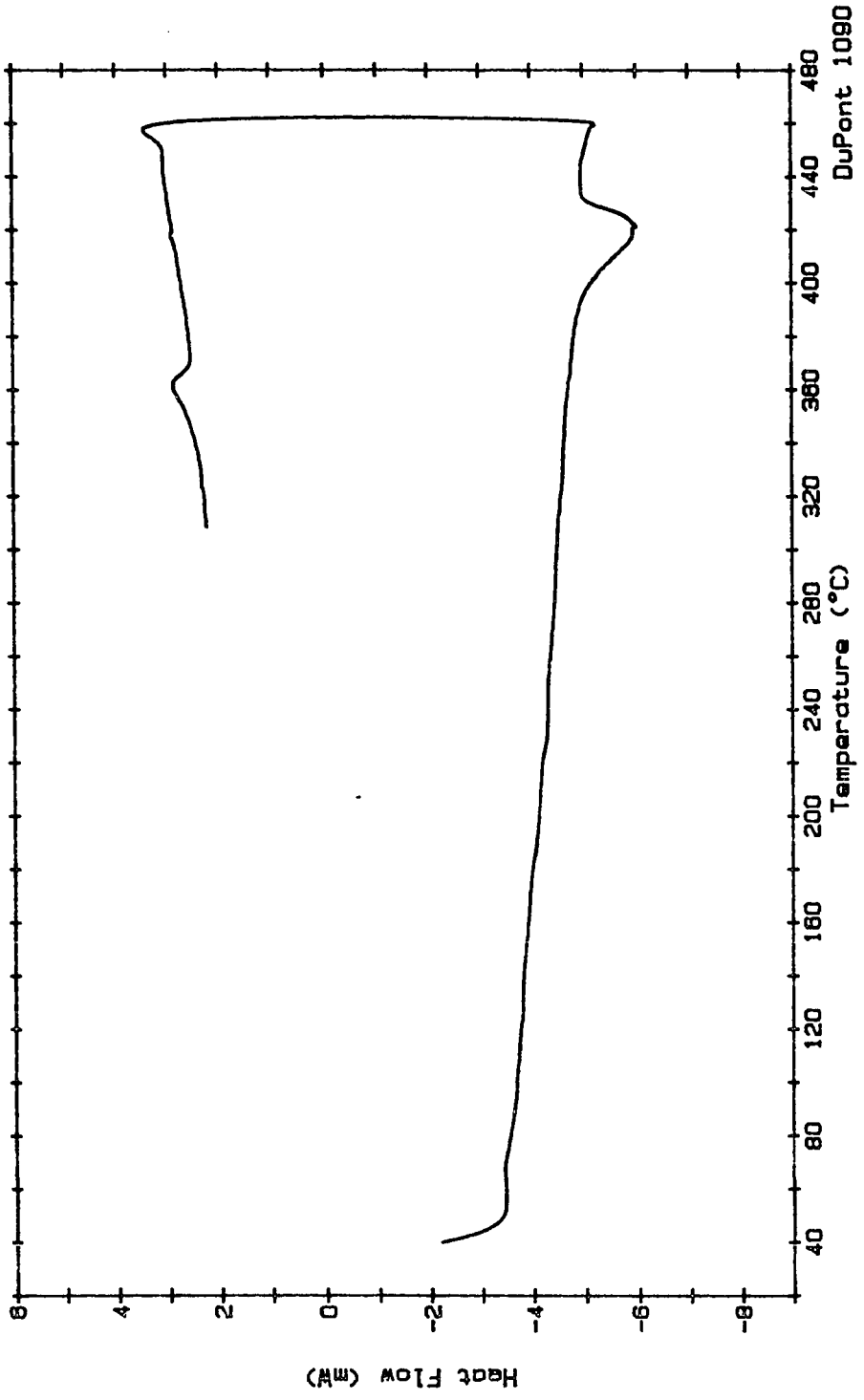

Figure 40. DSC trace for the third heating of a second portion from specimen 11.

of the four annealing conditions produce total specific energies which ranged from 11.2 J/g to 12.1 J/g for the crystalline-solid to liquid-crystal transition.(#) This is the case even though the peaks become sharper at higher annealing times and temperatures. This indicates, to a first approximation, that the same amount of energy is required to transform the molecules from both the solid structure, which produces the higher temperature peak, and the low temperature peak to the liquid-crystalline state. In addition, it indicates that one type of structure is built up at the expense of the other.

The specimens annealed at 300°C for 1 hour did not follow this trend, and it is likely that they were not at temperature for a sufficient amount of time to allow significant ordering to take place. This position is supported by the lack of a 100°C endotherm in two of the three specimens, and a very small endotherm seen for the remaining specimen. In addition, Field et al. indicate that annealing at 260°C can produce a return of the 100°C endotherm, but the process is relatively slow at that temperature.(23) The process does become rapid at temperatures above 350°C.(23)

(#) Specimen 17 with a specific energy of 9.29 J/g was the only exception to this, and it appears to be somewhat different from the other specimens.

The data presented here seem to indicate that the time required to produce a return of the 100°C endotherm for 300°C anneal cycles is somewhere between 1 and 24 hours, and that a one hour exposure at 360°C is sufficient to cause the return of the 100°C endotherm. If exposure at 300°C for one hour is not sufficient to reorganize the molecules to produce the 100°C endotherm, it is unlikely that the energy is sufficient to cause a significant change in the molecular structure which would be reflected in the energies exhibited by the higher temperature endotherms.

Another interesting piece of data produced by the DSC tests is that the specific energy of the liquid-crystal to isotropic-liquid transition seems to be approximately the same for all of the annealing conditions. This indicates that after all the material has passed through the liquid crystalline phase transition, it is essentially all in the same liquid-crystalline state. This makes sense if the analogy is made with a solid changing phase to a liquid and then to a gas. The energy required for the transition from a liquid to a gas is not dependent on the energy required to go from a solid to a liquid. The energy of each phase change is not dependent on previous phase changes. This is true as long as the previous phase changes were complete.

5.3 Overall X-ray Diffraction Results

The X-ray diffraction traces for the various pressed specimens and the injection molded plates can be seen in Figures 41 through 51. Figures 41 through 46 are for the pressed specimens. Each figure is for a specific heat treat condition and contains three traces. Figures 47 through 51 are for the injection molded plates. These figures contain one trace since only one injection molded plate specimen was subjected to each heat treatment. The X-ray diffraction traces presented in Figures 41 through 51 have not been normalized; they represent the raw data derived from the diffractometer. The traces in these figures were not normalized because there was no data on how specimen thickness affects the diffraction intensities. This would require a separate study with specimens of various thicknesses that have a structure which is known to be the same from specimen to specimen. These type of specimens require special processing techniques that were not available for this effort. As a result, it is not clear whether the intensity variations seen were due to specimen thickness or internal structure.

The relative size of the first two peaks does not match the literature.[23,27] This is the most noticeable feature of the diffraction traces. In the literature, the first peak is the largest and occurs around 19°. Except for the as

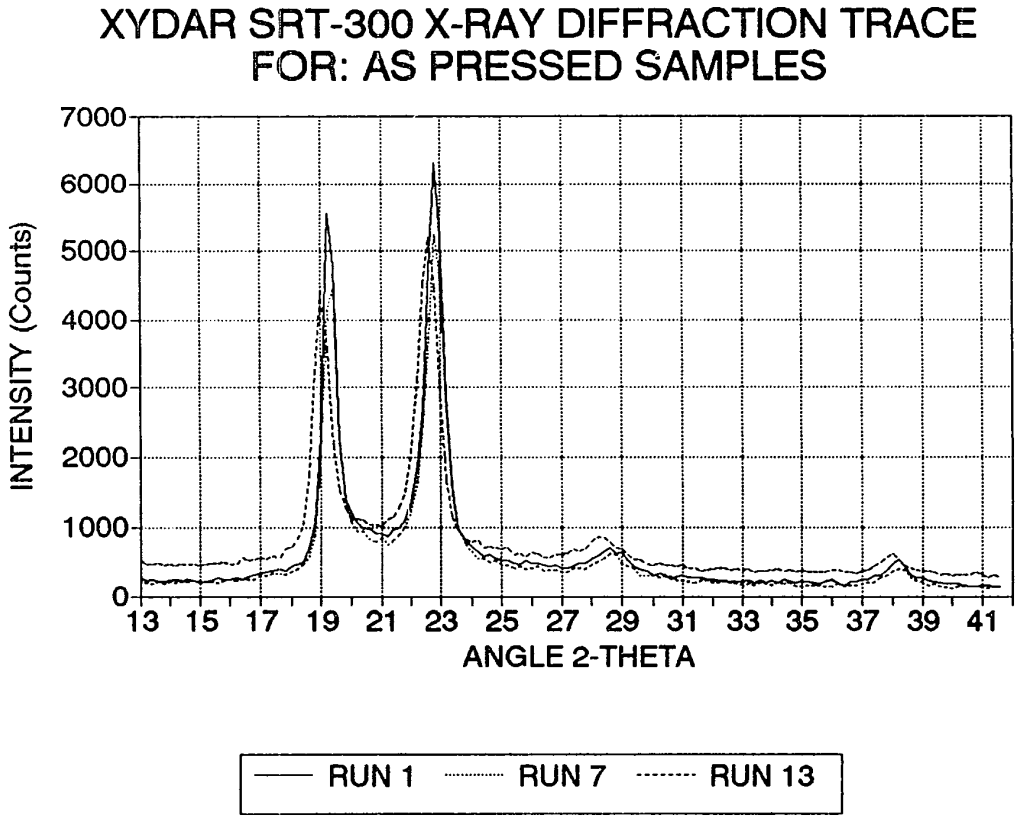

Figure 41. X-ray diffraction trace for as-pressed specimens. The run numbers listed correspond to the specimen numbers.

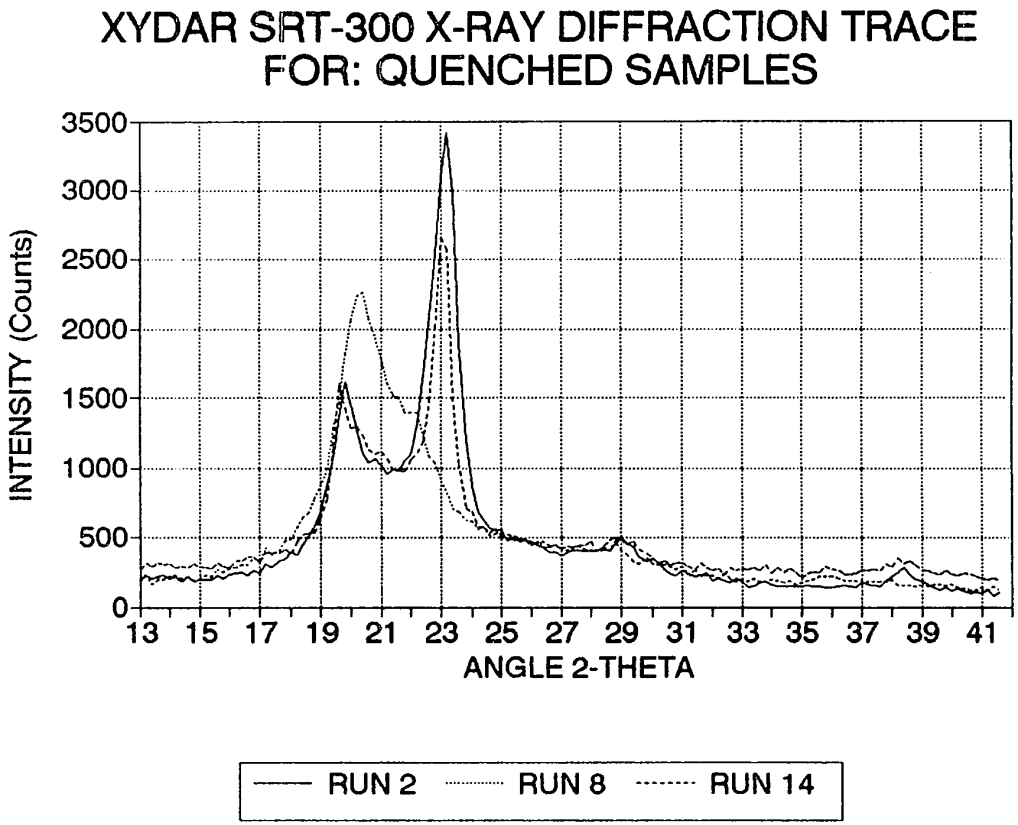

Figure 42. X-ray diffraction trace for quenched specimens. The run numbers listed correspond to the specimen numbers.

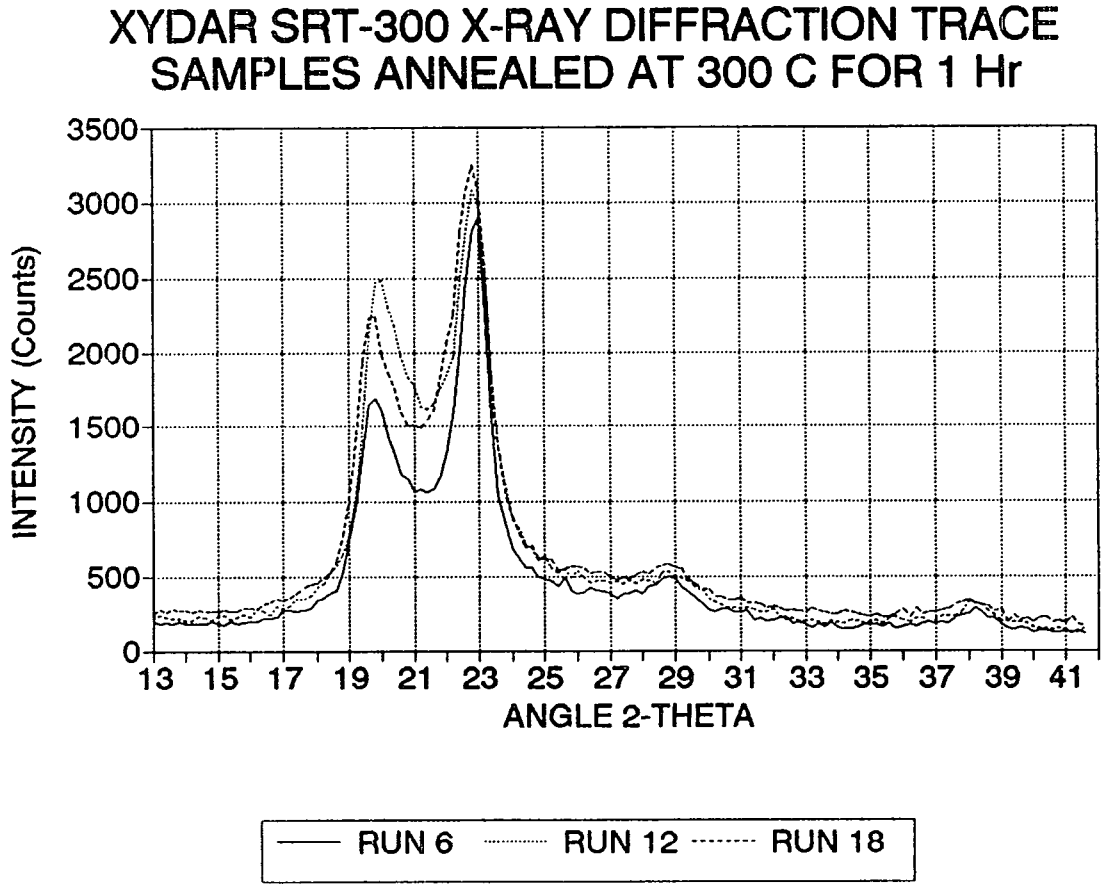

Figure 43. X-ray diffraction trace for specimens annealed at 300°C for 1 hour. The run numbers listed correspond to the specimen numbers.

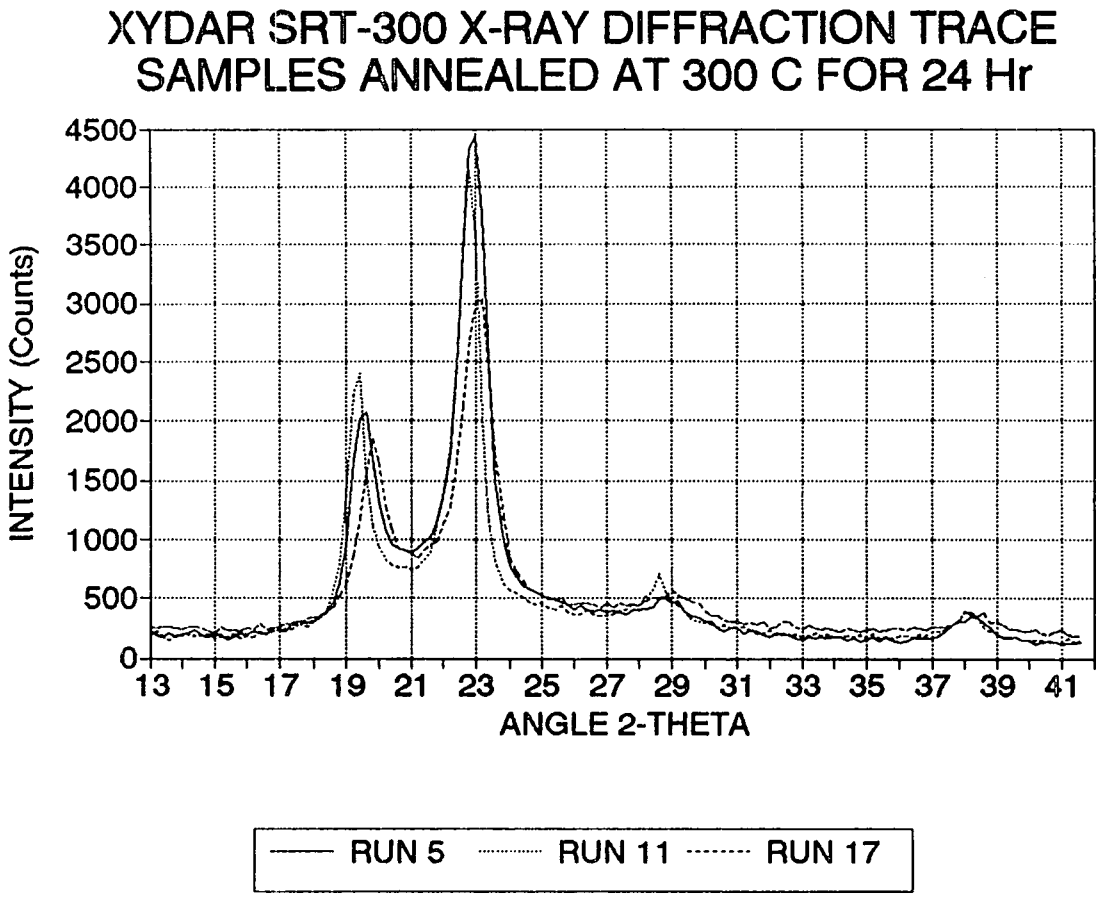

Figure 44. X-ray diffraction trace for specimens annealed at 300°C for 24 hours. The run numbers listed correspond to the specimen numbers.

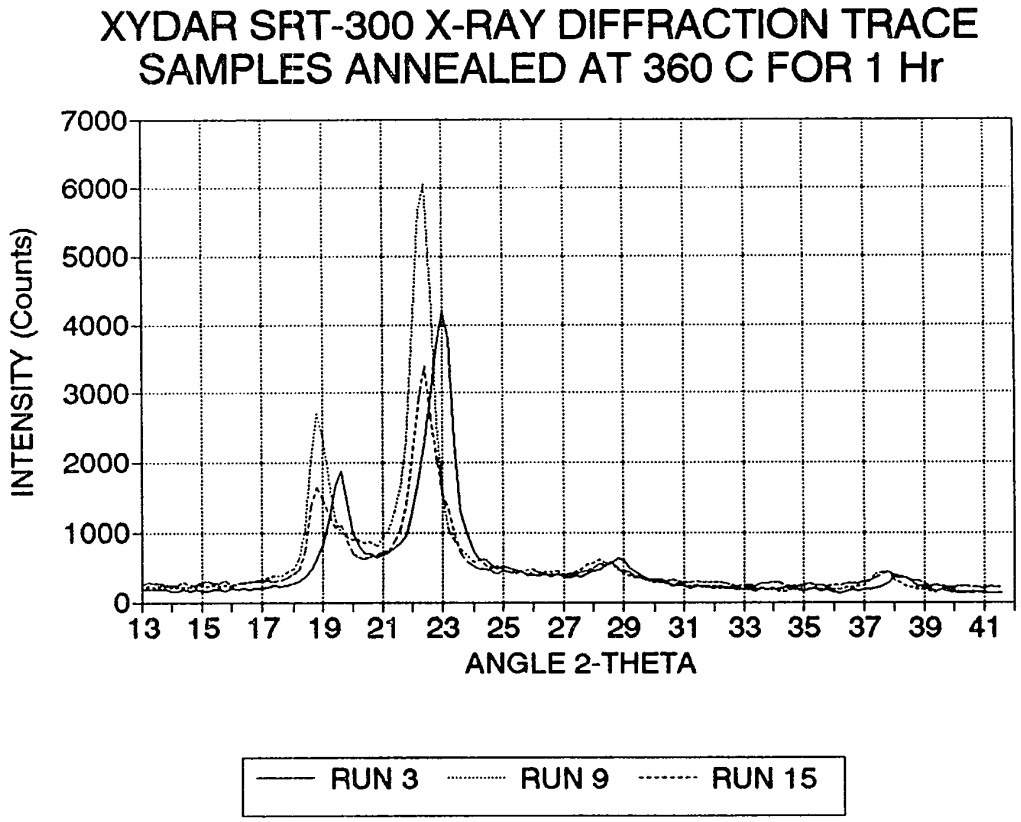

Figure 45. X-ray diffraction trace for specimens annealed at 360°C for 1 hour. The run numbers listed correspond to the specimen numbers.

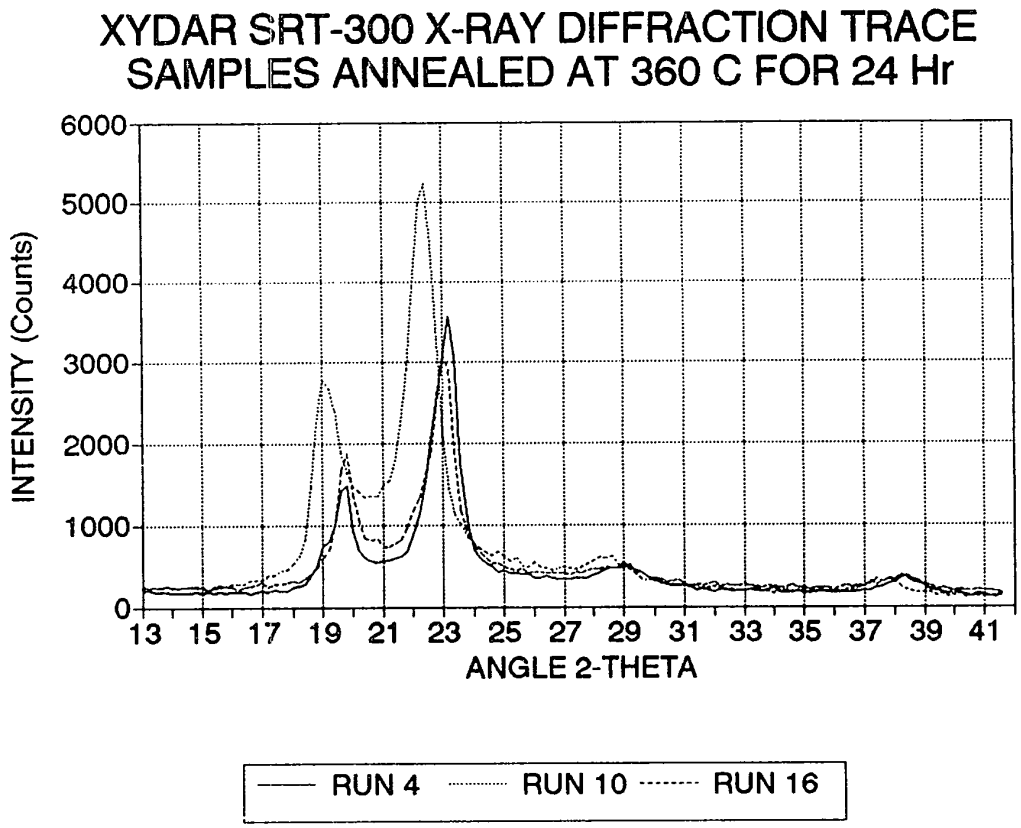

Figure 46. X-ray diffraction trace for specimens annealed at 360°C for 24 hours. The run numbers listed correspond to the specimen numbers.

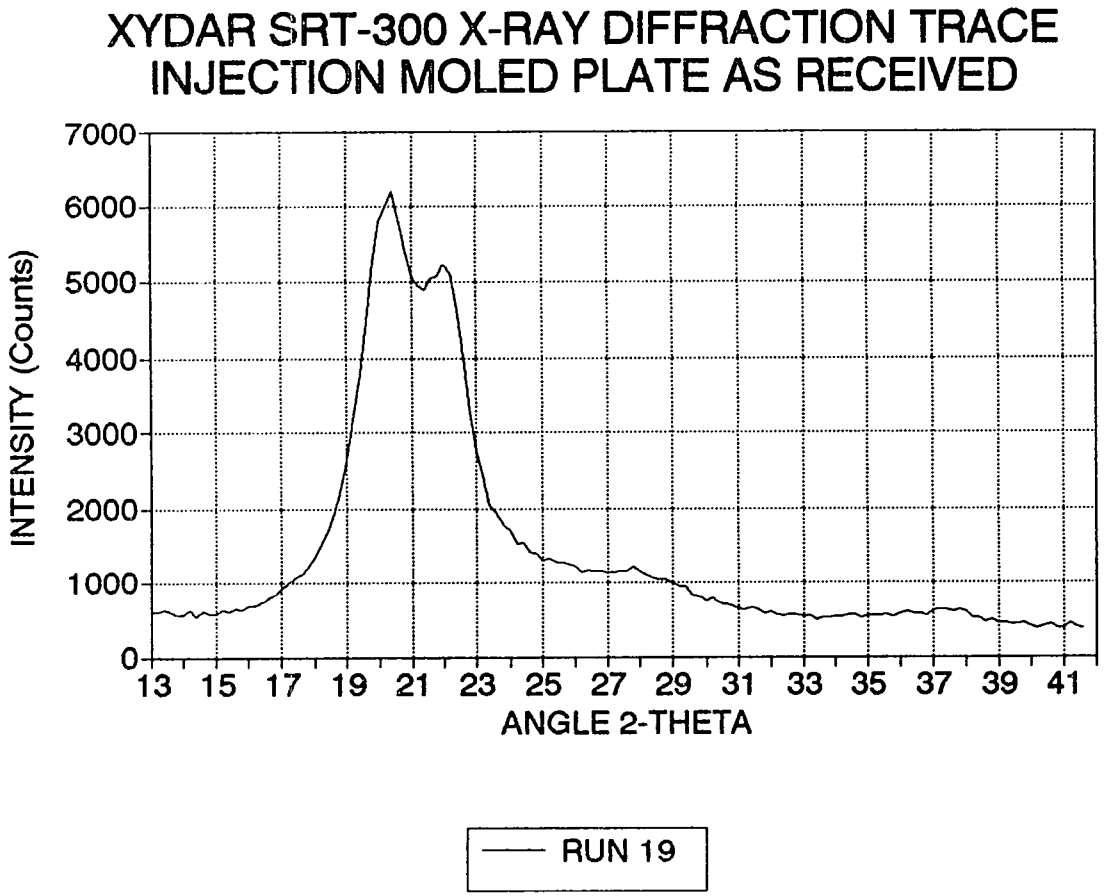

Figure 47. X-ray diffraction trace for an injection molded specimen in the as-received condition.

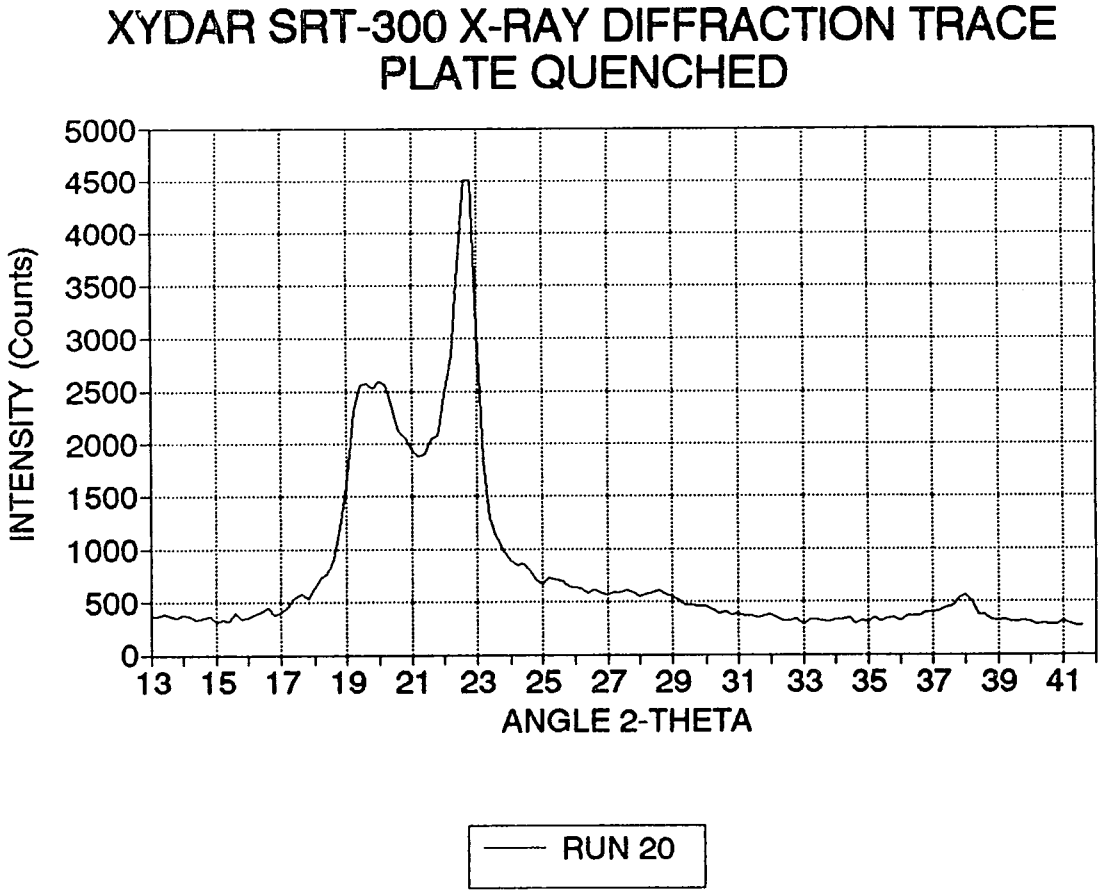

Figure 48. X-ray diffraction trace for an injection molded specimen in the quenched condition.

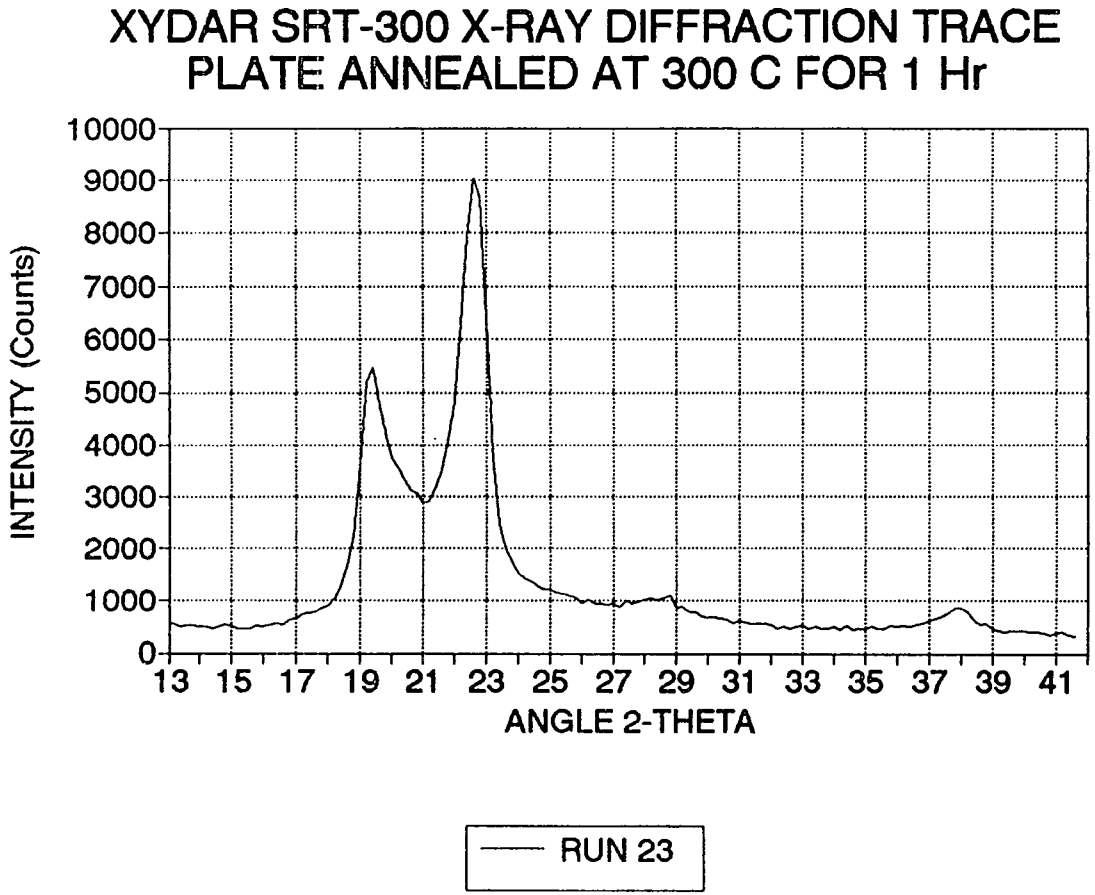

Figure 49. X-ray diffraction trace for an injection molded specimen annealed at 300°C for 1 hour.

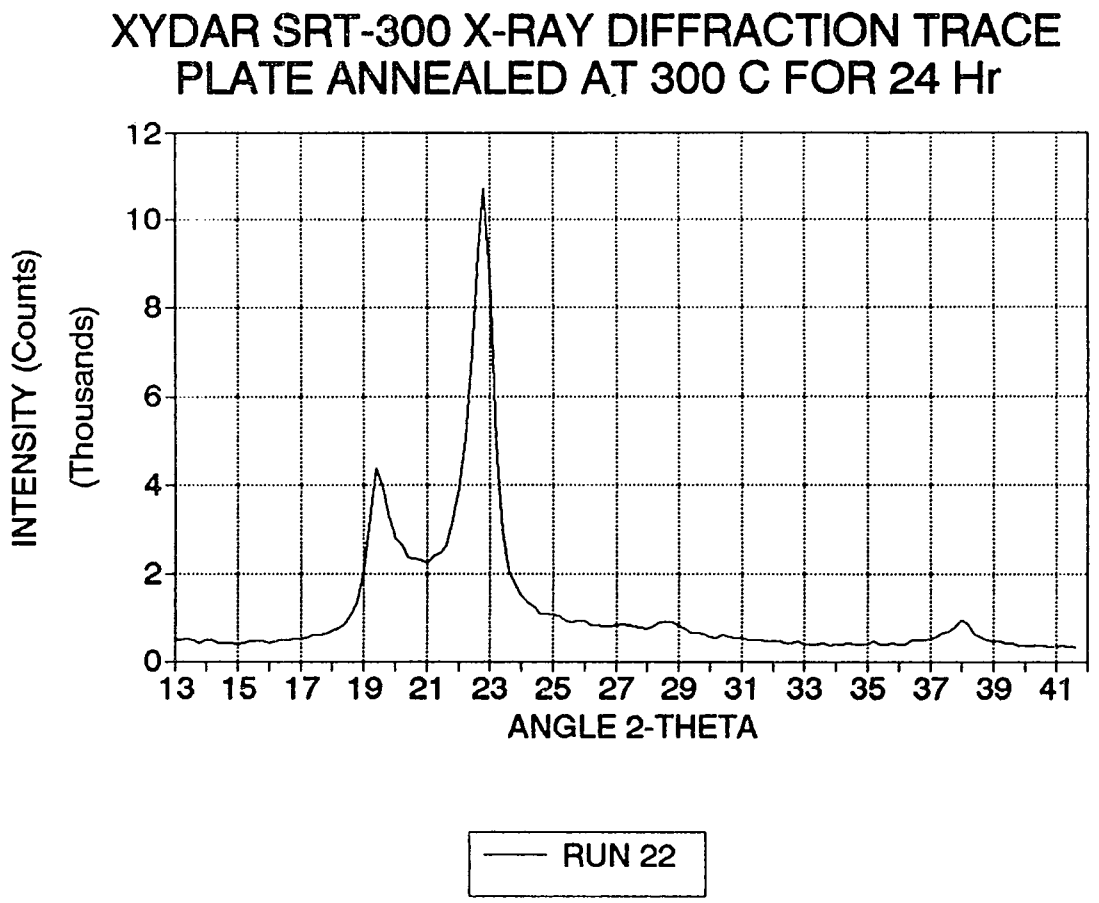

Figure 50. X-ray diffraction trace for an injection molded specimen annealed at 300°C for 24 hours.

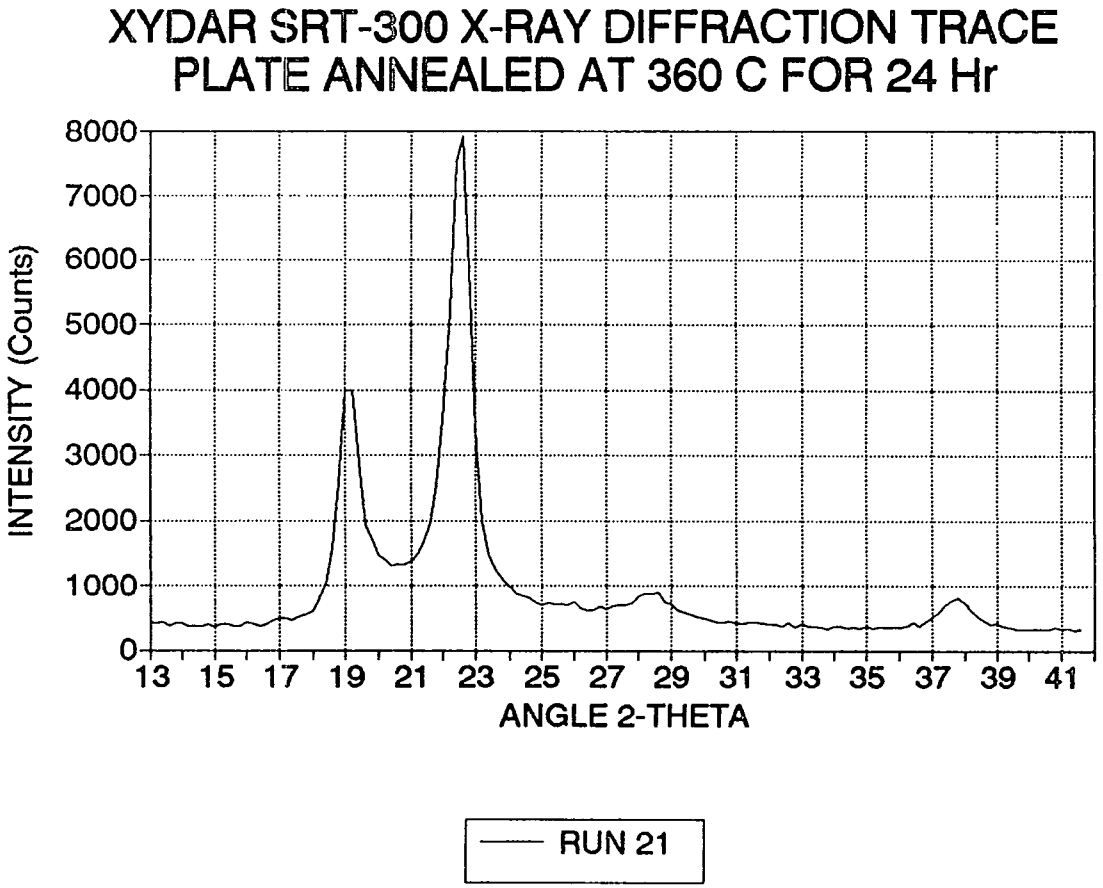

Figure 51. X-ray diffraction trace for an injection molded specimen annealed at 360°C for 24 hours.

received injection molded plate, seen in Figure 47, all the other specimens examined showed that the second peak, which occurs at about 22.8°, is the largest. While this effort was unable to produce a definitive explanation for this difference, there are a few possibilities. One answer could be that some kind of change occurs during the pressing process. Some supporting information for this explanation comes from the DSC studies. Recall that the first endotherm which was reported by Reference 23 occurs around 100°C, but in this study it occurred around 110°C. In addition, the material used for the X-ray diffraction studies in References 23 and 27 had not gone through the pressing step and consequently did not experience the additional thermal history associated with the pressing process. The argument is also supported by the X-ray results for injection molded plates. The as-received injection molded plate exhibits a first peak which is larger than the second peak. The other injection molded plates, which have additional thermal history, produced diffraction traces where the second peak is larger than the first.

Evidence that refutes the pressing-induced thermal history argument comes from Kalika et al.[27] This reference shows that after annealing the material at 350°C and cooling it to room temperature, the first peak is again the largest. This is also reported in by Field et al.[23] for specimens

which have been heated to 380°C, and 450°C; however, neither of these references indicates the length of time that the specimens were subjected to elevated temperatures.

Another possible explanation for the differences is the configuration of the specimens. References 23 and 27 used powder specimens for the X-ray diffraction studies. Kalika[27] used powder produced by sub-ambient fracture of the resin pellets, and Field[23] used the as-synthesized polymer powder. For the current study, the specimens were in the form of pressed disks. It is unclear whether this would explain the observed differences, but there is a clear difference in technique which is worthy of future exploration.

A third possibility is that the material used in the sited references is different from the material used in this study. Kalika et al.[27] clearly state that the material used in their study was XYDAR^R SRT-300, and Field also indicated that the material used in Reference 23 was XYDAR^R SRT-300.[28] Even though the material supplied for this effort was also identified as XYDAR^R SRT-300, it may not be exactly the same chemical compound. Review of the patent literature[13,14,15,29] indicates that there are at least two ways to produce XYDAR^R and several different additives which can be used in the process. It is not uncommon for resin manufactures to change their manufacturing processes

for commercial materials. These changes, though subtle, can produce the kinds of differences observed in the X-ray diffraction traces and DSC results.

5.3.1 Diffraction Traces of As-pressed Specimens

Review of the as-pressed diffraction traces in Figure 41 show that there are two primary peaks which occur between 18° and 24°, and two lesser peaks which reach maximum intensity around 28° and 38°. The variation in peak location appears to be a result of the experimental technique. For the diffraction studies, the pressed specimens were placed directly into the specimen holder with the specimen being held in place by spring clips at the top and bottom with no other support. Because some of the specimens exhibited a small amount of cupping after heat treatment, and the specimens were only gripped at the top and bottom, some of the curl in the horizontal direction remained causing a slight misalignment of the specimen. The misalignment was not considered critical because the purpose of the X-ray work was to find major changes in the structure, and to provide an assessment of the relative, rather than absolute crystallinity.

For the as-pressed specimens, the primary peaks are individually well defined. They are also fairly narrow with half height widths of about 0.6° for the first peak and 1°

for the second peak. They are very close to the same height with the first peak being smaller by an average of about 13 percent. On the other hand, the two remaining peaks are much smaller, fairly broad, and not very well defined.

5.3.2 Diffraction Traces for Quenched Specimens

The diffraction traces for the quenched specimens are shown in Figure 42. They are very different from the as-pressed specimens. There is also a major difference in the shape of the diffraction trace between quenched specimens with specimen 8 being different from the other two specimens. Earlier in the DSC discussions, it was suspected that this specimen was different from the others because the DSC results showed transition temperatures that were different from the other two quenched specimens. This difference is confirmed in the X-ray diffraction results which show that specimen 8 exhibits a very different shape in the region between 18° and 24°. Only one very broad peak is seen with the possibility that a second peak exists as a shoulder to the first. This correlates very well with some X-ray diffraction data obtained for one of the early attempts at molding a specimen disk which is described in Section 4-1. This particular specimen disk was severely discolored which clearly indicates decomposition. The shape of the diffraction trace for the disk specimen is very

similar to the one for specimen 8. Based on this, it is safe to assert that specimen 8 does suffer from decomposition.

For the two remaining quenched specimens, the height of the second major peak is about half that of the corresponding peak for the as-pressed specimens. In addition, the relative size of the first peak has changed such that it is only about half the intensity of the second peak.

The intensity of the minor peaks remains about the same as the as-pressed specimens, but the shape of the peaks is less defined.

5.3.3 Specimens Annealed at 300°C for 1 Hour

The diffraction traces for these specimens are very similar to quenched specimens. They can be seen in Figure 43. Two of the three traces show that the relative intensity of the first peak has increased slightly. Because these specimens have been annealed, one would expect that they would be more ordered than their quenched counterparts. The DSC data indicate that the difference in the degree of order is very slight, and the small difference in the diffraction traces appear to support this qualitatively. Meanwhile, the two minor peaks appear to be largely the same as those seen for the quenched specimens.

5.3.4 Specimens Annealed at 300°C for 24 Hours

Two of the three specimens shown in Figure 44 show a dramatic increase in the size of the second peak. This increase results in a reduction in the second peak to first peak intensity ratio. For these two specimens, the ratio has dropped such that the intensity of the first peak is now only 50 percent of the second peak. As a consequence of the increased intensity of the second peak, the two peaks appear to be better defined. The third specimen, specimen 17, does not appear to be very different from the specimens annealed at 300°C for one hour. It is interesting to note that the DSC results for specimen 17 showed a much lower specific energy for the crystalline-solid to liquid-crystal transition, than the other two specimens.

There was no major change in the minor peaks; however, one could argue that qualitatively the minor peaks appear to be better defined than they are for the quenched specimens.

5.3.5 Specimens Annealed at 360°C for 1 Hour

The diffraction traces for this group of specimens is shown in Figure 45. This group contains the specimen with the largest intensity peak. Specimen 9 is different from the other two specimens. The intensity of the second peak is about 40% higher than it is for the other two specimens. Unlike the earlier examples where the specimens exhibited

different X-ray traces and had different values of specific energy, the specific energy for specimen 9 is basically the same as the other two specimens. This discrepancy can be explained by variations within the specimens themselves. Another group of diffraction studies was performed on the same group of specimens. In this second set of studies, specimen 3 showed a very large pair of peaks similar to those obtained from specimen 9. In the same group of diffraction runs, specimen 9 exhibited intensities which were at the same level as those obtained for specimens 3 and 15 in the first set of diffraction runs. This suggests that the correlations between X-ray diffraction data and DSC data depend on the location from which the test material is extracted from the specimen.

Again the higher angle peaks did not change to any significant extent.

5.3.6 Specimens Annealed at 360°C for 24 Hours

Figure 46 contains the X-ray diffraction traces for the pressed specimens which were annealed at 360°C for 24 hours. Just like the previous group, only two of the three specimens produced traces which are similar. Further, the diffraction results do not agree with the DSC data. Specimen 10 shows much higher diffraction intensities while it has the lowest endotherm energy. Once again this appears to be a

consequence of variability within the specimen. The second run of the diffraction study showed specimen 4 to have the same kind of high intensities seen for specimen 10 in the first set of traces.

5.3.7 Injection Molded Specimens

The results of the X-ray diffraction studies on the injection molded specimens show basically the same behavior as the specimens that were pressed. The biggest difference was the relative intensities of the first and second diffraction peaks. The fact that the injection molded results were so closely related to those for the pressed specimens was surprising and encouraging, surprising because injection molded specimens start out with a very diverse internal structure. This view is supported by both DSC and X-ray diffraction results. A typical DSC trace for a section of injection molded material approximately 0.305 mm (0.012 in) thick is shown in Figure 52. The endotherm for the crystalline-solid to liquid-crystal transition is very broad and is almost unidentifiable. This is evidence of a variable structure. In Figure 47, the width of the diffraction peaks between 18° and 24° is very broad. This indicates that injection molded parts have a diverse structure.

Despite starting out with a very nonuniform structure, Figures 48 through 51 show that after heat treatment the

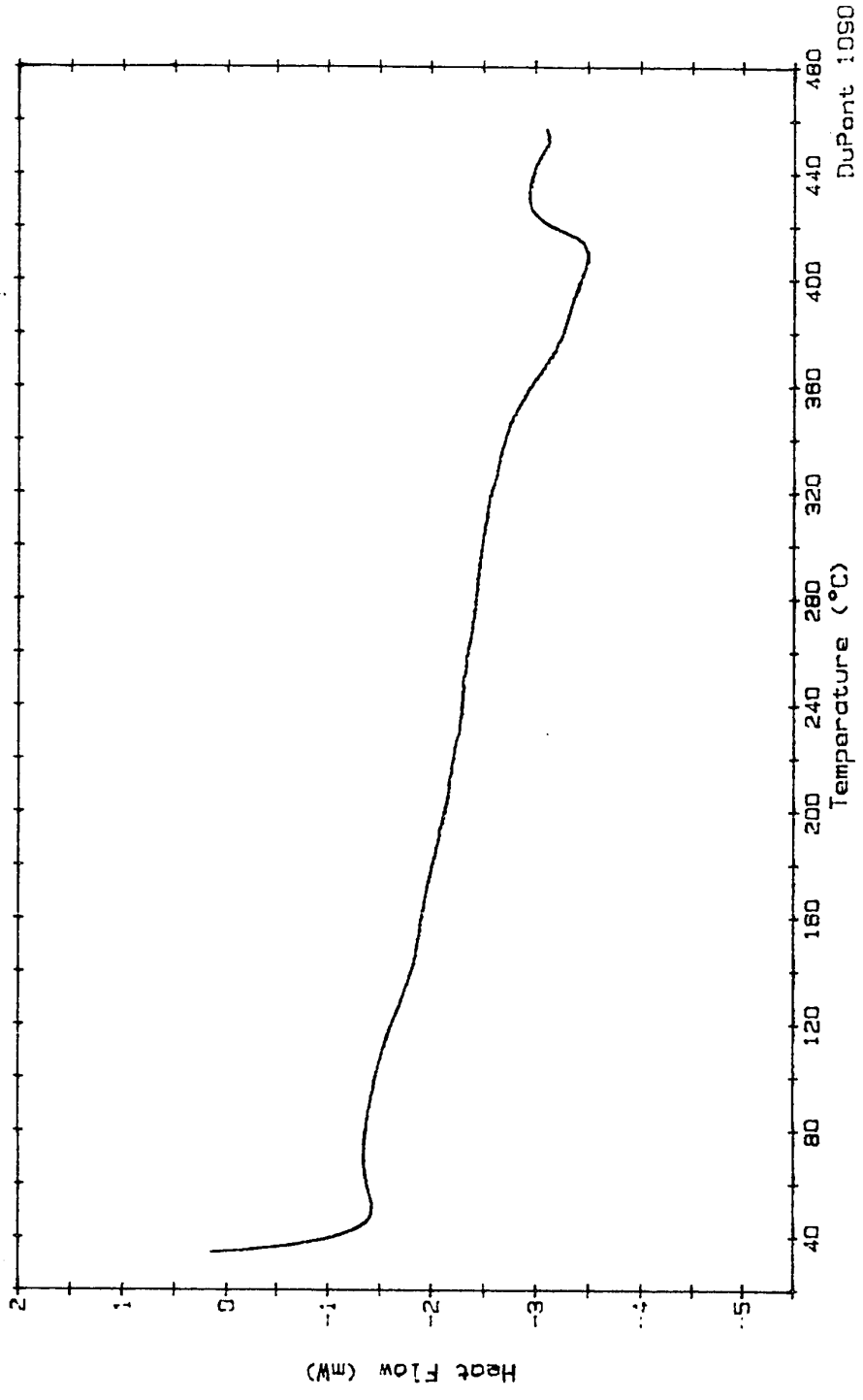

Figure 52. Typical DSC trace for an injection molded specimen in the as-received condition.

injection molded plates are able to produce X-ray diffraction traces which are similar to their pressed counterparts. This is encouraging because it indicates that changing the crystallinity of XYDAR^{R} SRT-300 does not require a uniform structure for the starting material. This is important because it implies that altering the level of molecular order in injection molded parts is possible.

5.4 Correlation of DSC and X-ray Diffraction Results

One possible explanation for the double peak endotherms seen in the DSC results is that some type of molecular reordering or change has taken place. Because there is a clear temperature difference between the two peaks, the process of peak splitting is reversible and each peak grows at the expense of the other. Changes in the crystalline structure could describe the type of molecular reordering which occurs. If the crystalline structure is changing, there should also be some kind of dramatic shift in the diffraction traces. While there is a clear difference between the quenched specimens and all the other specimens, the difference is much more subtle between the specimens annealed at 300°C for 24 hours and the specimens annealed at 360°C. There is a slight difference in the sharpness and intensities of the peaks, but there are none of the dramatic differences which are suggested by the DSC results. This

would tend to indicate that the material which produces the high temperature peaks possesses the same type of crystal structure as the material which produces the low temperature peaks.

The relative crystallinity of the test specimens was determined using the techniques described in Chapter 4. The calculated values are shown in Table 11. This table also includes the associated specific energy of the crystalline-solid to liquid-crystal transition. A quick review of Table 11 shows that there is no clear correlation between the relative percent crystallinity and the specific energy of the transition.

This lack of correlation could be the result of several factors. One likely source of the discrepancies is the variations within each specimen. These variations were seen in both the DSC data and the X-ray diffraction data. In order to truly define the condition of the specimens, additional work is required. Because of the different intensities seen in the X-ray diffraction results, it would be advisable to run several traces for each specimen with the specimen being moved between runs. The apparent variation in the DSC data could have been minimized by doing several DSC runs on material from several locations within the pressed specimens. This would have produced an average specific energy value for each specimen which could then be

Table 11. Relative Percent Crystallinity And Specific Energies Of The Crystalline-Solid To Liquid-Crystal Transition For The Various Specimens.

Condition	Specimen Number	Relative Percent Crystallinity	Specific Energy for the 2nd Endotherm
As-pressed			
	1	67.5	13.1
	7	63.1	11.7
	13	67.6	12.7
	Average	66.1	12.5
Quenched			
	2	57.7	9.16
	8	53.3	8.33
	14	45.7	7.64
	Average	52.2	8.38
Annealed at 300°C for 1 Hour			
	6	54.4	6.91
	12	65.4	7.57
	18	64.1	8.10
	Average	61.3	7.53
Annealed at 300°C for 24 Hours			
	5	60.8	11.4
	11	53.8	11.2
	17	50.5	9.29
	Average	55.0	10.6
Annealed at 360°C for 1 Hour			
	3	55.6	11.2
	9	65.4	11.3
	15	44.9	11.6
	Average	55.3	11.4
Annealed at 360°C for 24 Hours			
	4	46.9	11.6
	10	70.5	11.4
	16	46.3	12.1
	Average	54.6	11.7

compared with the average value for several determinations of relative percent crystallinity. If the variations seen in this study were due to structural variations within the specimens, the apparent variation between specimens would then be reduced.

The test techniques are another possible cause for the lack of correlation. The difference in crystallinity may be much smaller than initially expected. If this is the case, further refinement of the X-ray diffraction procedure is required. The 0.2° step interval is too large for precise determinations; it should have been reduced to 0.05° or at least 0.1° per step. This would provide better peak resolution. The actual maximum of the diffraction peak could be occurring at an angle of 2-theta which is between steps. If this situation occurred, it would cause the area under the sharpest diffraction traces to be under-estimated to a greater extent than the traces with broader peaks. Reducing the step size would also reduce the amount of error caused by the numerical block size integration of the area under the curve. In addition, the count times should be lengthened to several seconds to improve the counting statistics and reduce the amount of noise in the diffraction traces.

It was mentioned in Chapter 4 that several simplifying assumptions were made for the degree of crystallinity

determinations. Errors induced by these assumptions could have played a role in the correlation problem.

5.5 Indications that the Level of Orientation Changed as a Function of Thermal Treatment

Despite an overall lack of correlation between the DSC and X-ray diffraction data, there are some indications that the level of crystallinity and order within the specimens did indeed change with thermal treatment. While the calculated relative percent crystallinity data had a wide variation, when the maximum values for each thermal treatment condition are examined, there appears to be a trend. The quenched specimens have the lowest level of crystallinity and the specimens annealed at 360°C for 24 hours have the highest. The maximum values for the DSC data also follow this pattern. Specimens annealed at 300°C for 1 hour are the exception. They have higher than expected relative crystallinity values and lower than expected specific energies. The data appear to be inconsistent with the other specimens in the same condition and with specimens in different states. A possible explanation for this situation is that the material is in a state of transition. The DSC traces tend to support this argument by exhibiting a variation in size for the two peaks. Recall that for one of the specimens the second peak was larger, while for the

other two specimens the first peak was larger. In addition, only one of the three specimens showed signs of the first endotherm. Examination of Figure 43 shows that the first two diffraction peaks are not as well defined at the base, and the saddle between the two peaks for specimens 12 and 18 are above 1500 counts. At the same time, the estimated amorphous trace has a maximum of 500 counts in the same area. This clearly shows a problem with the estimated amorphous curve and the method used to calculate relative crystallinity.

5.6 Comparisons Between the As-pressed and Highly Annealed Specimens

The as-pressed specimens show a very high relative percent crystallinity, and high specific energy. On average they are slightly higher than the values obtained for the specimens which were annealed at 360°C for 24 hours; however, there are some distinct differences between them. The DSC traces have very different shapes for the second endotherm. The as-pressed specimens have a very broad endotherm while the annealed specimens have a very sharp endothermic peak. In addition, the peaks on the X-ray diffraction traces are much sharper for the annealed specimens. These somewhat qualitative differences indicate that some type of reorganization has occurred within the material. The form of this reorganization is not entirely

clear. Since there are no major energy or X-ray diffraction differences, a strong possibility is that rather than an increase in crystallinity existing in the annealed specimens there is an increase in the degree of uniformity of the material. This could also be explained by an increase in short range ordering which cannot be detected with the X-ray diffraction methods used.

5.7 The Progression of Thermal Treatment Affects as Determined by DSC and X-ray Diffraction

A helpful way to summarize the effects of the thermal treatment is to examine the changes in the DSC and X-ray diffraction traces as a function of the thermal history as it progresses from a minimum level for the as-pressed condition to a maximum level for the annealed at 360°C for 24 hours condition.

The DSC characterizes the as-pressed condition as possessing a very broad, high energy endotherm for the crystalline-solid to liquid-crystal transition. At the same time, the X-ray diffraction trace has relatively large, semi-broad peaks. Both the DSC and X-ray diffraction data indicate that there could be a high degree of order within the material but, this order is not uniform.

Heating the specimens quickly to 430°C and then quickly quenching them in liquid nitrogen causes a decrease in the

apparent order observed by both DSC and X-ray diffraction. This is characterized by a major drop in the energy for the crystalline-solid to liquid-crystal transition, and in the size of the X-ray diffraction peaks. While there is a drop in the energy of the endotherm, the peak becomes sharper. This is thought to be indicative of increased uniformity.

Subsequent annealing at 300°C for 1 hour results in a very limited increase in the peak height for the first x-ray diffraction peak. This indicates a slight increase in molecular order. The initial splitting of the endotherm for the crystalline-solid to liquid-crystal transition detected by DSC is the most striking change observed.

Extending the annealing time at 300°C from 1 to 24 hours produces a taller and sharper profile for the second x-ray diffraction peak; however, the calculated relative percent crystallinity is reduced. This apparent inconsistency in the x-ray diffraction data is thought to be a result of the diffraction parameters employed. At the same time, the splitting of the crystalline-solid to liquid-crystal endotherm becomes more pronounced and the energy of the transition rises.

Changing the annealing conditions to 360°C for 1 hour causes a shift in the split peak so that the size of the low temperature side of the peak becomes smaller than the high temperature side. As the high temperature peak becomes

larger, it appears to sharpen, and there is an increase in the energy of the transition. This indicates both increased order and uniformity within the structure. While the DSC results indicate a dramatic change, the X-ray diffraction data show no major change.

Increasing the time for the 360°C anneal to 24 hours causes the low temperature portion of the double peak to completely disappear and the average energy of the transition to increase slightly. This is thought to indicate that restructuring is complete. Once again, the changes observed by the DSC were not observed by X-ray diffraction.

The tests which were conducted to see if the changes brought on by the annealing cycles were reversible did determine that these changes were indeed reversible. This strongly suggests that the changes are physical rather than chemical in nature.

Chapter 6. CONCLUSIONS AND RECOMMENDATIONS

The goal of this investigation was to determine if it is possible to alter the degree of crystallinity of the liquid crystalline polymer know as XYDAR^{R} SRT-300, through the use of thermal processing, or annealing techniques. The results of this study have clearly shown that there is an obvious difference between quenched and annealed specimens. Both the X-ray diffraction and DSC data indicate that the differences between these two conditions is the degree of crystallinity.

The DSC results also indicate that there are differences between specimens annealed under different conditions; however, these differences are not as clearly observed in the X-ray diffraction results. Consequently, the nature of the differences between annealed specimens is not completely clear.

The data show that all the changes, with the exception of inadvertent decomposition, are reversible. This clearly indicates that the changes which result from annealing are not chemical in nature. This leads to the conclusion that the differences observed in the DSC traces are a result of short range molecular ordering which cannot be observed with the X-ray diffraction methods used in this investigation.

Even though the results are not conclusive, they clearly show that there are changes that take place within the material as a result of thermal treatment, and that this phenomenon is worthy of further investigation.

6.1 Confirmation of Earlier Studies

Earlier work by others has shown that it is possible to quench the material from the liquid-crystal state to produce a structure which is different from the starting material. It was also shown that the initial structure could be recovered by annealing the specimens at temperatures between 260°C and 354°C.[22,23,27] This investigation was able to confirm these results. It also showed that extended annealing times (*) are capable of producing changes in the material which were not reported in the earlier studies.

The earlier papers explored annealing times of approximately one hour, and they did not discuss the effects of extended annealing times. In addition, these earlier works focus on changes in the X-ray diffraction traces as a function of thermal treatment. Discussions on changes in the DSC traces centered around the return of the crystalline-solid to crystalline-solid transition but the changes in higher temperature endotherms were not discussed.

(*) In this case the term extended annealing times is used to refer to annealing times of 24 hours.

Both 1 hour and 24 hour annealing times at 300°C and 360°C were investigated in this study. In general, the results support the previous findings in that the quenched specimens show less order than the as-pressed specimens in both the DSC and X-ray diffraction studies. Furthermore, the one hour at 300°C anneal was only marginally capable of producing a return of the low temperature endotherm, while the other annealing conditions were able to produce a return of this endotherm. This directly supports the results of Field et al.[23]

The relative heights of the first two X-ray diffraction peaks did not match those reported in the literature[22,23,27]; but, the X-ray diffraction results qualitatively show that there was a structural difference between the as-pressed starting material and the quenched specimens. This investigation also shows that the quenched material was less crystalline than the starting material, and that given enough time at the annealing temperatures, a significant amount of order returns to the structure. This became apparent through an increase in peak sharpness for both the DSC and X-ray diffraction traces. All of these results agree with earlier works.[22,23,27]

While some of the details of the X-ray diffraction work do not exactly correspond with those reported in the literature, the general changes in peak height and sharpness

previously reported for the material were repeated in this study.

6.2 Expansion of Other Studies

The results of this study indicate that by concentrating on the X-ray diffraction data rather than DSC data, other investigators may have overlooked some refinement in the detail of the structure or an additional type of ordering exhibited by the material. The specimens annealed at 300°C for 24 hours and the specimens annealed at 360°C for 1 hour clearly show that there is a splitting of what has been described here, and in earlier works as the crystalline-solid to liquid-crystal transition.[23] The fact that the splitting was found almost uniformly within this study is a strong indication that the phenomenon is real, even though there is no sign of major changes in the X-ray diffraction data. A more detailed study may reveal that there is a type of short range molecular ordering taking place which wide angle X-ray diffraction cannot resolve.

6.3 Changes in the DSC Endotherm Peaks

At this point, it is difficult to determine what is causing the changes seen in the second endotherm; however, there are many things which the data are able to show are not the cause. The endotherm changes cannot be attributed to

major changes in the chemical structure. Changes such as cross linking, a large degree of chain extension or even decomposition would produce permanent changes in the material and a permanent shift in the endotherm positions. It was clearly shown in Figures 35 through 37 and Figures 38 through 40 that the endotherm temperatures and the splitting of the second endotherm can be reversed by the use of subsequent thermal cycles.

There are many possible explanations for the peak splitting seen in this study; but, the fact that no major changes are seen in the X-ray diffraction data limits the number of possible explanations. One explanation is that the annealing treatments refine the distribution of molecules. Both the as-pressed and quenched specimens have a fairly wide range for the degree of order within the specimen. This is evidenced by the broad endothermic peaks which were observed in the DSC traces. The annealing process acts to refine this distribution into clearly defined crystalline and amorphous regions. Because it is less ordered, the amorphous solid material can convert to a liquid-crystal phase at a lower temperature than the crystalline-solid material. This occurs because the forces that bind the amorphous solid material are slightly weaker than those that bind the crystalline material. During the annealing process, the amorphous regions are consumed by the crystalline

regions until the situation observed in the specimens annealed at 360°C for 24 hours is reached. At this time, all of the material is in a well organized uniform crystalline structure exhibiting a single, very sharp high temperature endotherm.

The amorphous region explanation accounts for the endotherm peak splitting and allow for the lack of structure observed in the quenched specimens. One would expect that a quenched structure would have a fully amorphous structure; however, the temperature limitations used for the quenching step may have clouded the results with residual crystallinity in the quenched specimens. The likely cause of the residual crystallinity in the quenched material is the temperature employed during the quench treatment. Recall that the specimens were not heated to the clearing or isotropic liquid temperature. They were only heated to a temperature which is within the liquid-crystalline transition range. In other words, the quenched specimens were quenched from the liquid-crystal phase rather than the isotropic-liquid phase. This is likely to have resulted in quenched specimens that still had a considerable amount of crystalline character. This can explain the presence of peaks in the X-ray diffraction traces for quenched specimens. It must be pointed out that this explanation is supposition. Without additional work, a definitive

explanation of the peak splitting phenomenon is not possible, but this explanation does fit all the data generated by this study.

It can be argued that the longer annealing times produce an increase in the short range molecular order which cannot be observed with the X-ray diffraction techniques used. This explanation is also consistent with the results.

6.4 Recommendations for Additional Work

In order to truly understand what is causing the second endotherm to split, additional work is required. The basic study should be repeated with some improvements made in the test procedures, and an emphasis placed on statistical experimental design. The primary improvements relate to principles of statistical design of the experiments. The data from this investigation show that there can be a large degree of variation from specimen to specimen, and there is some evidence that there is variation within each specimen. This requires that more area of each specimen be tested. Any future X-ray diffraction work should include several scans of the specimens with the specimens being moved between scans. The average of the X-ray intensities would then be used for crystallinity determinations. Along the same lines, DSC testing should use as much of the specimen as possible. The average specific energy derived from several runs using

material from the same specimen should be obtained. Comparing average DSC and X-ray diffraction data should have more meaning and correlate better. In addition, a statistically significant number of specimens should be used. Because of the limited availability of material, this effort has been a type of feasibility study and not a statistically precise effort.

In addition, the X-ray diffraction data could be improved by reducing the step size and increasing the scan times. Both these changes would result in improved resolution of the diffraction peaks.

Expansion of the test matrix to fill in the data gaps between 1 and 24 hour annealing times, and the addition of temperature between 300°C and 360°C may also shed some light on the exact nature of the reordering process.

Future work should also focus on the material in its final form, such as injection molded parts. At the start of this program, it was thought that the various structures present within the injection molded parts would interfere with obtaining accurate test results. The X-ray diffraction results for injection molded parts indicate that this may not be the case, and that the annealed injection molded parts may actually have a more uniform structure than the pressed test specimens used for this study. The use of

material in the final configuration, or part form is also advisable from a produceability standpoint.

Another important consideration is the effect that annealing has on the mechanical properties. This study was only designed to determine if changes in the structure were possible. The next step, after confirmation of the results of this work, is to see if the process has any significance relative to material performance. For this evaluation, the standard set of mechanical properties such as tensile strength and modulus determination would be a logical first choice. In addition, study of the physical properties relating to electrical and thermal characteristics may be revealing.

Improvements in the thermal treatment process should center around higher heating rates and trying to increase the temperature to which the material is heated as part of the quench process. This could be precipitated by the development of a technique which would allow the specimens to be quenched while in the thermal treatment chamber inside the oven.

Beyond these suggestions, more advanced techniques such as solid state nuclear magnetic resonance (NMR) and sophisticated X-ray techniques may be required to determine the nature of the highly annealed structure.

6.5 Summary

This study has produced strong indications that thermal annealing cycles alone are capable of producing differences in the structure of XYDAR^{R} SRT-300, and that this technique for altering the structure is worthy of further investigation.

REFERENCES

1. Duska, Joseph J., "Liquid-crystal Polymers: How They Process and Why". Plastics Engineering, Vol. 42, No. 12, (1986) pp. 39-42.

2. Cottis, S.G., Economy, J., Storm R.S., Wohrer, L.C., U.S. Patent 3,974,250, (1976).

3. Priestley, E.B., Wojtowicz, Peter J., Sheng, Ping, Introduction to Liquid Crystals, Plemum Press, N.Y. NY, (1974,1975) pg 1-22.

4. McChesney, C.E., "Liquid Crystal Ploymers (LCP)". Engineered Materials Handbook Vol. 2, Engineering Plastics, ASM International, Metals Park, OH (1990) pp. 179-182.

5. Rusek, J.J., "Thermotropic Liquid Crystal Polymers", Proceedings of the AIAA/SAE/ASME 27th Joint Propulsion Conference, Sacramento, CA, June 24-26, 1991, AIAA Paper No. 91-3375.

6. de Vries, Adriaan, "Structure and Classification of Thermotropic Liquid Crystals", Liquid Crystals the Fourth State of Matter, Seava, Franklin D. ed., Marcel Dekker, Inc, N.Y. NY, (1979), pp. 1-72.

7. Hashimoto, Takeji, "Laser Light Scattering From Cholesteric Liquid Crystals", U.S. - Japan Seminar on Polymer Liquid Crystals Journal of Applied Polymer Science: Applied Polymer Symposium 41, John Wiley and Sons, (1985) pp. 83-103.

8. Barrett, Craig R., Nix, William D., Tetelman, Alan S., The Principles of Engineering Materials, Prentice-Hall, Inc. Englewood Cliffs, NJ, (1973), pg. 91.

9. Atkins, P. W., Physical Chemistry, W.H. Freeman and Company, San Francisco, CA, (1978), pg. 17.

10. Jastrzebski, Zbigniew D., The Nature and Properties of Engineering Materials 2nd Ed, John Wiley and Sons, N.Y., NY, (1977), pg. 80.

11. White, James Lindsay, "Historical Survey of Polymer Liquid Crystals" U.S. - Japan Seminar on Polymer Liquid Crystals Journal of Applied Polymer Science: Applied Polymer Symposium 41, John Wiley and Sons, (1985) pp. 3-24.

12. Field, N.D., Polymer Associates, Personal Communication (September, 1991)

13. Cottis, S.G., U.S. Patent 4,639,504, (1987).

14. Duska, J.J., Finestone, A.B., Maher, J.B., U.S. Patent 4,626,557, (1986).

15. Cottis, S.G., Layton, R., Field, N.D., U.S. Patent 4,563,508, (1986).

16. Fein, Marvin M., "Introducing Xydar", 30th National SAMPE Symposium and Exhibition, Anahime, CA March 19-21 1985, Society for The Advancement of Materials and Process Engineering, Covina, CA, (1985) pp.556-564.

17. Rodriguez, F., Principles Of Polymer Systems 2nd Ed., Hemisphere Publishing Corp. N.Y. NY (1982), pg. 38.

18. Brady, Don G., "Polyphenylene Sulfides (PPS)", Engineered Materials Handbook Vol. 2, Engineering Plastics, ASM International, Metals Park, OH (1990), pp. 186-191.

19. Kelly, William E., "Polyaryletherketones (PAEK, PEK, PEEK, PEKK)", Engineered Materials Handbook Vol. 2, Engineering Plastics, ASM International, Metals Park, OH (1990) pp. 142-144.

20. Economy, J., "Liquid Crystalline Aromatic Polyesters" J. Macromol. Sci.-Chem., A21(13 &14), (1983), pp. 1705-1724.

21. Volksen, W., Lyerla, J.R. Jr., Economy J., Dawson, B., "Liquid-Crystalline Copolyester Based on Poly(p-Oxybenzoate) and Poly(p,p-Biphenylene Terephthalate)", Journal of Polymer Science; Polymer Chemistry Edition, vol. 21, (1983), pp. 2249-2259

22. Blackwell, J., Cheng, H.-M. and Biswas, A., "X-ray Analysis Of The Structure Of The Thermotropic Copolyester XYDAR", Macromolecules, No. 21, (1988), pp. 39-45.

23. Field, N.D., Baldwin, R., Layton, R., Frayer, P., and Scardiglia, F., "Polymorphism In A Liquid Crystalline Polyester Based On 4,4"-Biphenol, Terephthalic Acid, and p-Hydroxybenzoic Acid (1:1:2)", Macromolecules, No. 21, (1988), pp 2155-2160.

24. Dartco Manufacturing, Inc., Technical Information XYDAR™ High-Perfomance Engineering Resins, Dart Industries Inc., (February 1985), pp. 2-3.

25. Shelley, J., "Propulsion Applications for Thermotropic Liquid Crystal Polymers", Proceedings of the AIAA/SAE/ASME 27th Joint Propulsion Conference, Sacramento, CA, June 24-26, 1991, AIAA Paper No. 91-3376.

26. Rusek, J.J., Phillips Laboratory, Personal Communiction (July 1991).

27. Kalika, Douglass S., Yoon, Do Y., Iannelli, Pio, Parrish, William, "Structural, Dielectric, and Rheological Characterization of Thermotropic Liquid Crystalline Copolyesters Based on 4-Hydroxybenzoic Acid, 4,4'-Dihydroxybiphenyl, Terephthalic Acid, and Isophthalic Acid", Macromolecules, No. 24, (1991), pp. 3413-3422.

28. Field, N.D., Polymer Associates, Personal Communication (October, 1991).

29. Cottis, S.G., Economy, J., Nowak, B.E., U.S. Patent 3,637,595, (1972).